Electronic Supplementary Material (ESI) for Polymer Chemistry.
This journal is © The Royal Society of Chemistry 2018

SUPPORTING INFORMATION

Highly active Mg(II) and Zn(II) complexes for the ring opening polymerisation of lactide

*Paul McKeown,[a] Strachan N. McCormick,[b] Mary F. Mahon,[a] and Matthew D. Jones[a,]**

[a] *Department of Chemistry, University of Bath, Claverton Down, Bath, BA2 7AY, UK*

[b] *Doctoral Training Centre in Sustainable Chemical Technologies, University of Bath, Claverton Down, Bath, BA2 7AY, UK*

General experimental methods

The preparation and characterisation of all metal complexes was carried out under inert argon atmosphere using standard Schlenk or glovebox techniques. All chemicals used were purchased from Aldrich and used as received except for *rac*-LA and *L*-LA which were recrystallised from dry toluene. ^{1}H and ^{13}C{^{1}H} NMR spectra were recorded on a Bruker 400 MHz instrument and referenced to residual solvent resonances. $CDCl_3$ was dried over CaH_2 prior to use with metal complexes. C_6D_6 was degassed and stored over molecular sieves. Coupling constants are given in Hertz. Diffusional ordered spectroscopy (DOSY) NMR analysis was carried out on a Bruker 500 MHz instrument; the standard Bruker pulse sequence ledgp2s[1] was used, with d_1 of 5 seconds, 64k data points and 8 scans per gradient level. Typically the gradient pulse was 1750 μs, with a diffusion time of 0.05 s. Ten gradient strengths were used between 10 and 90 %. Data were processed using DOSY methods.[2] All ligands were characterised by electron-spray ionisation-mass spectrometry (ESI-MS) in positive mode. CHN microanalysis was performed by Mr. Stephen Boyer of London Metropolitan University. In certain cases, satisfactory elemental analysis results were not achieved, with samples being consistently low in carbon. This is despite reasonable characterisation by other techniques (^{1}H/^{13}C{^{1}H} NMR spectroscopy and X-ray crystallography).

All crystallographic data was collected on a SuperNova or Excalibur, EOS detector diffractometer using radiation CuKα (λ = 1.54184 Å) or Mo-Kα (λ = 0.71073 Å) radiation all recorded at 150(2) K. All structures were solved by direct methods and refined on all F^2 data using the SHELXL-2014 suite of programs. All hydrogen atoms were included in idealised positions and refined using the riding model, all refinement details are given in the .cif file. All models were straightforward with the following exceptions: Zn(**1**)$_2$ the methyl groups of one tBu (C29) were disordered over two positions in a 70:30 ratio; Zn(**2**)$_2$ refined as a 2-component inversion twin in the ratio 93:7. Two independent complex molecules are connected via hydrogen bonding. Disorder, of one ligand backbone, in the ratio 70:30 in one complex molecule is observed and the minor part has been refined with ADP restraints. All NH hydrogen atoms, with exception of the one involved in the disorder, have been refined freely with bond length restraints. One solvent toluene in the asymmetric unit which is disordered over two sites in the ratio 70:30. This has been refined with geometric constraints and ADP restraints; Mg(**1**)$_2$ the methyl groups of one tBu (C47) are disordered over two positions in a 60:40 ratio; Mg(**7**)$_2$ the ligand has disorder in the backbone over two positions in a ca. 70:30 ratio.

Polymerisations were carried out in a Young's ampoule under inert argon conditions. All polymerisations were carried out in the absence of solvent. Initial polymerisations were performed with *rac*-lactide (1 g, 6.94 mmol) at 130 °C. Immortal polymerisation was carried out with *L*LA (3 g, 20.8 mmol) at both 130 °C and 180 °C. After polymerisation, the flask was exposed to air to quench and the product was dissolved in CH_2Cl_2 which was then removed *in vacuo* and a crude ^{1}H NMR spectrum recorded. For immortal polymerisation, the polymer was precipitated from methanol to remove LA and initiator. IR kinetic measurements were recorded using a Bruker Matrix-MF FTIR spectrometer equipped with a diamond ATR probe (IN350 T) suitable for Mid-IR in situ reaction monitoring was used. These reactions were performed with *L*-LA (15 g) at 180 °C. The decrease of the C-O-C lactide peak was monitored. Several known LA:PLA ratios were measured to set up a calibration curve to relate peak area to LA concentration. Stereocomplexation was achieved by sequential addition of monomers under a flow of argon. Overhead stirring was used to ensure a homogeneous polymerisation.

All polymer molecular weights were characterised by gel permeation chromatography (GPC). GPC was carried out at 1 ml min^{-1} at 35 °C with a THF eluent using a PLgel 5 µm MIXED-D 300 × 7.5 mm column. The system was referenced against 11 narrow molecular weight standards polystyrene standards with detection *via* refractive index response. A correction factor of 0.58 was applied to measured values.[3] Epimerisation was assessed *via* ^{1}H NMR spectroscopy ($CDCl_3$) analysis of the homonuclear decoupled methine region. MALDI-ToF mass spectra were determined on a Bruker Autoflex speed instrument using DCTB (trans-2-[3-(4-tert-Butylphenyl)-2-methyl-2-propenylidene]malononitrile) as the matrix and ionised using NaTFA. DSC analysis was recorded on a TA Instruments DSC Q20. The sample was held at 40 ºC for 1 minute, heated to 250 ºC at 10 ºC/min held at this temperature for 1 minute, cooled to 40 ºC at 10 ºC/min held at this temperature for 1 minute and finally heated to 250 ºC at 5 ºC/min - the T_m values are quoted for the second heating cycle.

Materials characterisation (GPC, ESI-MS MALDI-TOF) facilities were provided through the Chemical Characterisation and Analysis Facility (CCAF) at the University of Bath.

Synthesis and characterisation

Ligand synthesis and characterisation

1-7H: All ligands were prepared in Schlenk tubes and made directly prior to complexation. Substituted aldehyde (2 mmol) was dissolved in methanol (3 ml) and diamine (2 mmol) was added dropwise to afford a yellow or orange solution. To ensure complete conversion, this solution was stirred at room temperature for 16 hours. Solvent was removed *in vacuo* to yield a quantitative yield of product.

1H (3,5-di-*tert*-butyl-2-hydroxybenzaldehyde + N-methylethylenediamine, yellow oil)

^{1}H NMR ($CDCl_3$, 400 MHz) δ = 13.65 (s, 1H; OH), 8.41 (s, 1H; ArCHN), 7.40 (d, *J* = 2.3 Hz, 1H; ArH), 7.10 (d, *J* = 2.4 Hz, 1H; ArH), 3.74 (t, *J* = 5.7 Hz, 2H; CH_2), 2.93 (t, *J* = 5.7 Hz, 2H; CH_2). 2.48 (s, 3H; CH_3) 1.46 (s, 9H; $(CH_3)_3$), 1.32 (s, 9H; $(CH_3)_3$).^{13}C{^{1}H} NMR ($CDCl_3$, 100 MHz) δ = 167.1 (ArCHN), 158.0, 140.1, 136.7, 127.0, 125.9, 117.8 (Ar), 59.5, 51.9 (CH_2), 36.3 ($C(CH_3)_3$), 35.0 (CH_3), 34.1 ($C(CH_3)_3$), 31.5, 29.4 ($C(CH_3)_3$).

ESI-MS (MeOH): Calcd *m/z* $[C_{18}H_{30}N_2ONa]^+$ = 313.2250, found *m/z* = 313.2246.

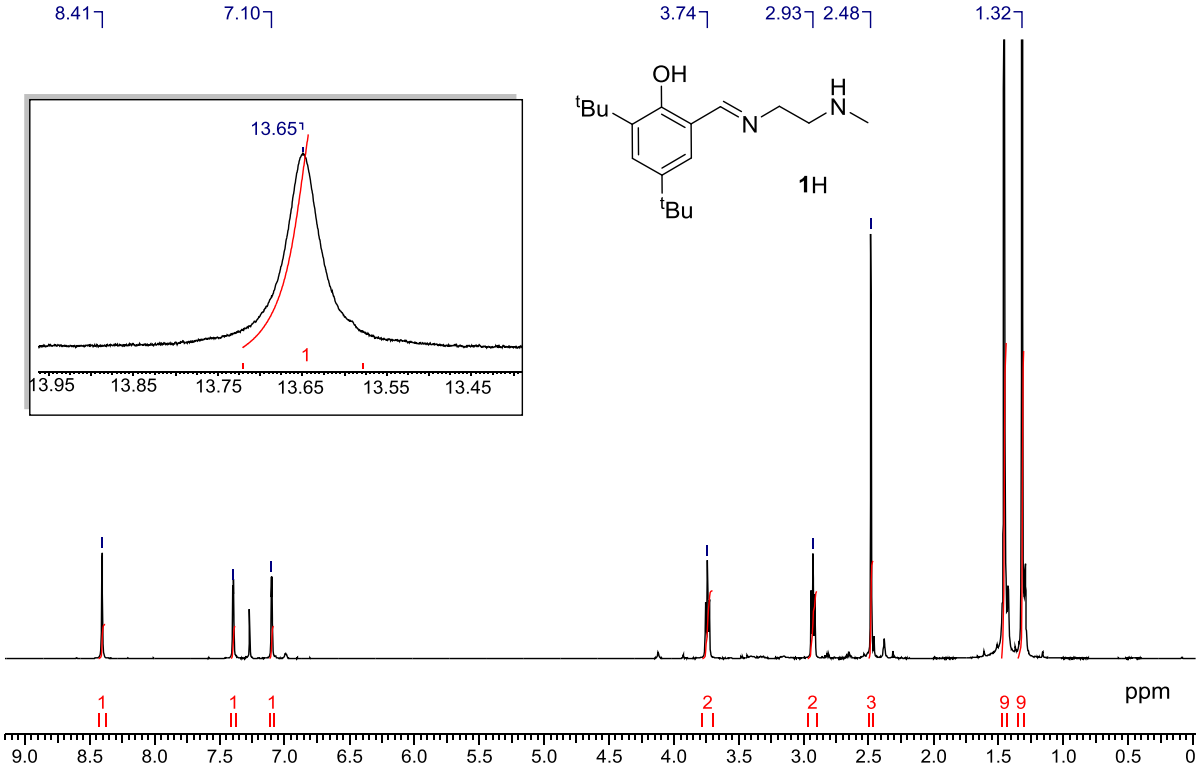

Figure SI1: ^{1}H NMR spectra (400 MHz, $CDCl_3$) of **1**H. Inset: OH resonance.

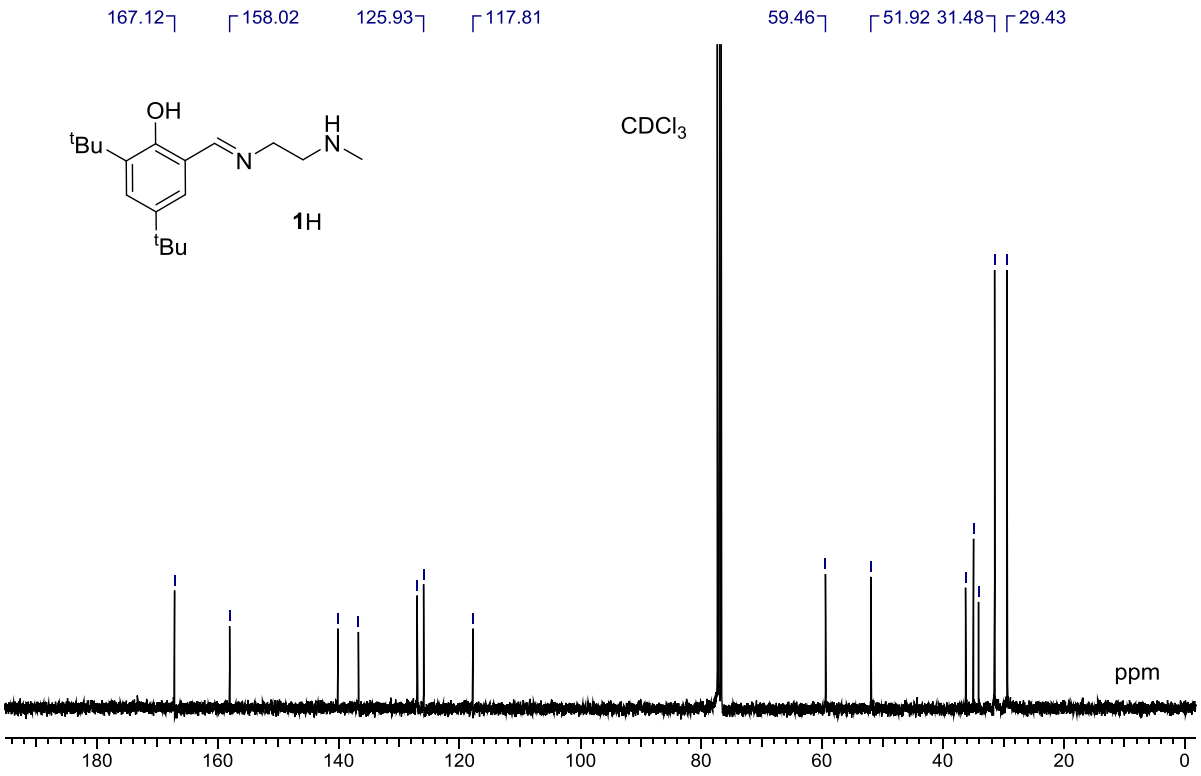

Figure SI2: $^{13}C\{^{1}H\}$ NMR spectra (100 MHz, $CDCl_3$) of **1**H.

2H (Salicylaldehyde + N-methylethylenediamine, orange oil)

^{1}H NMR ($CDCl_3$, 400 MHz) δ = 13.27 (s, 1H; OH), 8.39 (s, 1H; ArCHN), 7.31 (m, 1H; ArH), 7.25 (m, 1H; ArH), 6.96 (br d, *J* = 7.5 Hz, 1H; ArH), 6.88 (br t, *J* = 7.4 Hz, 1H; ArH), 3.74 (br s, 2H; CH_2), 2.92 (br s, 2H; CH_2). 2.47 (br,s, 4H; CH_3 /NH).$^{13}C\{^{1}H\}$ NMR ($CDCl_3$, 100 MHz) δ = 166.0 (ArCHN), 161.1, 132.3, 131.3, 120.0, 117.0 (Ar), 59.5, 51.8 (CH_2), 36.3 (CH_3). Broadness of spectra due to ligand cyclisation.

ESI-MS (MeOH): Calcd *m/z* $[C_{10}H_{15}N_2O]^+$ = 179.1179, found *m/z* = 179.1199.

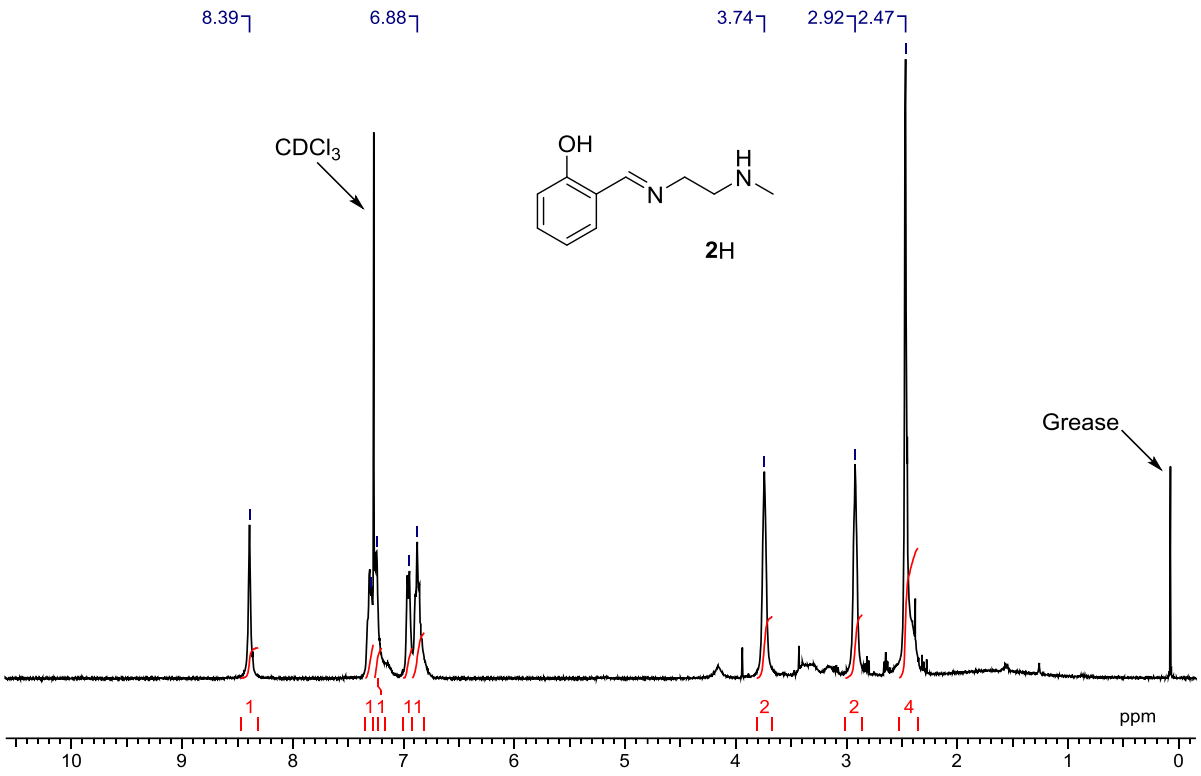

Figure SI3: ^{1}H NMR spectra (400 MHz, $CDCl_3$) of **2**H.

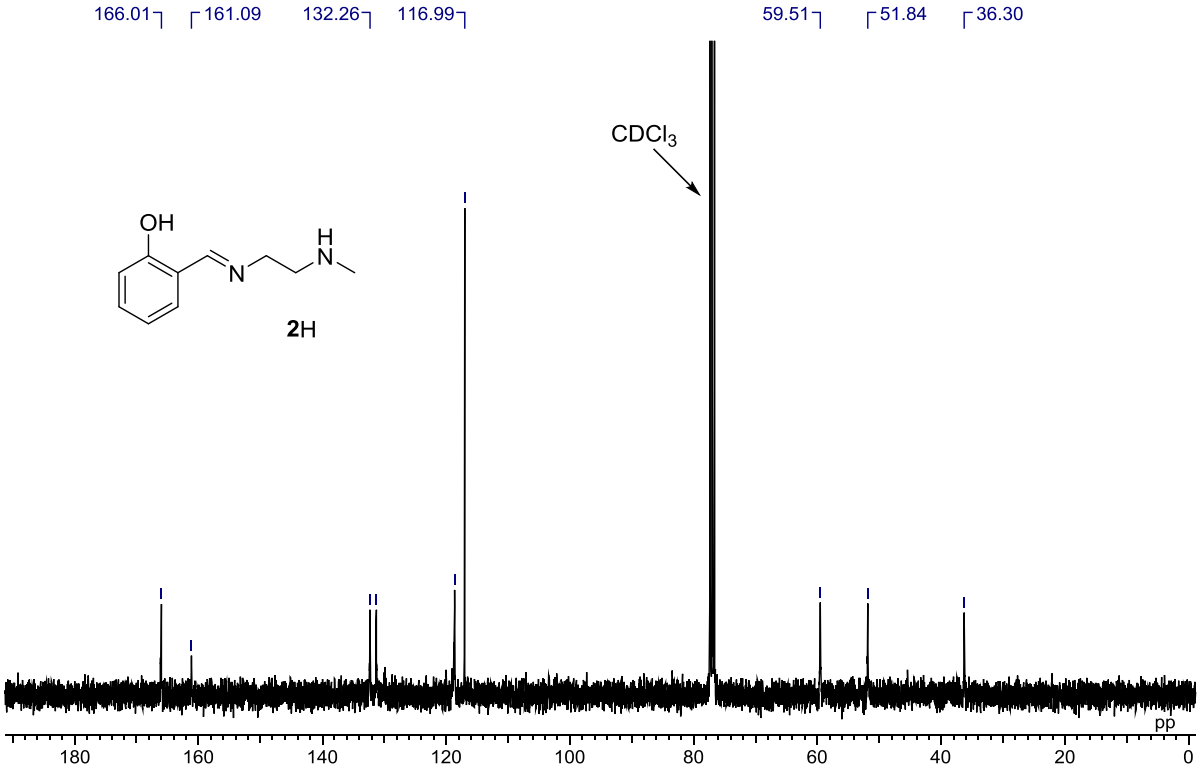

Figure SI4: $^{13}C\{^{1}H\}$ NMR spectra (100 MHz, $CDCl_3$) of **2**H.

3H (3,5-Dichlorosalicylaldehyde + N-methylethylenediamine, orange oil).

^{1}H NMR ($CDCl_3$, 400 MHz) δ = 7.35 (br s, 1H; ArH), 7.09 (br s, 1H; ArH), 3.49 (br s, 2H; CH_2), 2.96 (br s, 2H; CH_2). 2.44 (s, 3H; CH_3).^{13}C{^{1}H} NMR ($CDCl_3$, 100 MHz) δ = 128.5, 122.7 (Ar).

Notes: No OH and imine resonance observable in ^{1}H NMR spectra. Broadness of spectra due to ligand cyclisation.

ESI-MS (MeOH): Calcd *m/z* $[C_{10}H_{13}Cl_2N_2O]^+$ = 247.0399, found *m/z* = 247.0382.

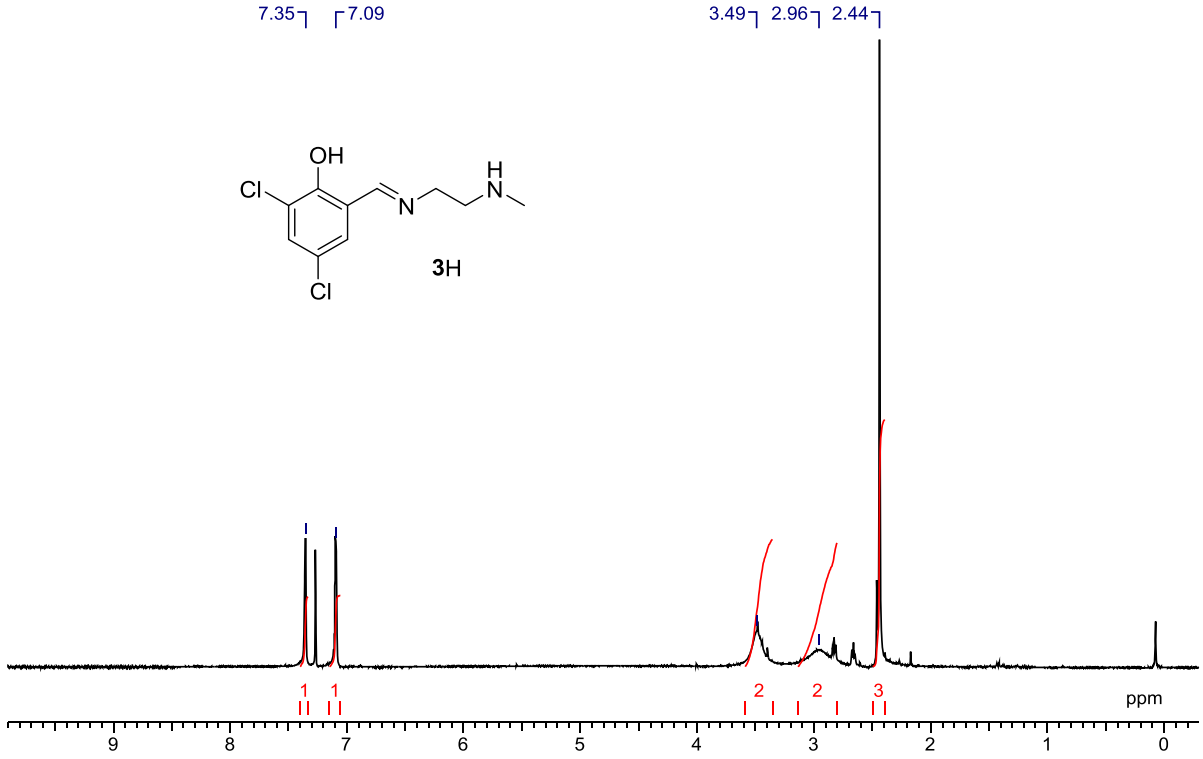

Figure SI5: ^{1}H NMR spectra (400 MHz, $CDCl_3$) of **3**H.

4H (3-adamantyl-2-hydroxy-5-*tert*-butylbenzylaldehyde[4] + N-methylethylenediamine, yellow oil).

^{1}H NMR ($CDCl_3$, 400 MHz) δ = 13.69 (s, 1H; OH), 8.40 (s, 1H; ArCHN), 7.33 (d, *J* = 2.5 Hz, 1H; ArH), 7.09 (d, *J* = 2.4 Hz, 1H; ArH), 3.73 (t, *J* = 5.8 Hz, 2H; CH_2), 2.92 (t, *J* = 5.8 Hz, 2H; CH_2). 2.48 (s, 3H; CH_3), 2.21 (m, 6H; $CH_{2,ad}$), 2.10 (m, 3H; CH_{ad}), 1.81 (m, 6H; $CH_{2,ad}$), 1.32 (s, 9H; $(CH_3)_3$). ^{13}C{^{1}H} NMR ($CDCl_3$, 100 MHz) δ = 167.2 (ArCHN), 158.2, 140.2, 136.9,

126.9, 125.8, 117.7 (Ar), 59.4, 51.8 (CH_2), 40.3 ($CH_{2,ad}$), 37.2 (C_{ad}), 37.1 ($CH_{2,ad}$), 36.2 (CH_3), 34.1 ($C(CH_3)_3$), 31.4, 29.1 ($C(CH_3)_3$).

ESI-MS (MeOH): Calcd *m/z* $[C_{24}H_{37}N_2O]^+$ = 369.2900, found *m/z* = 369.2933.

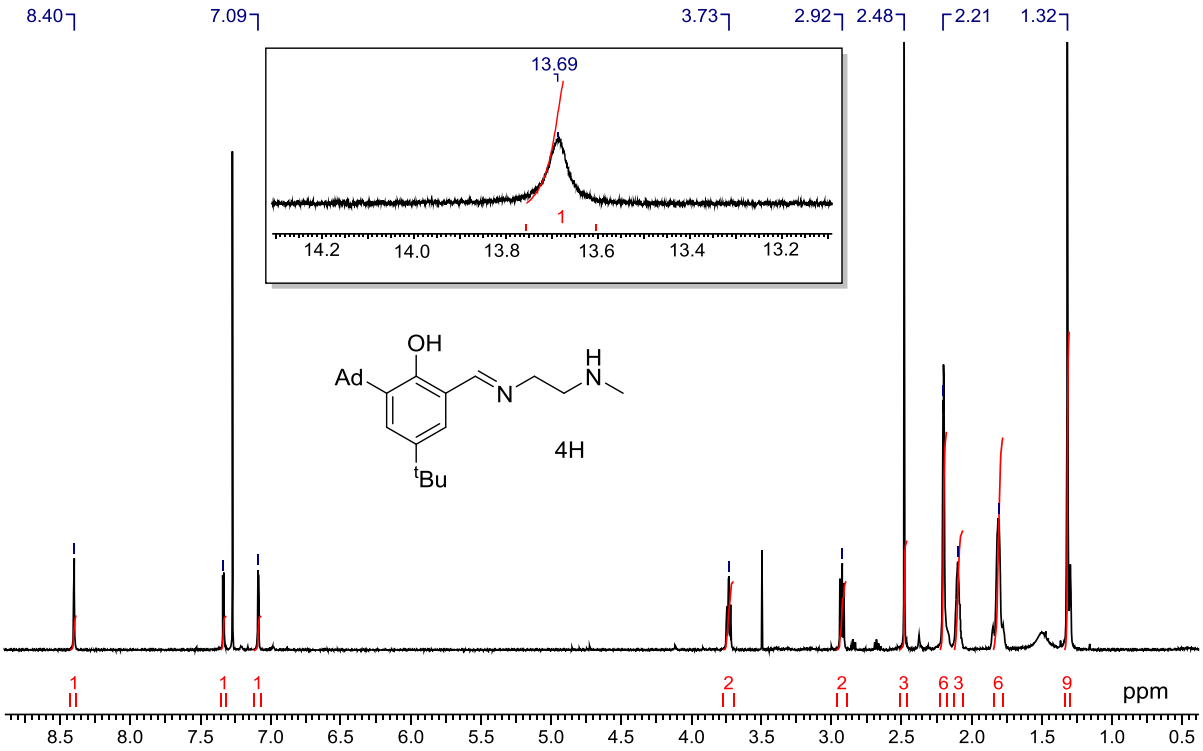

Figure SI6: ^{1}H NMR spectra (400 MHz, $CDCl_3$) of **4**H. Inset: OH resonance.

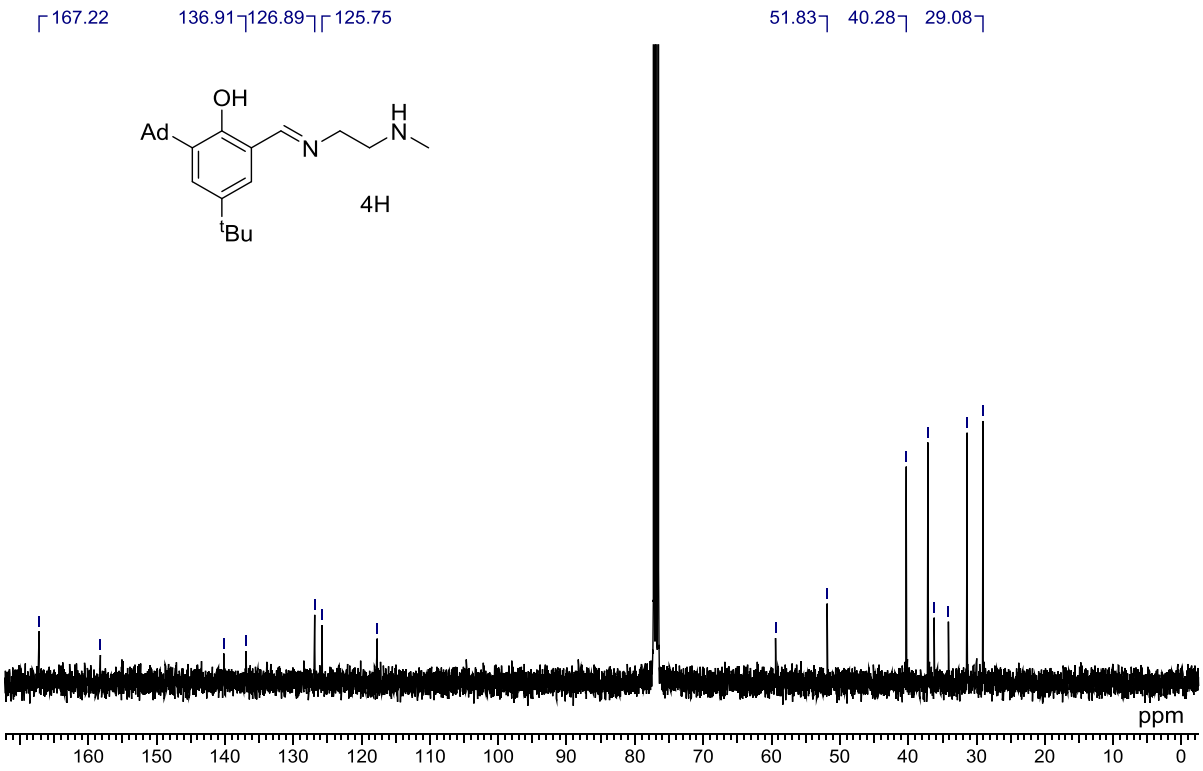

Figure SI7: $^{13}C\{^{1}H\}$ NMR spectra (100 MHz, $CDCl_3$) of **4**H.

5H (3,5-di-*tert*-butyl-2-hydroxybenzaldehyde + N,N-dimethylethylenediamine, yellow solid)

^{1}H NMR ($CDCl_3$, 400 MHz) δ = 13.77 (s, 1H; OH), 8.39 (s, 1H; ArCHN), 7.38 (d, *J* = 2.5 Hz, 1H; ArH), 7.09 (d, *J* = 2.4Hz, 1H; ArH), 3.71 (td, *J* = 7.0, 1.1 Hz, 2H; CH_2), 2.66 (t, *J* = 7.2 Hz, 2H; CH_2), 2.32 (s, 6H; 2 × CH_3) 1.45 (s, 9H; $(CH_3)_3$), 1.32 (s, 9H; $(CH_3)_3$).$^{13}C\{^{1}H\}$ NMR ($CDCl_3$, 100 MHz) δ = 166.6 (ArCHN), 158.1, 139.9, 136.7, 126.8, 125.8,117.9 (Ar), 60.1, 57.8 (CH_2), 45.8 (CH_3), 35.0, 34.1 ($C(CH_3)_3$), 31.5, 29.4 ($C(CH_3)_3$).

ESI-MS (MeOH): Calcd *m/z* $[C_{19}H_{33}N_2O]^+$ = 305.2593, found *m/z* = 305.2607.

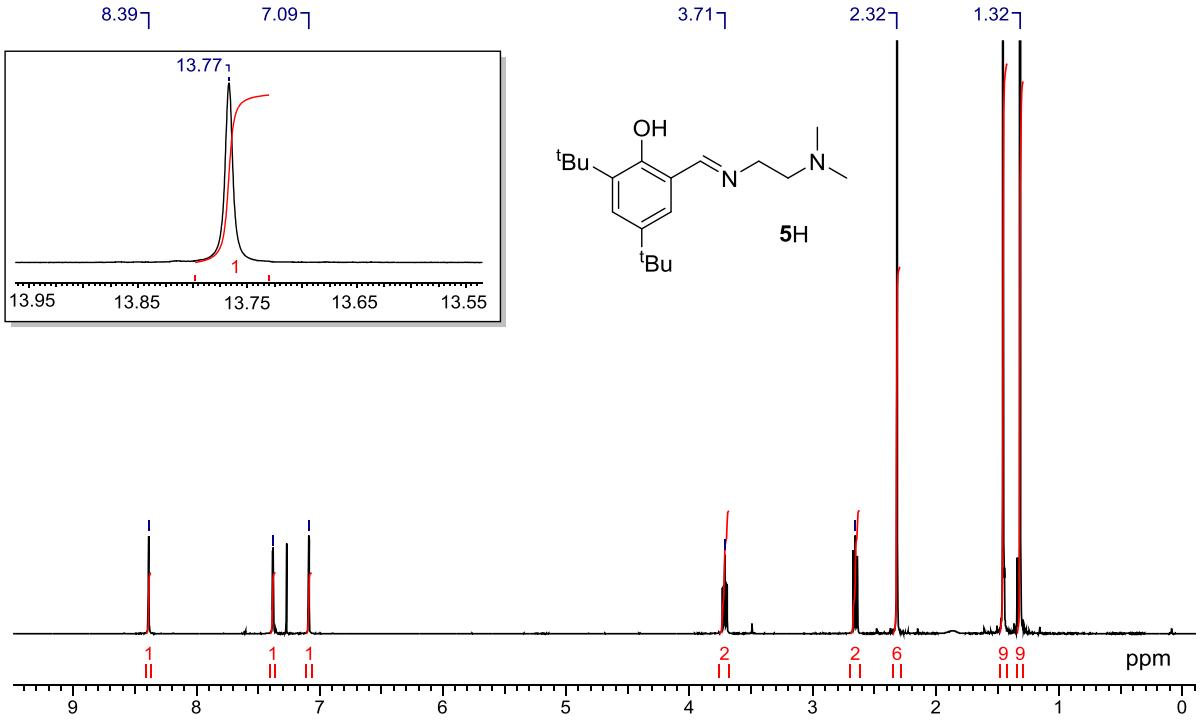

Figure SI8: ^{1}H NMR spectra (400 MHz, $CDCl_3$) of **5**H. Inset: OH resonance.

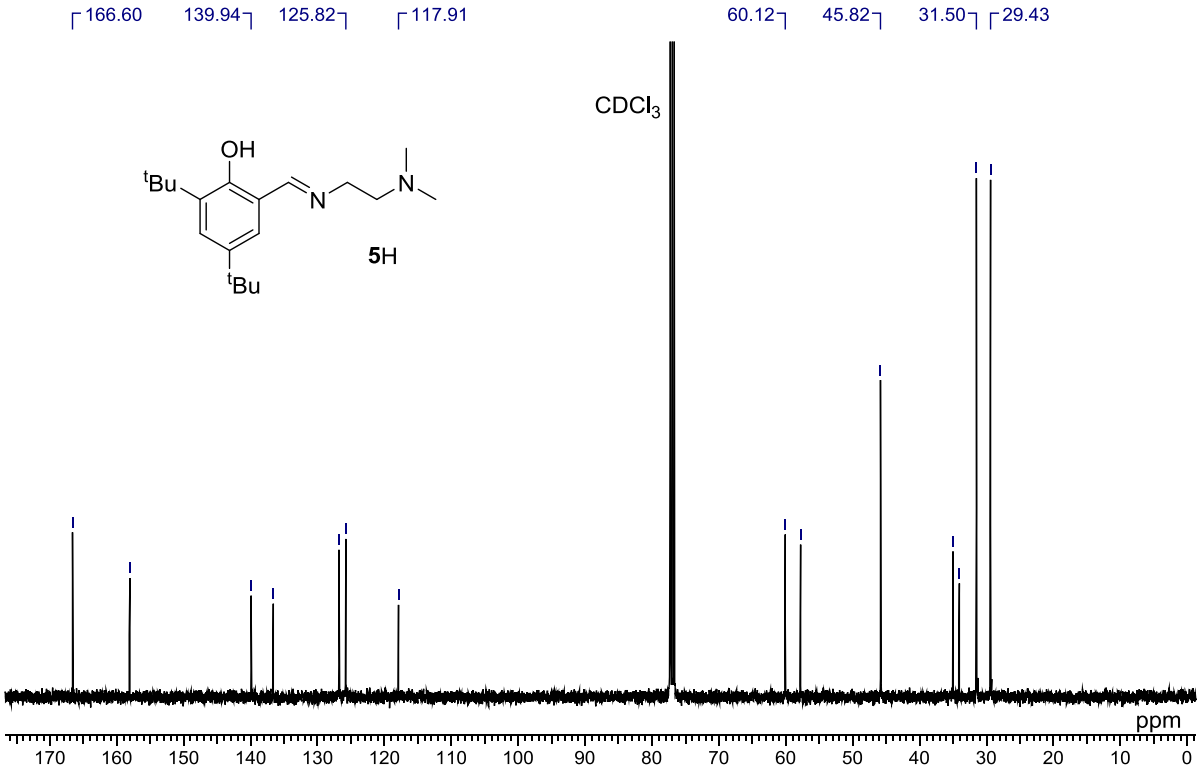

Figure SI9: ^{13}C{^{1}H} NMR spectra (100 MHz, $CDCl_3$) of **5**H.

6H (Salicylaldehyde + N,N-dimethylethylenediamine, orange oil).

^{1}H NMR ($CDCl_3$, 400 MHz) δ = 13.42 (s, 1H; OH), 8.37 (s, 1H; ArCHN), 7.30 (td, *J* = 7.3, 1.8 Hz, 1H; ArH), 7.25 (dd, *J* = 7.7, 1.6 Hz, 1H; ArH), 6.96 (d, *J* = 8.3 Hz, 1H; ArH), 6.87 (td, *J* = 7.5, 1.1 Hz, 1H; ArH), 3.72 (dt, *J* = 6.8, 1.2 Hz, 2H; CH_2), 2.65 (t, *J* = 6.7 Hz, 2H; CH_2). 2.31 (s, 6H; 2 × CH_3).^{13}C{^{1}H} NMR ($CDCl_3$, 100 MHz) δ = 165.5 (ArCHN), 161.2, 132.1, 131.2, 118.8, 118.4, 117.0 (Ar), 59.9, 57.8 (CH_2), 45.8 (CH_3).

ESI-MS (MeOH): Calcd *m/z* $[C_{11}H_{16}N_2ONa]^+$ = 215.1155, found *m/z* = 215.1145.

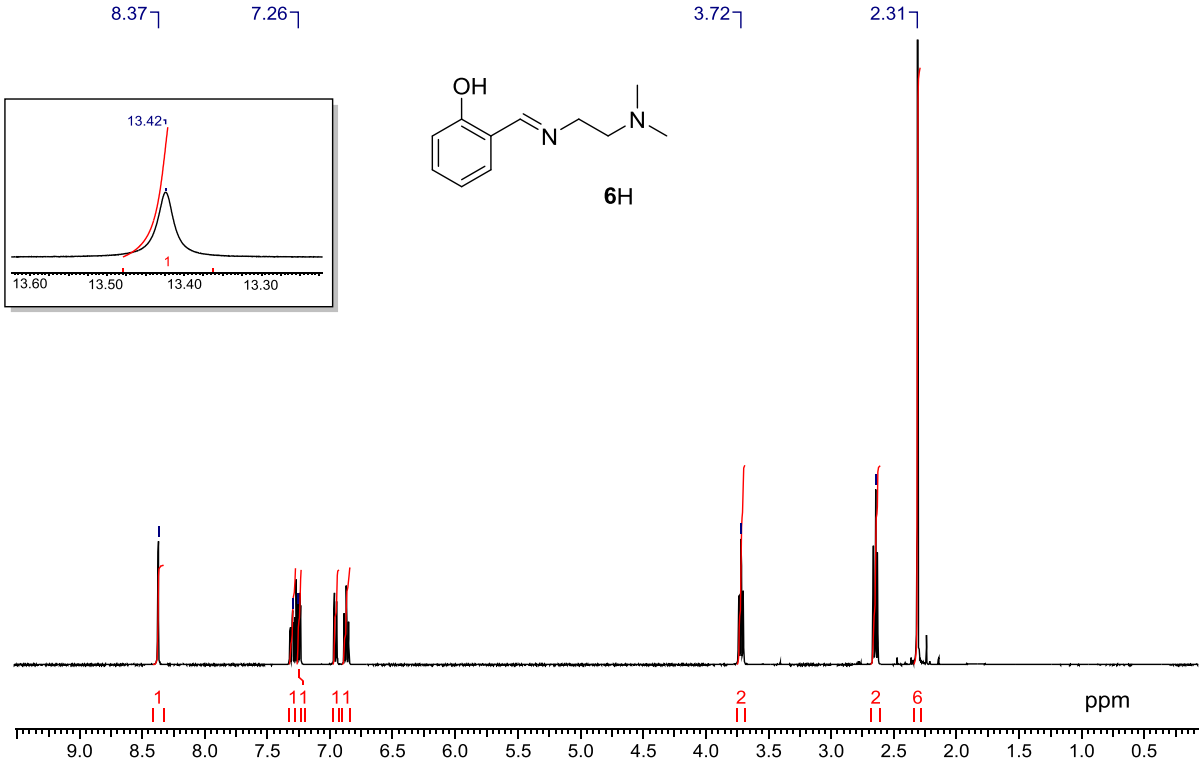

Figure SI10: ^{1}H NMR spectra (400 MHz, $CDCl_3$) of **6**H. Inset: OH resonance.

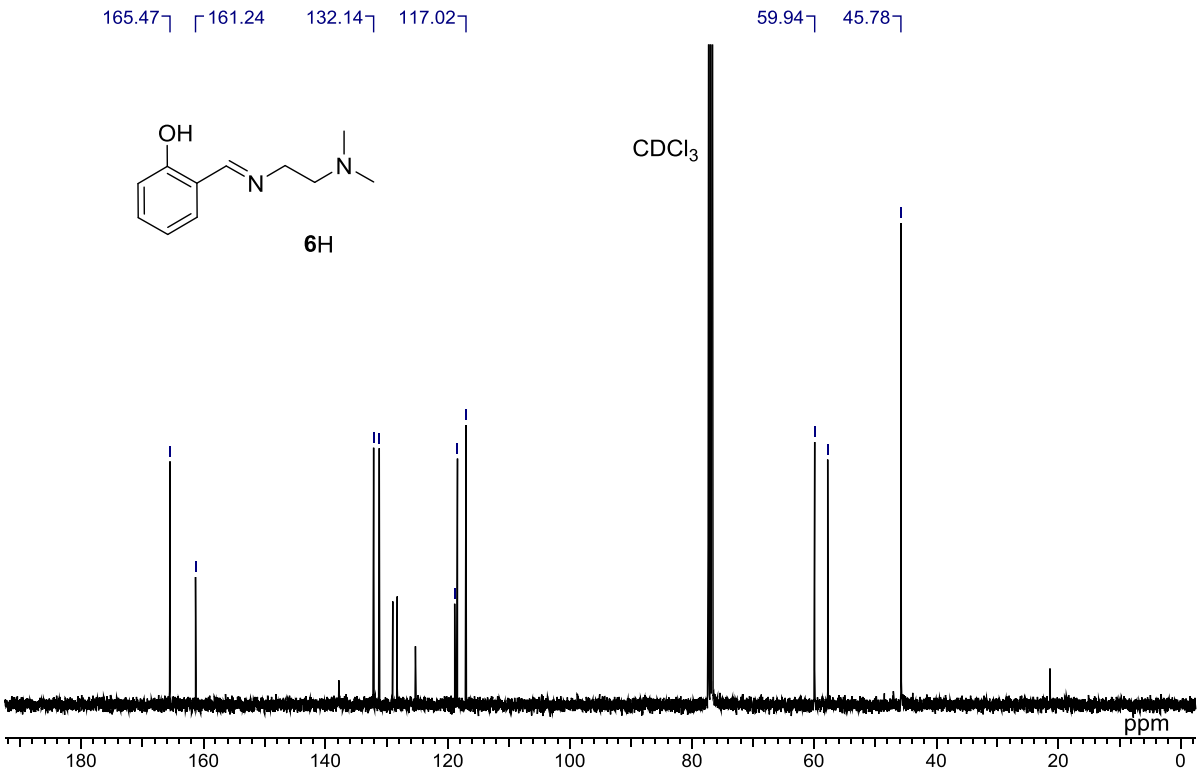

Figure SI11: $^{13}C\{^{1}H\}$ NMR spectra (100 MHz, $CDCl_3$) of **6**H.

7H (3,5-Dichlorosalicylaldehyde + N,N-dimethylethylenediamine, orange oil).

^{1}H NMR ($CDCl_3$, 400 MHz) δ = 14.55 (s, 1H; OH), 8.25 (s, 1H; ArCHN), 7.40 (d, *J* = 2.5 Hz, 1H; ArH), 7.15 (d, *J* = 2.6 Hz, 1H; ArH), 3.73 (dt, *J* = 6.4, 1.1 Hz, 2H; CH_2), 2.64 (t, *J* = 6.4 Hz, 2H; CH_2). 2.29 (s, 6H; 2 × CH_3).$^{13}C\{^{1}H\}$ NMR ($CDCl_3$, 100 MHz) δ = 164.0 (ArCHN), 158.3, 132.4, 129.0, 123.5, 121.8, 119.0 (Ar), 59.4, 55.9 (CH_2), 45.7 (CH_3).
ESI-MS (MeOH): Calcd *m/z* $[C_{11}H_{15}Cl_2N_2O]^+$ = 261.0562, found *m/z* = 261.0541.

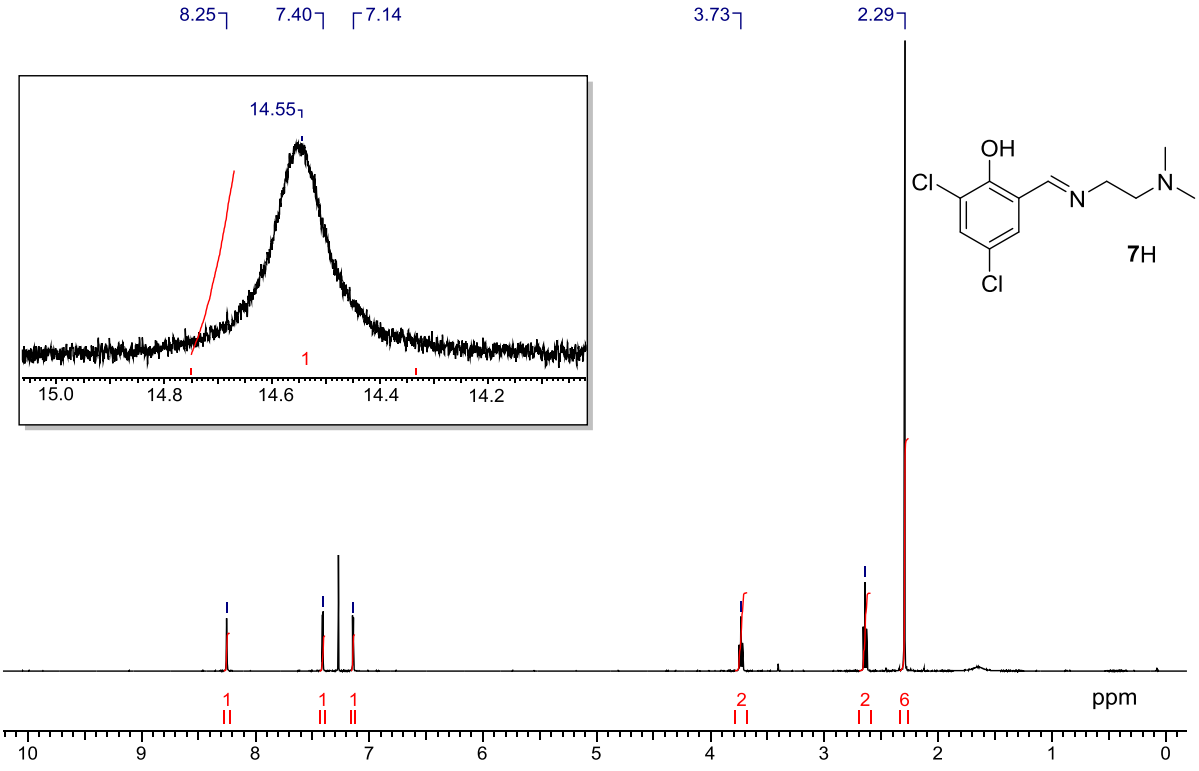

Figure SI12: ^{1}H NMR spectra (400 MHz, $CDCl_3$) of **7**H. Inset: OH resonance.

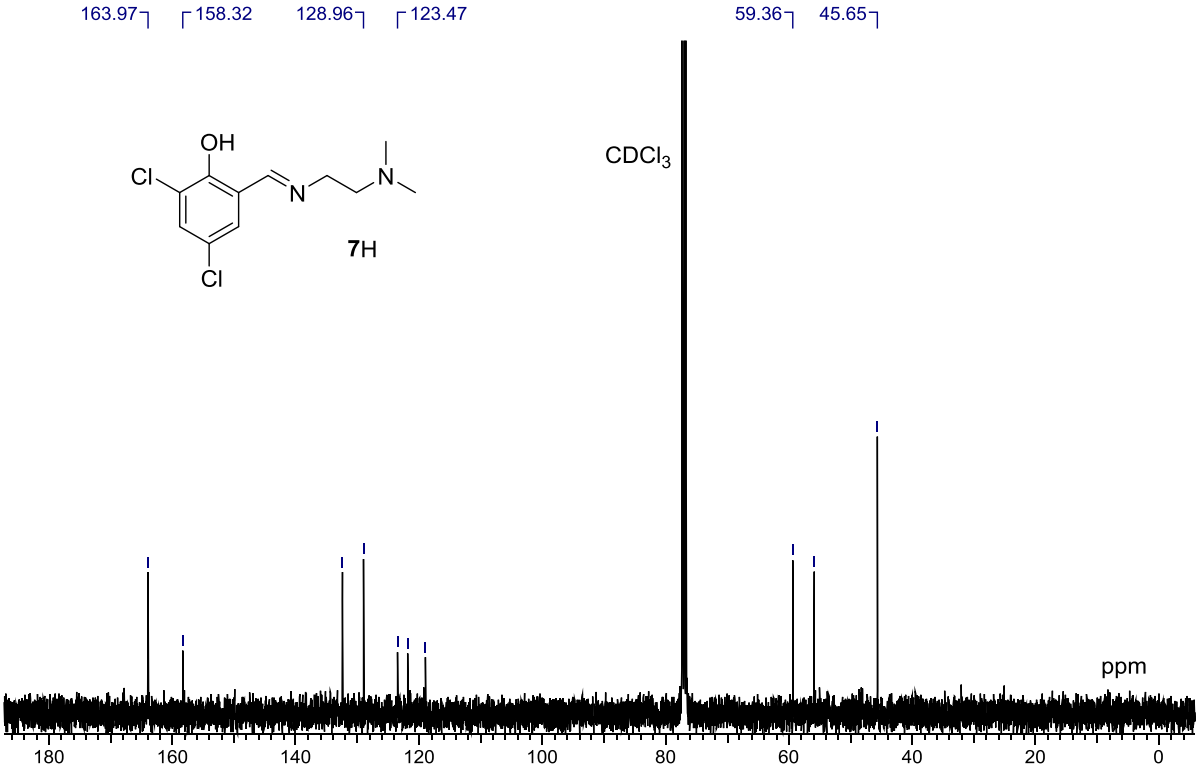

Figure SI13: ^{13}C{^{1}H} NMR spectra (100 MHz, $CDCl_3$) of **7**H.

Zn(II) complexes

Synthesis of imino monophenolate zinc complexes, Zn(1-7)$_2$: $Zn(Et)_2$ (1M, 1 ml, 1 mmol) was added to a solution of ligand (2 mmol) in toluene (10 ml). After complete addition, the solution was stirred for 1 hour before solvent removal. The desired complex was purified *via* washing or recrystallisation from hexane.

Zn(1)$_2$: Recrystallised from hexane. Isolated as pale yellow crystals (0.40 g, 0.62 mmol, 62%). ^{1}H NMR (C_6D_6, 400 MHz) δ = 7.88 (s, 1H; ArCHN), 7.57 (d, *J* = 2.5 Hz, 1H; ArH), 6.96 (d, *J* = 2.5 Hz, 1H; ArH), 3.26 (m, 1H; CH_2), 2.91 (m, 1H; CH_2), 2.59 (m, 1H; CH_2), 2.15 (m, 1H; CH_2), 1.81 (d, *J* = 6.2 Hz, 3H; CH_3), 1.61 (s, 9H; $C(CH_3)_3$), 1.41 (s, 9H; $C(CH_3)_3$), 0.93 (m, 1H; NH). ^{13}C{^{1}H} NMR (C_6D_6, 100 MHz) δ = 171.1 (ArCHN), 169.9, 144.8, 132.8, 129.6, 118.5 (Ar), 58.0, 51.7 (CH_2), 36.3 (CH_3), 36.2, 34.4 ($C(CH_3)_3$), 32.4, 30.2 ($C(CH_3)_3$).
Elemental analysis ($C_{36}H_{58}ZnN_4O_2$) Calcd in %: C, 67.11; H, 9.07; N, 8.70. Found: C, 66.94; H, 8.91; N, 8.64.
Note: Complexation scaled up to 54 mmol in reduced solvent volume (toluene, 50 ml). Solution was cooled with an ice batch during $Zn(Et)_2$ addition. Solvent was removed and product washed with hexane (2 x 50 ml). Isolated as yellow powder (25.0 g, 39 mmol, 72 %).

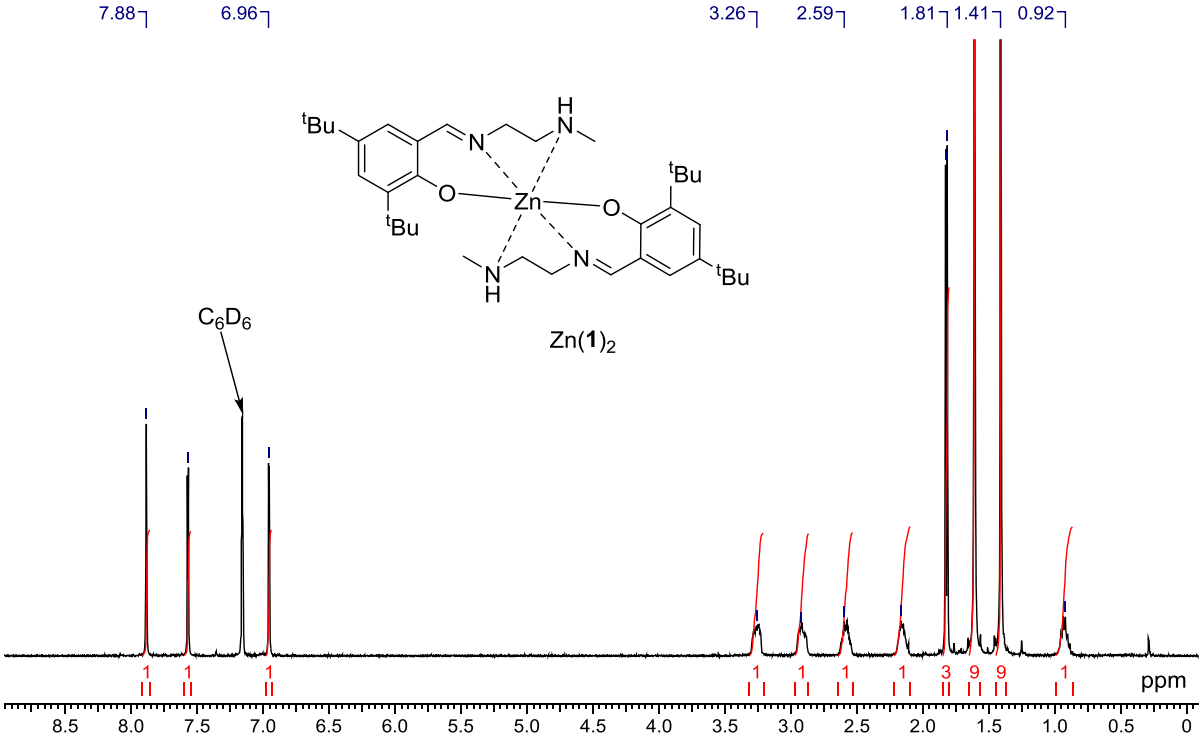

Figure SI14: ^{1}H NMR spectra (400 MHz, C_6D_6) of Zn(**1**)$_2$.

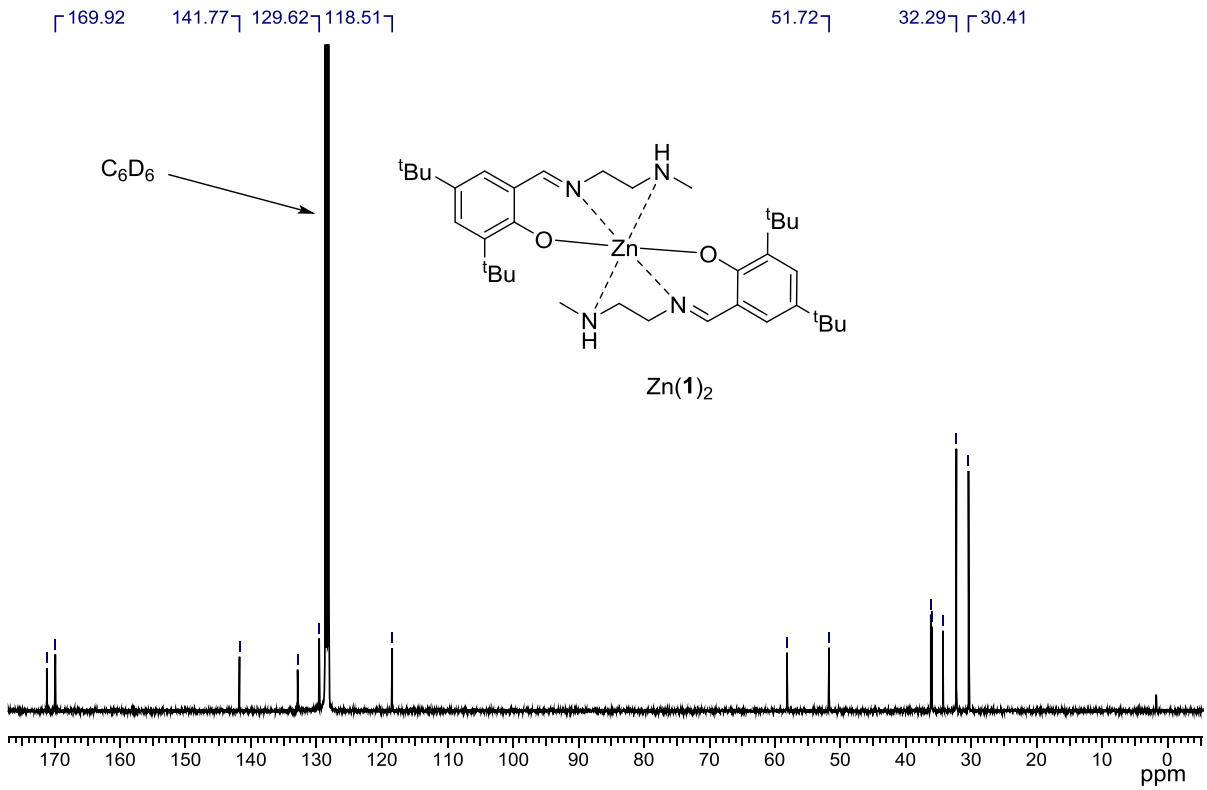

Figure SI15: $^{13}C\{^{1}H\}$ NMR spectra (100 MHz, C_6D_6) of Zn(**1**)$_2$.

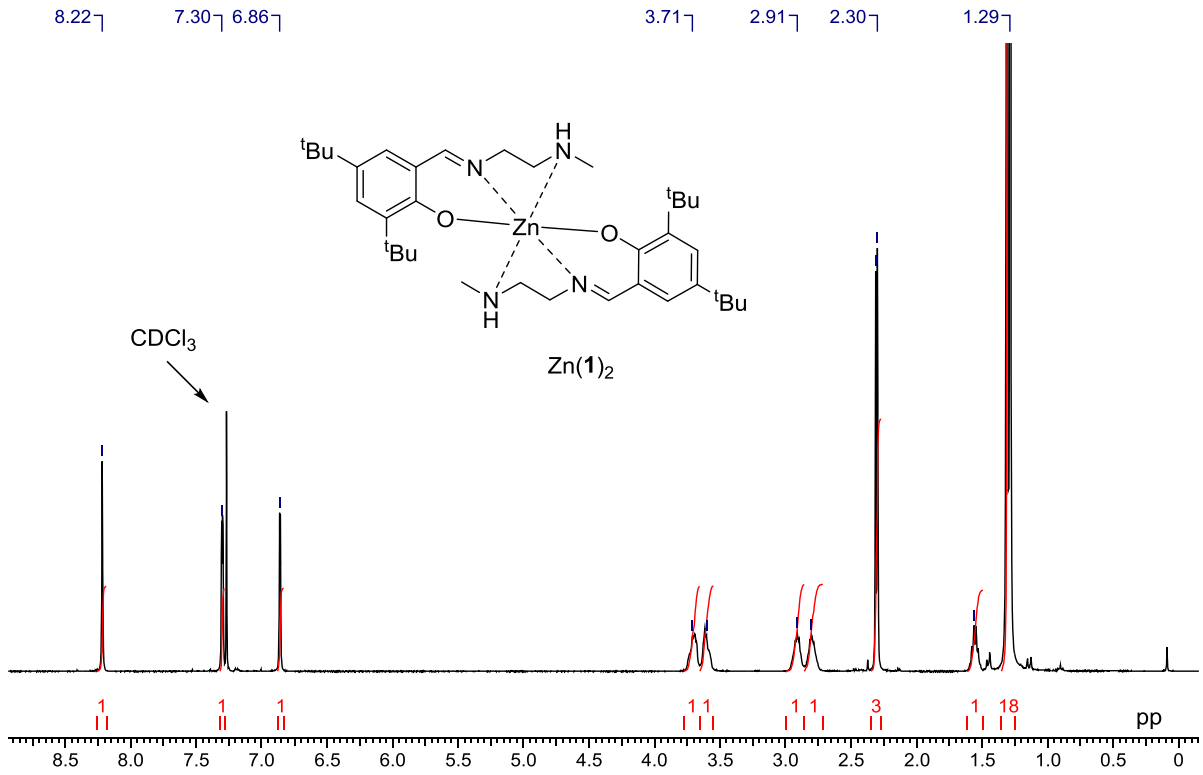

Figure SI16: ^{1}H NMR spectra (400 MHz, $CDCl_3$) of Zn(**1**)$_2$.

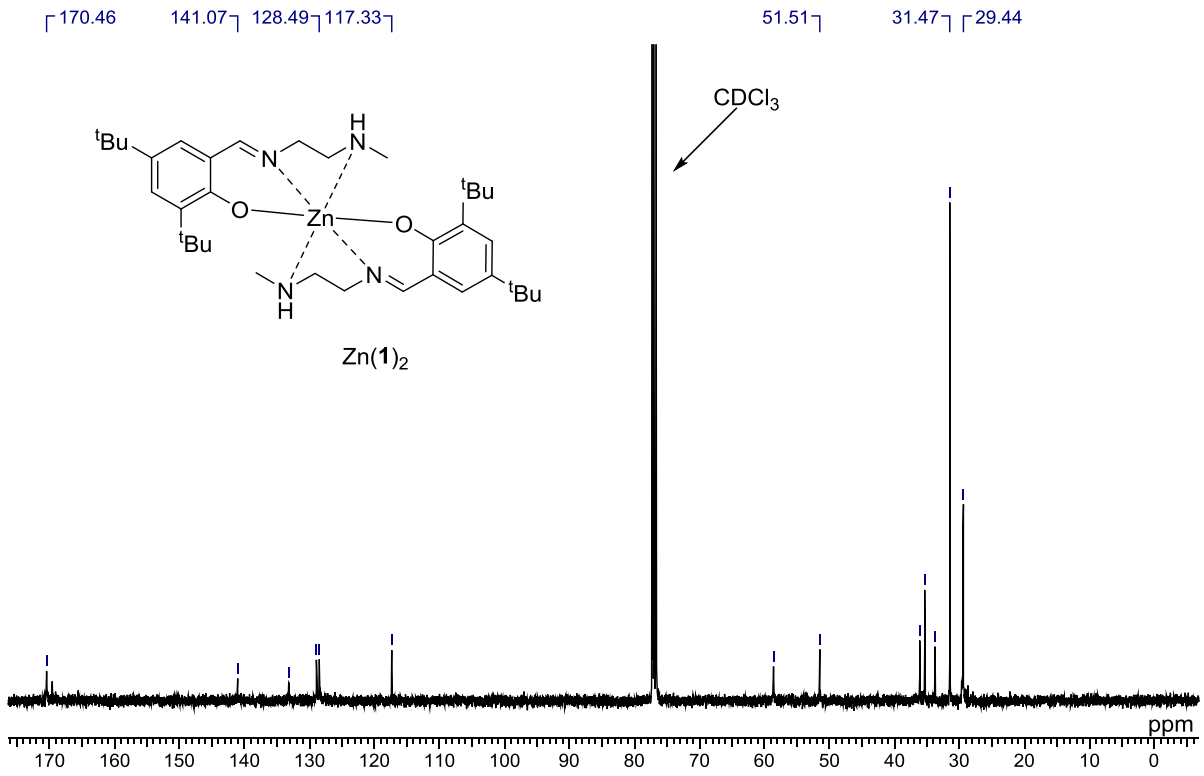

Figure SI17: $^{13}C\{^{1}H\}$ NMR spectra (100 MHz, $CDCl_3$) of Zn(**1**)$_2$.

Zn(2)$_2$: Recrystallised from hexane. Isolated as pale yellow crystals (0.20 g, 0.47 mmol, 47%). ^{1}H NMR ($CDCl_3$, 400 MHz) δ = 8.19 (s, 1H; ArCHN), 7.15 (m, 1H; ArH), 7.02 (dd, *J* = 7.8, 1.5 Hz, 1H; ArH), 6.75 (d, *J* = 8.5 Hz, 1H; ArH), 6.42 (d, *J* = 7.4 Hz, 1H; ArH), 3.69 (br s, 2H; CH_2), 2.83 (br s, 2H; CH_2), 2.24 (d, *J* = 6.4 Hz, 3H; CH_3), 0.93 (hept, *J* = 6.5 Hz, 1H; NH). $^{13}C\{^{1}H\}$ NMR ($CDCl_3$, 100 MHz) δ = 172.0 (Ar), 168.8 (ArCHN), 135.1, 133.5, 123.6, 119.0, 112.2 (Ar), 57.7, 51.2 (CH_2), 36.2 (CH_3).

Elemental analysis ($C_{20}H_{26}ZnN_4O_2$) Calc %, C 57.22, H 6.24, N 13.35; found %, C 57.31, H 6.33, N 13.16.

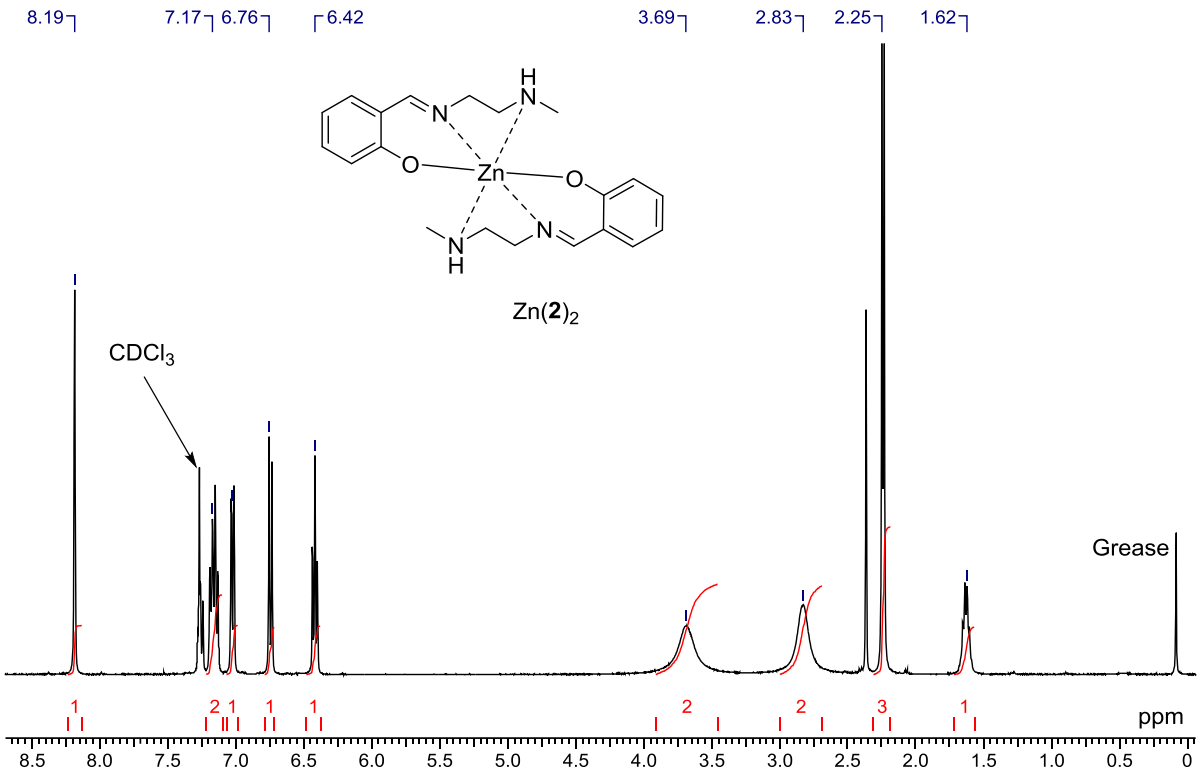

Figure SI18: ^{1}H NMR spectra (400 MHz, $CDCl_3$) of Zn(**2**)$_2$.

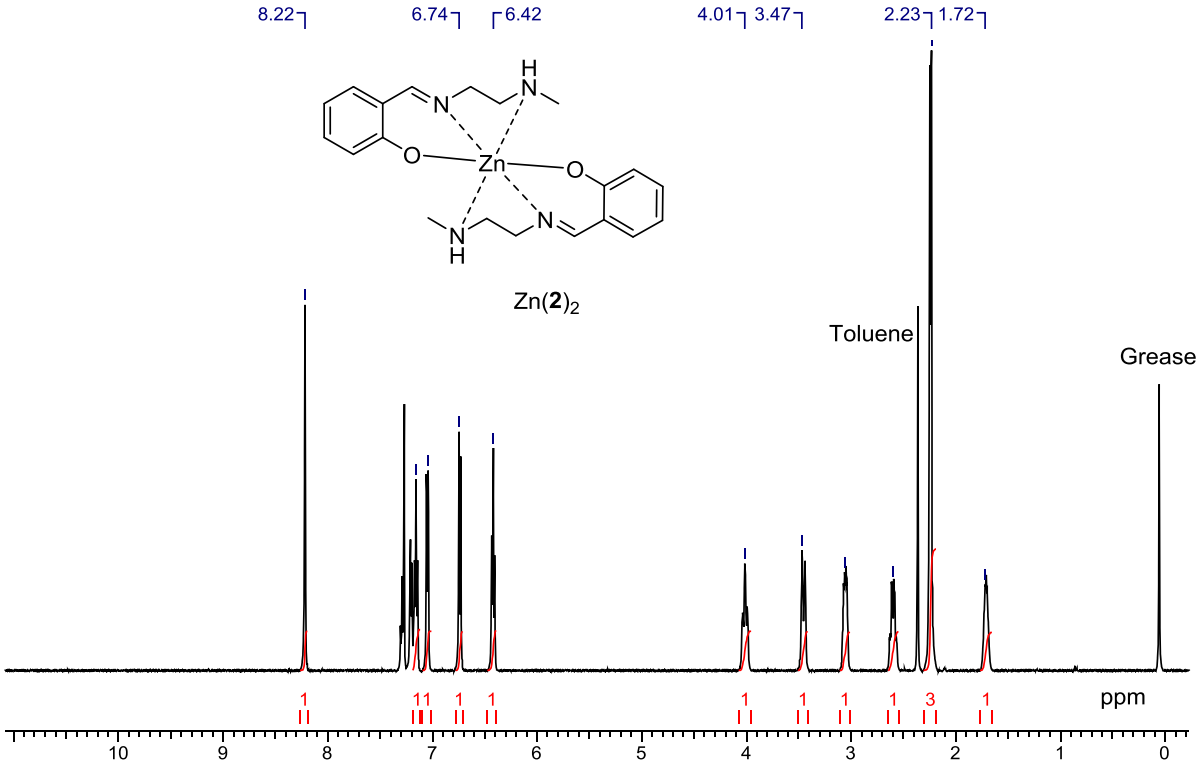

Figure SI19: ^{1}H NMR spectra (400 MHz, 233 K, $CDCl_3$) of Zn(**2**)$_2$.

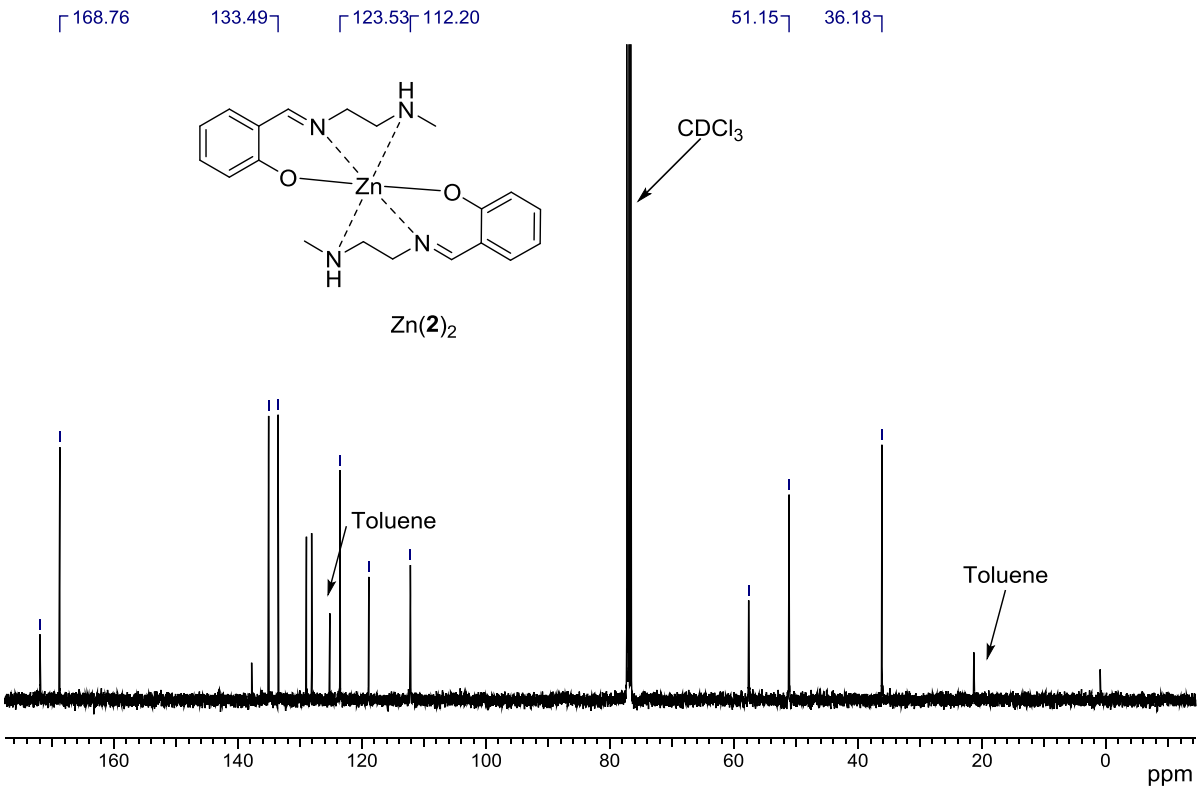

Figure SI20: $^{13}C\{^{1}H\}$ NMR spectra (100 MHz, $CDCl_3$) of Zn(**2**)$_2$.

Zn(3)$_2$: Recrystallised from hexane/toluene mixture. Isolated as pale yellow crystals (0.34 g, 0.61 mmol, 61%).

^{1}H NMR ($CDCl_3$, 400 MHz) δ = 8.16 (s, 1H; ArCHN), 7.30 (br s, 1H; ArH), 6.95 (br s, 1H; ArH), 3.82 (br s, 2H; CH_2), 2.91 (br s, 2H; CH_2), 2.27 (s, 3H; CH_3), 1.73 (br s, 1H; NH). Note: Due to low solubility, $^{13}C\{^{1}H\}$ NMR was not recorded.

Elemental analysis ($C_{20}H_{22}Cl_4ZnN_4O_2$) : Calc %, C 43.08, H 3.98, N 10.05; found %, C 43.23, H 4.21, N 9.86.

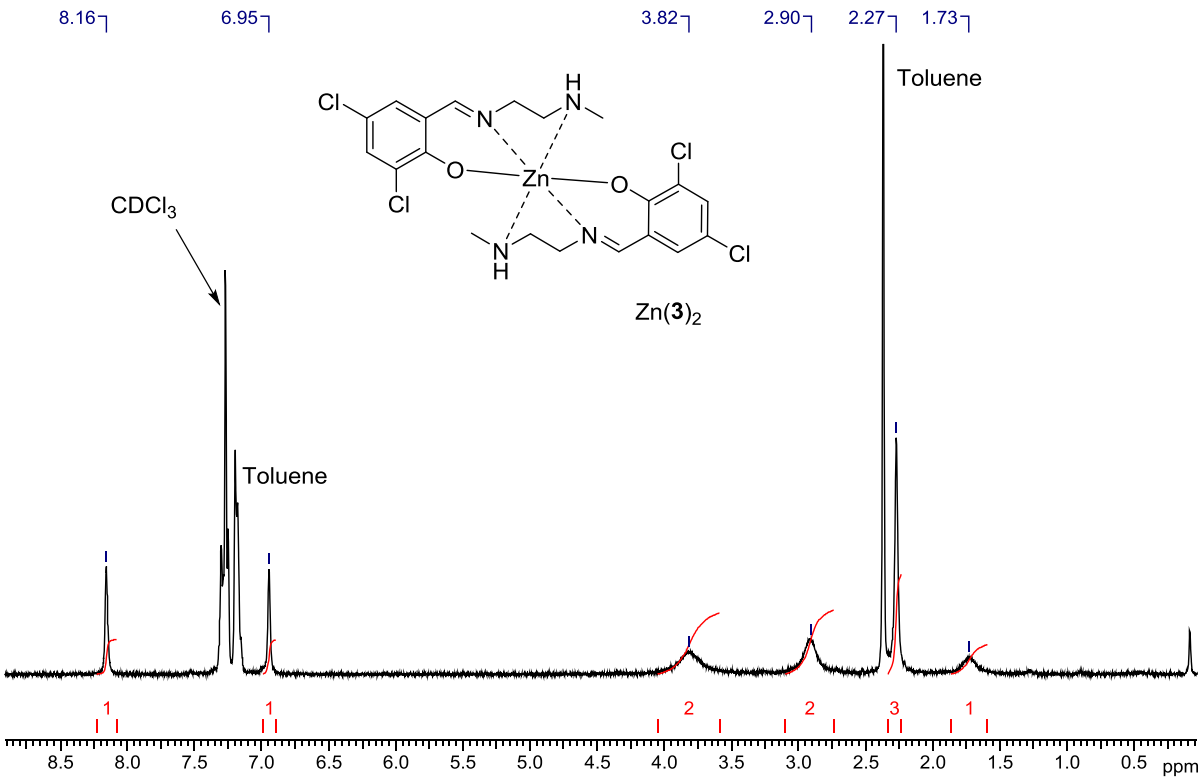

Figure SI21: ^{1}H NMR spectra (400 MHz, $CDCl_3$) of Zn(**3**)$_2$.

Zn(4)$_2$: Recrystallised from mixture of hexane/toluene. Isolated as pale yellow crystals (0.33 g, 0.41 mmol, 41%).

^{1}H NMR (C_6D_6, 400 MHz) δ = 8.01 (s, 1H; ArCHN), 7.47 (d, *J* = 2.5 Hz, 1H; ArH), 6.96 (d, *J* = 2.5 Hz, 1H; ArH), 3.08 (br t, *J* = 4.6 Hz, 2H; CH_2), 2.76 (m, 1H; CH_2), 2.29 (br s, 6H; CH_{2ad}), 2.20 (m, 1H; CH_2), 2.06 (br s, 3H; CH_{ad}), 1.87 (d, *J* = 6.2 Hz, 3H; CH_3), 1.84 (br s, 6H; CH_{2ad}), 1.44 (s, 9H; $C(CH_3)_3$), 0.83 (m, 1H; NH). ^{13}C{^{1}H} NMR (C_6D_6, 100 MHz) δ = 171.7 (Ar), 169.8 (ArCHN), 141.8, 132.6, 129.2, 128.3, 119.0 (Ar), 58.2, 51.7, 40.9, 38.6 (CH_2), 38.4 (CH_3), 36.0 (C_{ad}), 34.4 ($C(CH_3)_3$), 32.3 ($C(CH_3)_3$), 30.4 (CH) .

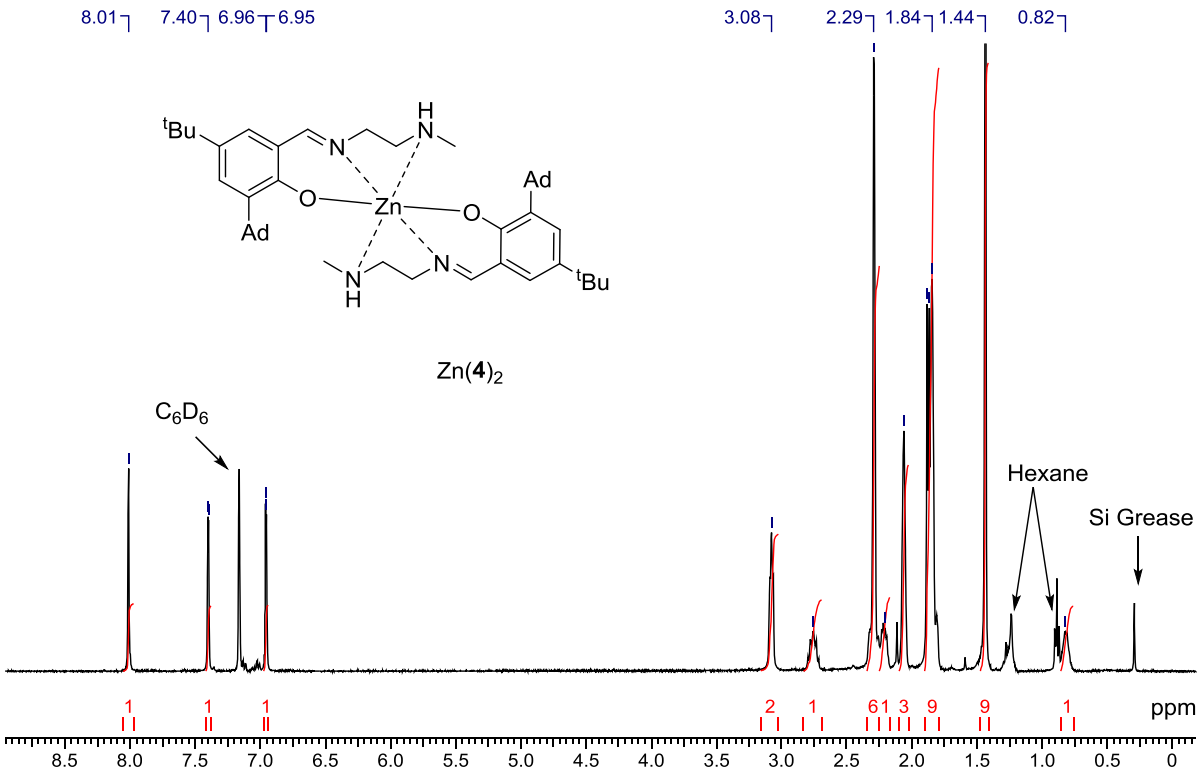

Figure SI22: ^{1}H NMR spectra (400 MHz, C_6D_6) of Zn(**4**)$_2$.

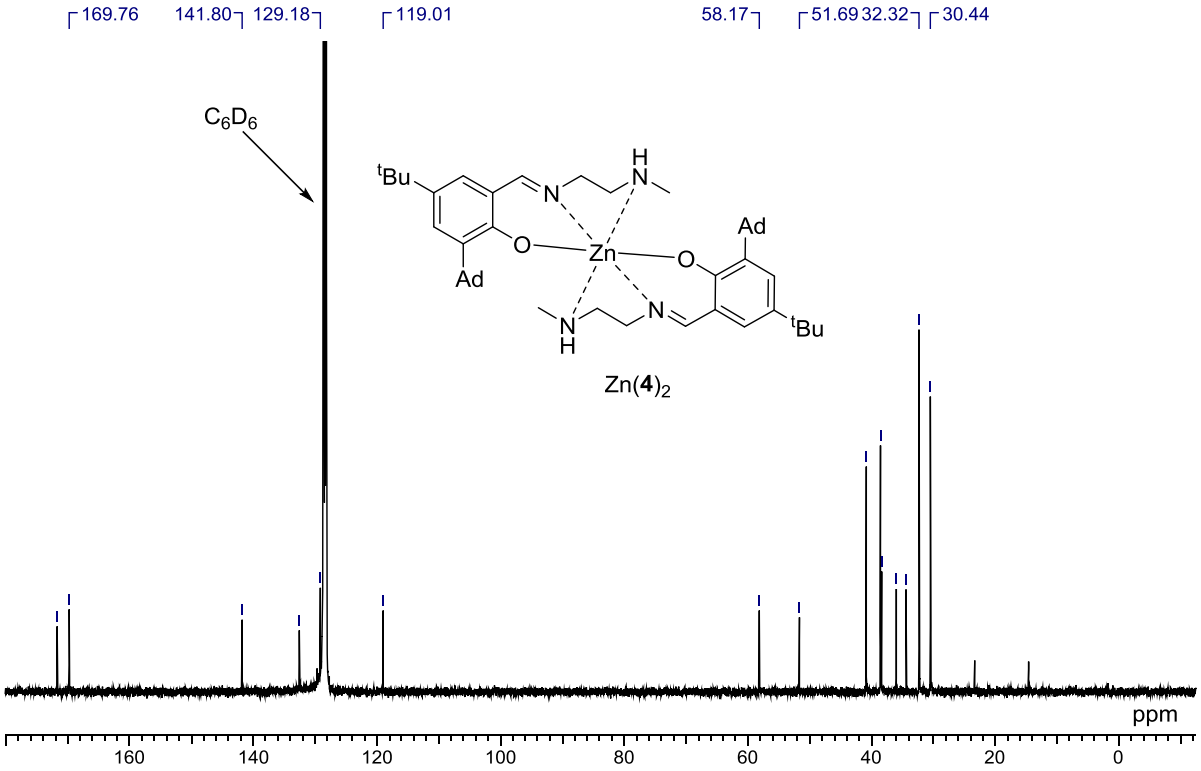

Figure SI23: $^{13}C\{^{1}H\}$ NMR spectra (100 MHz, C_6D_6) of Zn(**4**)$_2$.

Zn(5)$_2$: Recrystallised from hexane. Isolated as yellow crystals (0.33 g, 0.49 mmol, 49%). ^{1}H NMR (C_6D_6, 400 MHz) δ = 7.80 (s, 1H; ArCHN), 7.64 (d, *J* = 2.6 Hz, 1H; ArH), 6.91 (d, *J* = 2.5 Hz, 1H; ArH), 3.14 (2, *J* = 6.3 Hz, 1H; CH_2), 2.37 (sept, *J* = 6.4 Hz, 1H; CH_2), 2.11 (sept, *J* = 6.3 Hz, 1H; CH_2), 1.88 (s, 6H; 2 × CH_3), 1.70 (s, 9H; $C(CH_3)_3$), 1.39 (s, 9H; $C(CH_3)_3$). ^{13}C{^{1}H} NMR (C_6D_6, 100 MHz) δ = 172.0 (Ar), 170.7 (ArCHN), 142.2, 134.2, 129.9, 129.6, 118.2 (Ar), 56.0, 57.7 (CH_2), 45.9 (CH_3), 36.3, 34.4 ($C(CH_3)_3$), 32.2, 30.5 ($C(CH_3)_3$). Elemental analysis ($C_{38}H_{62}ZnN_4O_2$) Calcd in %: C, 67.89; H, 9.30; N, 8.33. Found: C, 67.98; H, 9.20; N, 8.33.

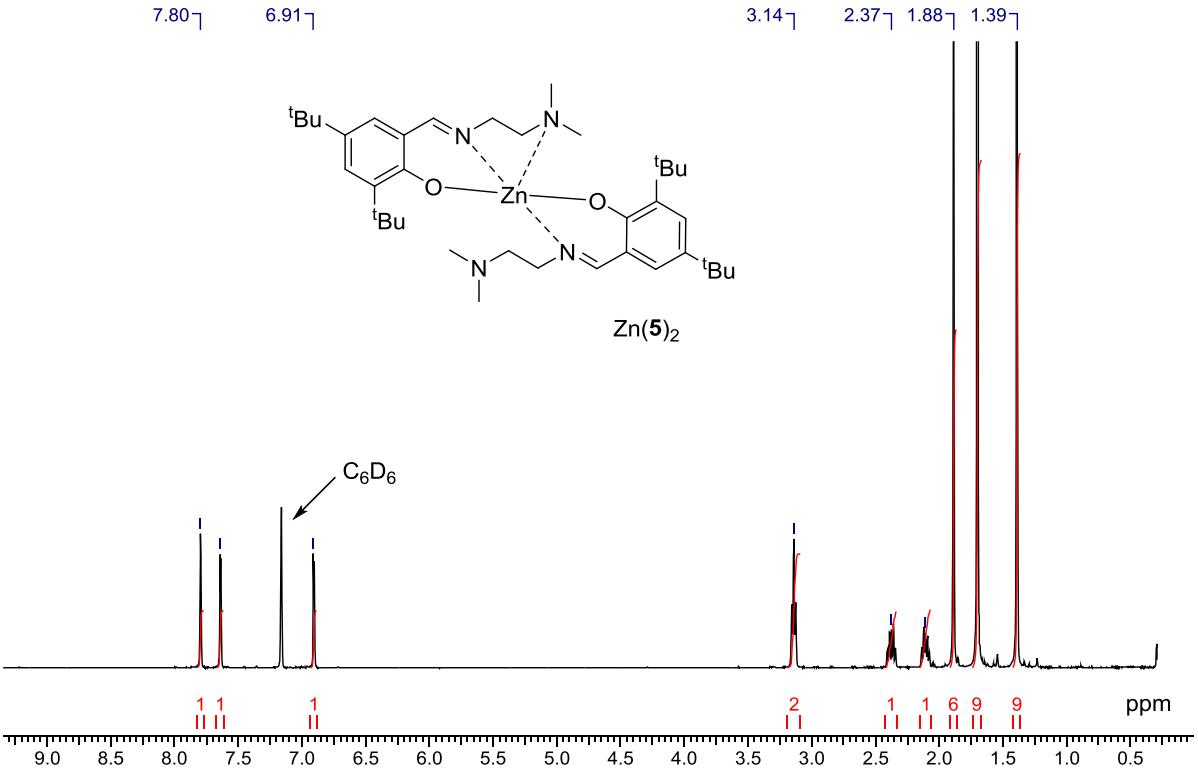

Figure SI24: ^{1}H NMR spectra (400 MHz, C_6D_6) of Zn(**5**)$_2$.

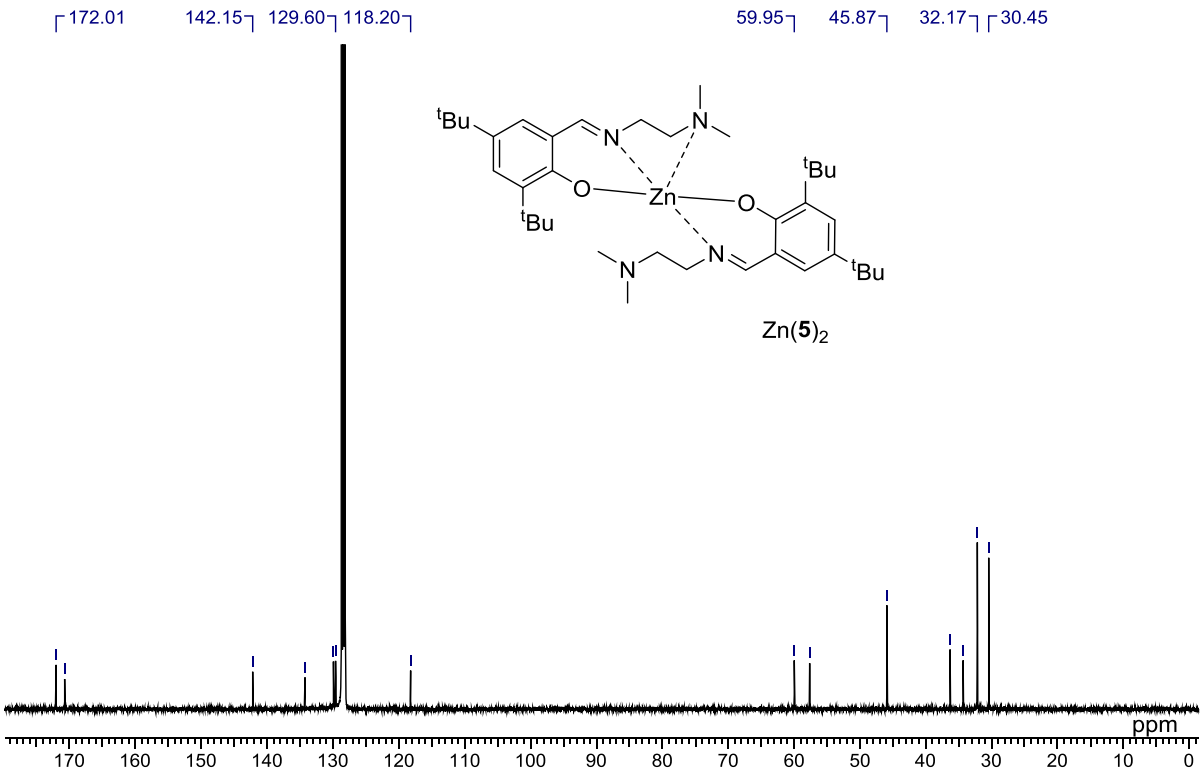

Figure SI25: $^{13}C\{^{1}H\}$ NMR spectra (100 MHz, C_6D_6) of Zn(**5**)$_2$.

Zn(6)$_2$: Washed with hexane. Isolated as pale yellow powder (0.23 g, 0.51 mmol, 51%). ^{1}H NMR ($CDCl_3$, 400 MHz) δ = 8.19 (s, 1H; ArCHN), 7.21 (m, 1H; ArH), 7.05 (dd, *J* = 7.8, 1.5 Hz, 1H; ArH), 6.81 (d, *J* = 8.5 Hz, 1H; ArH), 6.48 (t, *J* = 7.3 Hz, 1H; ArH), 3.69 (br t, *J* = 6.2 Hz, 2H; CH_2), 2.54 (m, 2H; CH_2), 2.09 (s, 6H; 2 × CH_3).$^{13}C\{^{1}H\}$ NMR ($CDCl_3$, 100 MHz) δ = 171.7 (Ar), 170.8 (ArCHN), 135.2, 134.3, 123.6, 118.5, 113.1 (Ar), 59.4, 57.2 (CH_2), 45.6 (CH_3).

Elemental analysis ($C_{22}H_{30}ZnN_4O_2$) Calc %, C 59.00, H 6.75, N 12.51; found %, C 58.96, H 6.79, N 12.38.

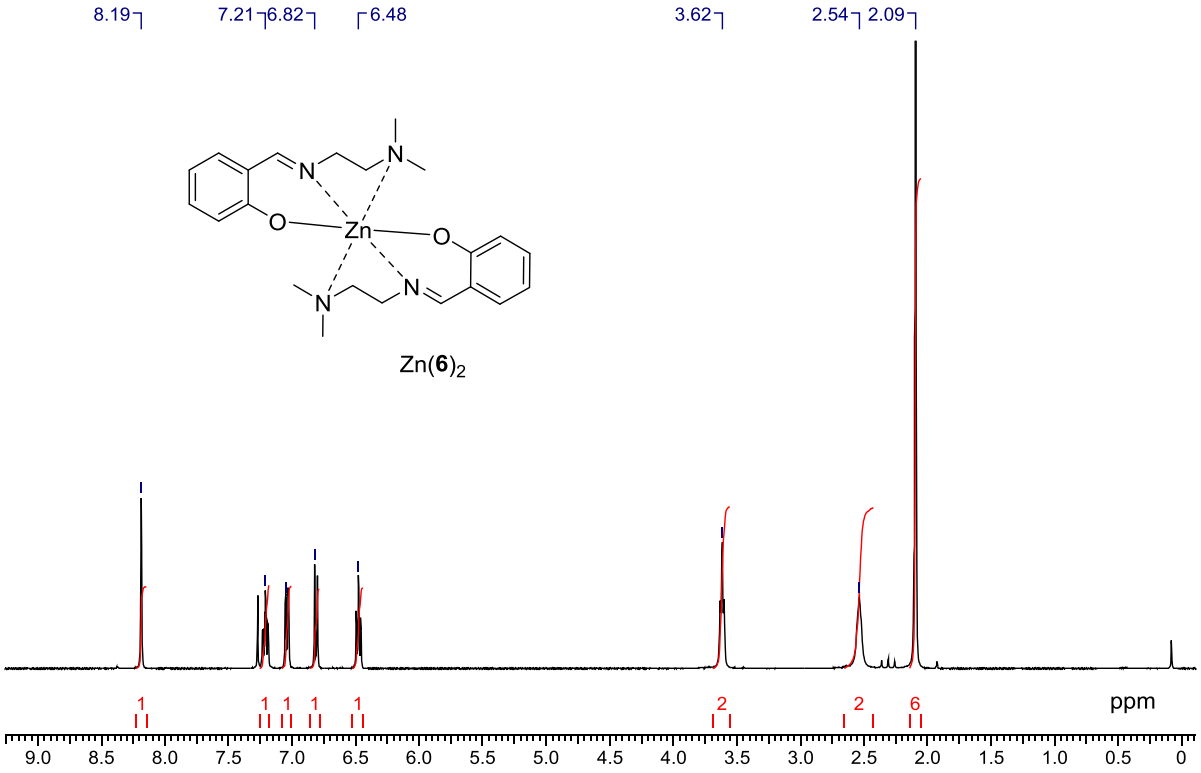

Figure SI26: ^{1}H NMR spectra (400 MHz, $CDCl_3$) of Zn(**6**)$_2$.

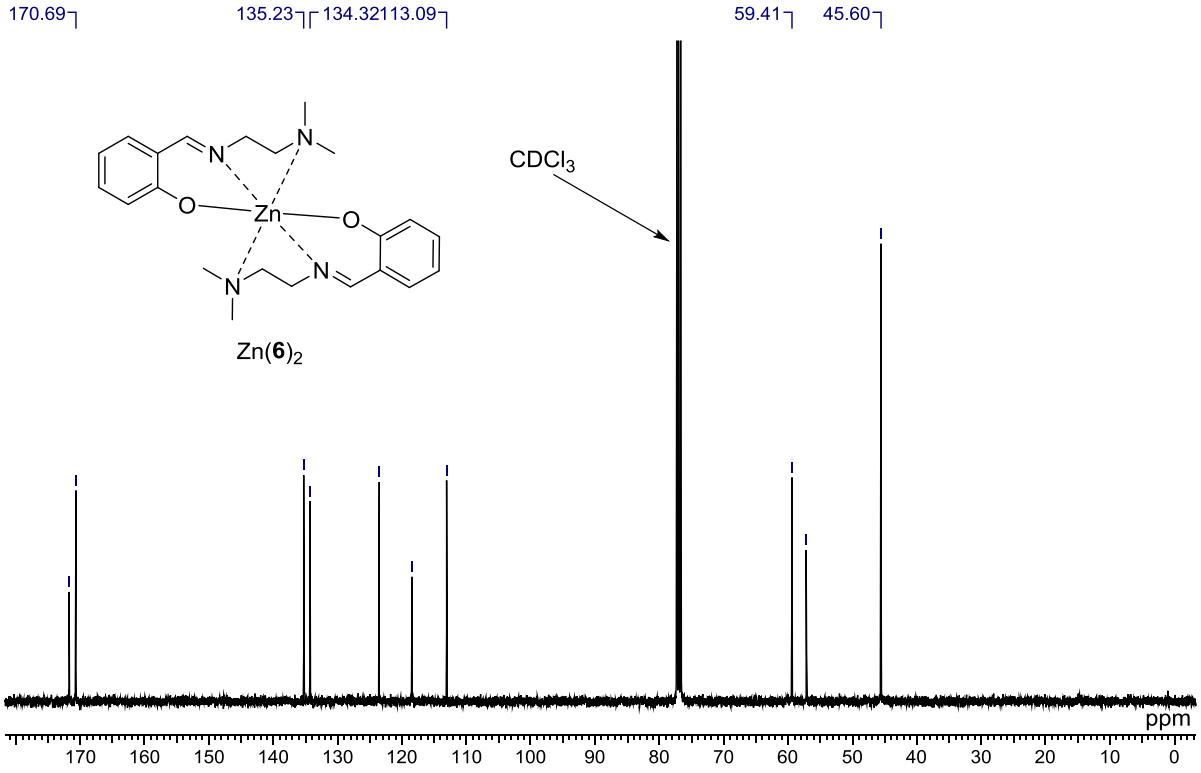

Figure SI27: $^{13}C\{^{1}H\}$ NMR spectra (100 MHz, $CDCl_3$) of Zn(**6**)$_2$.

Zn(7)$_2$: Washed with hexane. Isolated as pale yellow powder (0.28 g, 0.48 mmol, 48%).

^{1}H NMR ($CDCl_3$, 400 MHz) δ = 8.17 (s, 1H; ArCHN), 7.21 (d, *J* = 2.8 Hz, 1H; ArH), 6.98 (d, *J* = 2.8 Hz, 1H; ArH), 3.72 (m, 2H; CH_2), 2.65 (t, *J* = 5.5 Hz, 2H; CH_2), 2.15 (s, 6H; 2 × CH_3).

^{13}C{^{1}H} NMR ($CDCl_3$, 100 MHz) δ = 169.0 (ArCHN), 164.7, 133.2, 132.2 127.7, 119.3, 115.9 (Ar), 59.2, 56.4 (CH_2), 45.7 (CH_3).

Elemental analysis ($C_{22}H_{26}Cl_4ZnN_4O_2$) Calc %, C 45.12, H 4.47, N 9.57; found %, C 45.21, H 4.33, N 9.38.

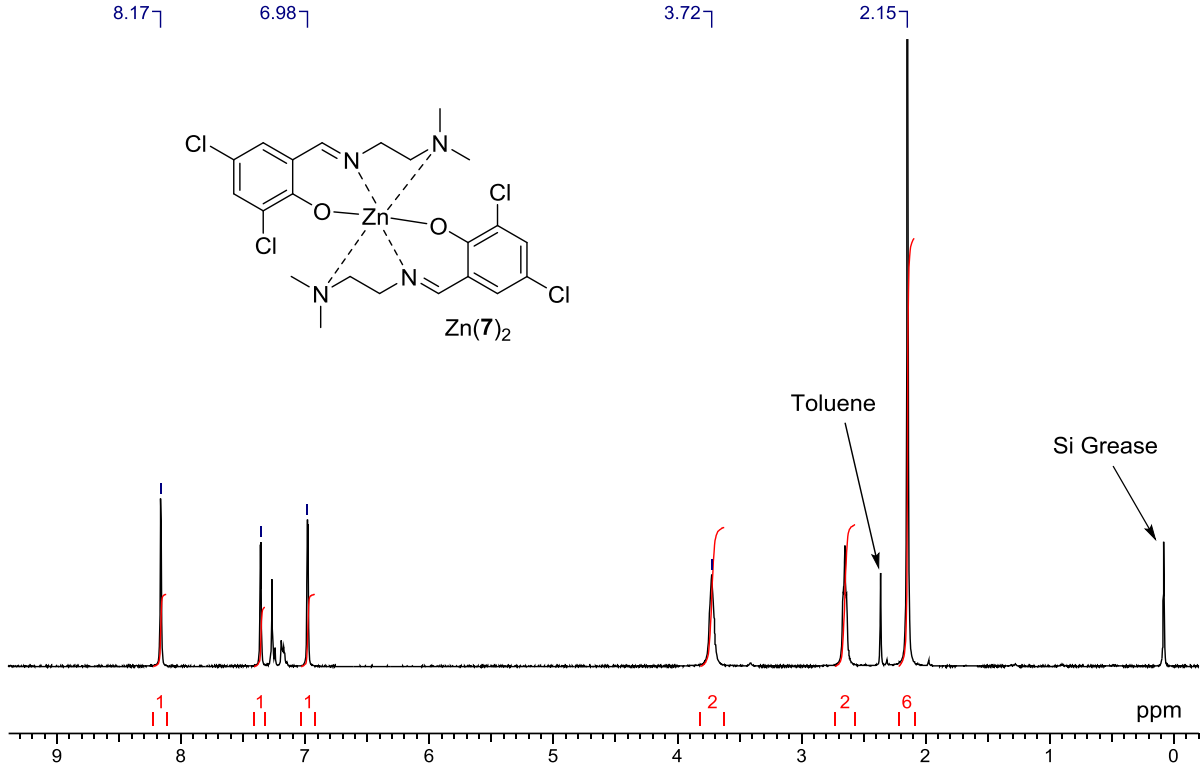

Figure SI28: ^{1}H NMR spectra (400 MHz, $CDCl_3$) of Zn(**7**)$_2$.

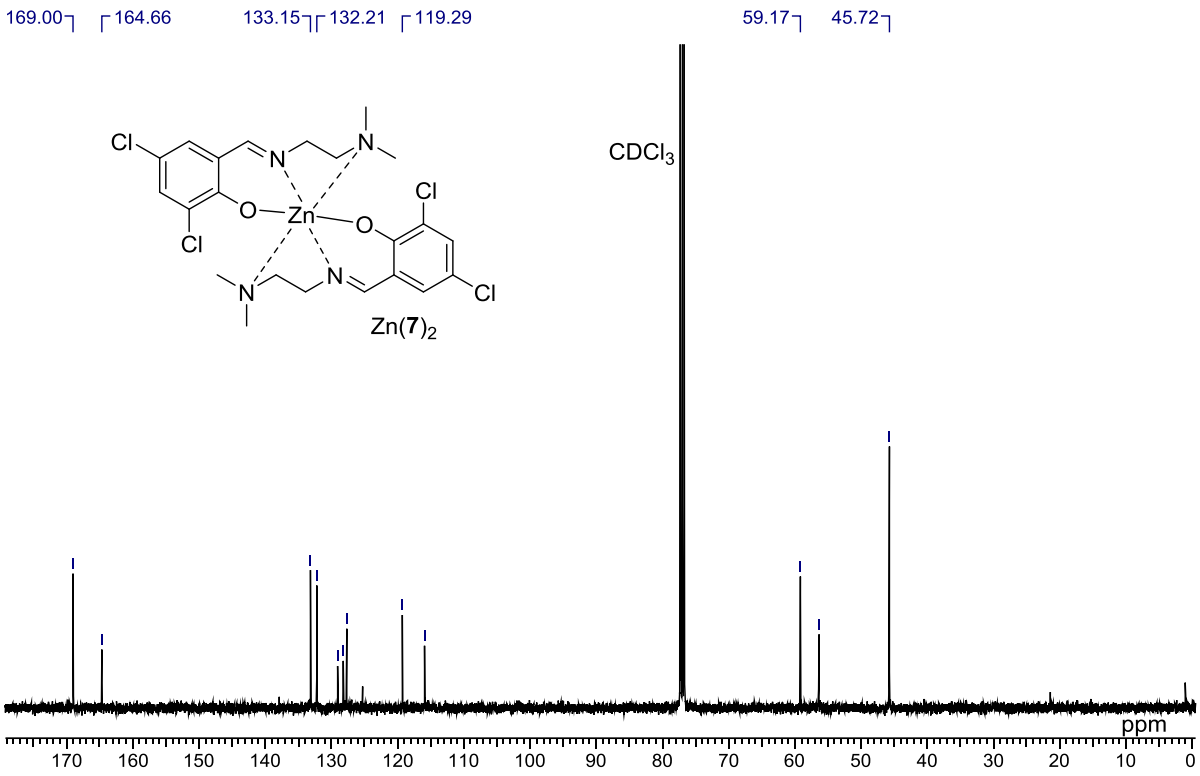

Figure SI29: $^{13}C\{^{1}H\}$ NMR spectra (100 MHz, $CDCl_3$) of Zn(**7**)$_2$.

DOSY NMR spectra

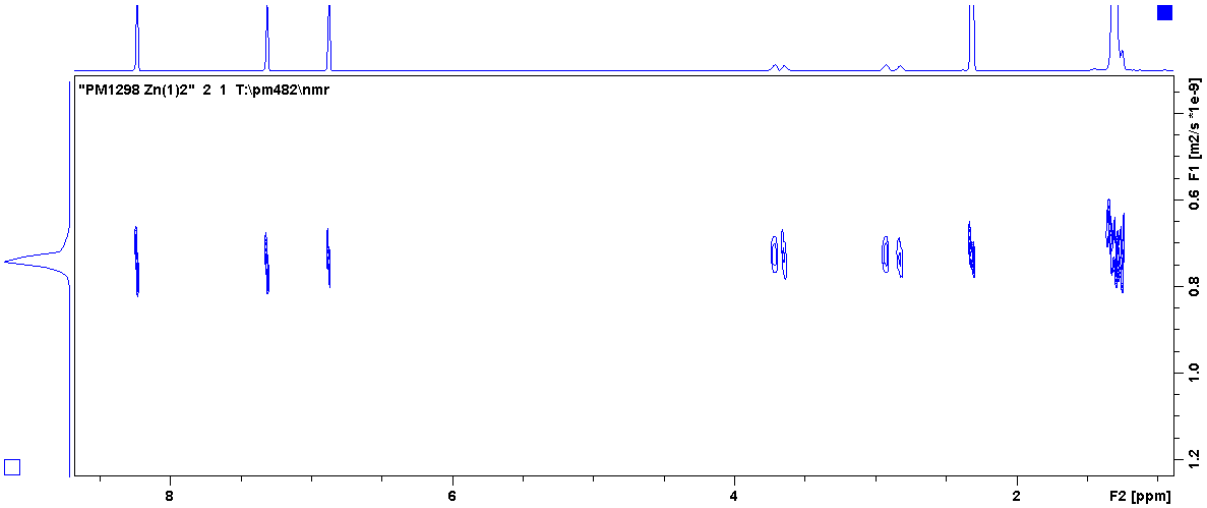

Figure SI30: Zn(**1**)$_2$ DOSY NMR spectra ($CDCl_3$, 500 MHz, D = 7.39 × 10^{-10} m^2s^{-1}).

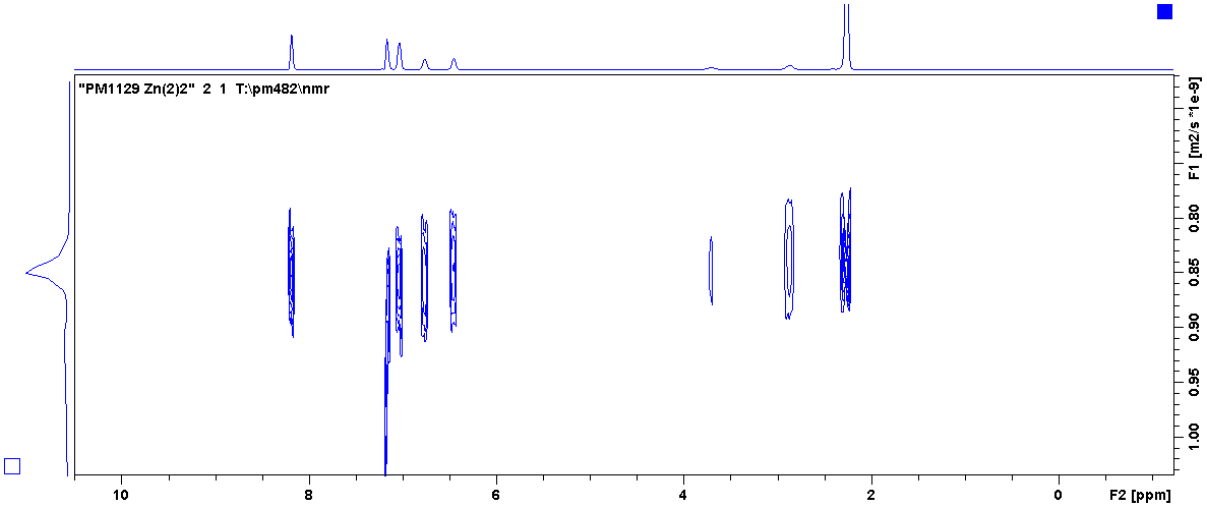

Figure SI31: Zn(**2**)$_2$ DOSY NMR spectra ($CDCl_3$, 500 MHz, D = 8.49 × 10^{-10} m^2s^{-1}).

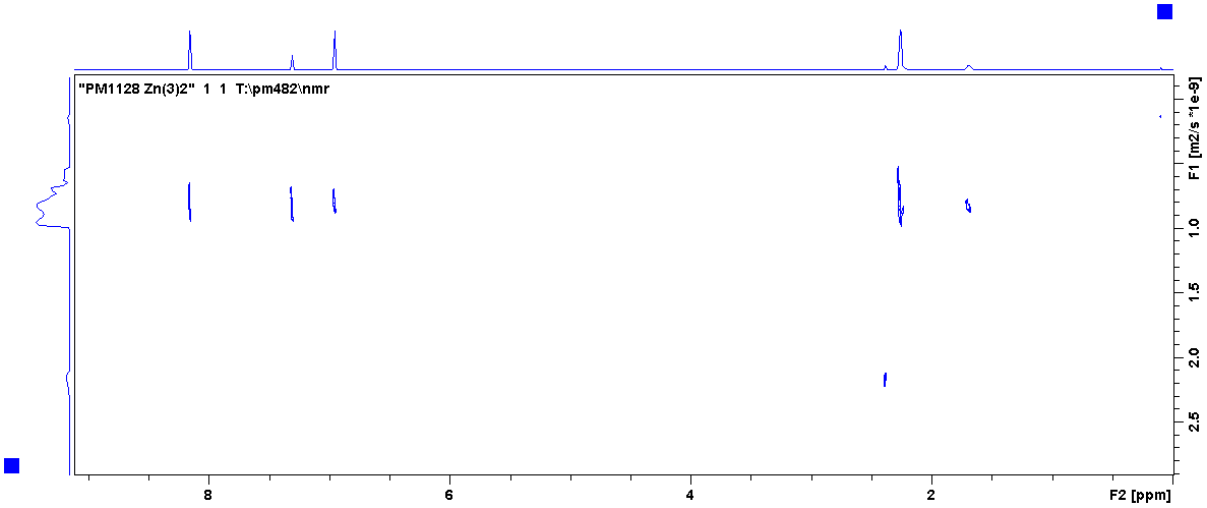

Figure SI32: Zn(**3**)$_2$ DOSY NMR spectra ($CDCl_3$, 500 MHz, D = 8.25 × 10^{-10} m^2s^{-1}). Note: Complex precipitated during experiment.

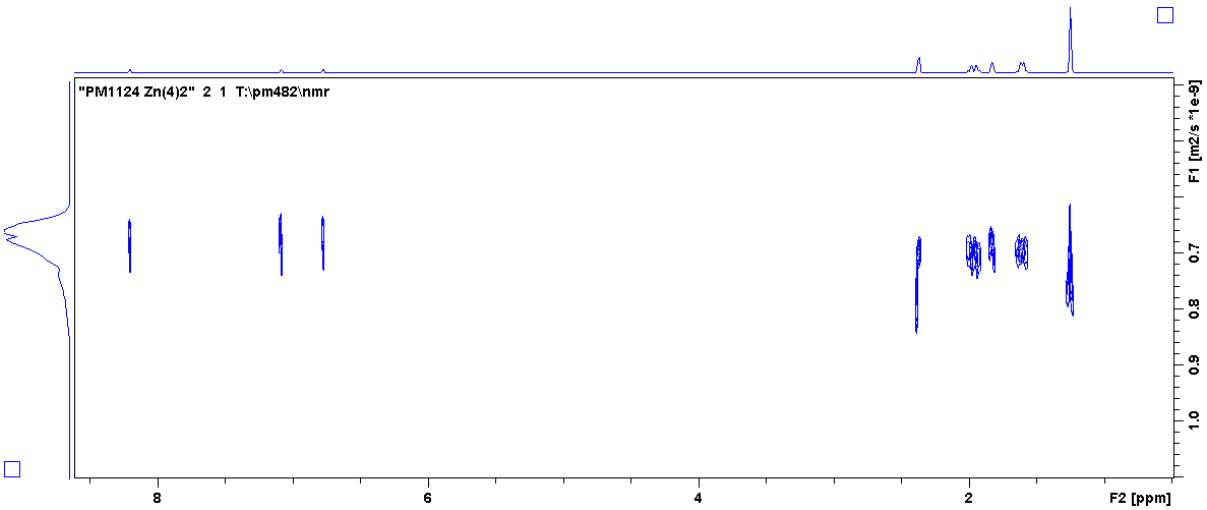

Figure SI33: Zn(**4**)$_2$ DOSY NMR spectra ($CDCl_3$, 500 MHz, D = 6.66 × 10^{-10} m^2s^{-1}).

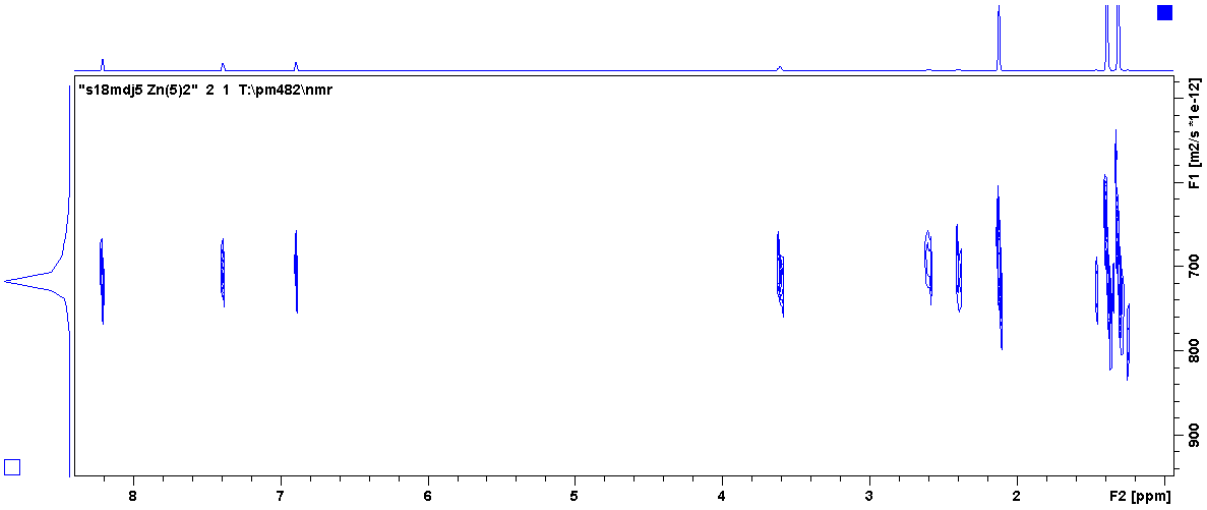

Figure SI34: Zn(**5**)$_2$ DOSY NMR spectra ($CDCl_3$, 500 MHz, D = 7.16 × 10^{-10} m^2s^{-1}).

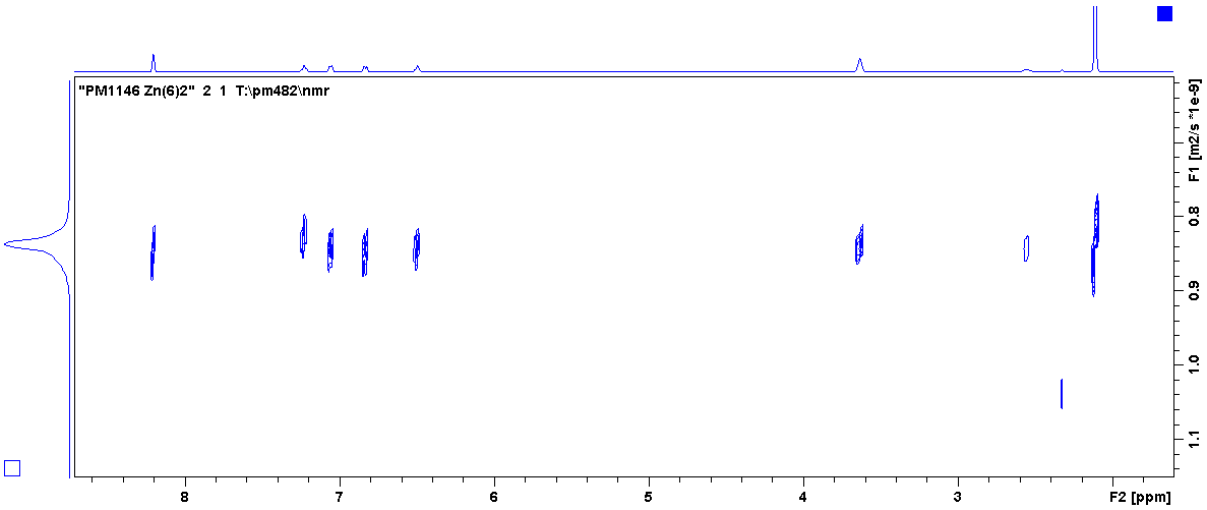

Figure SI35: Zn(**6**)$_2$ DOSY NMR spectra ($CDCl_3$, 500 MHz, D = 8.36 × 10^{-10} m^2s^{-1}).

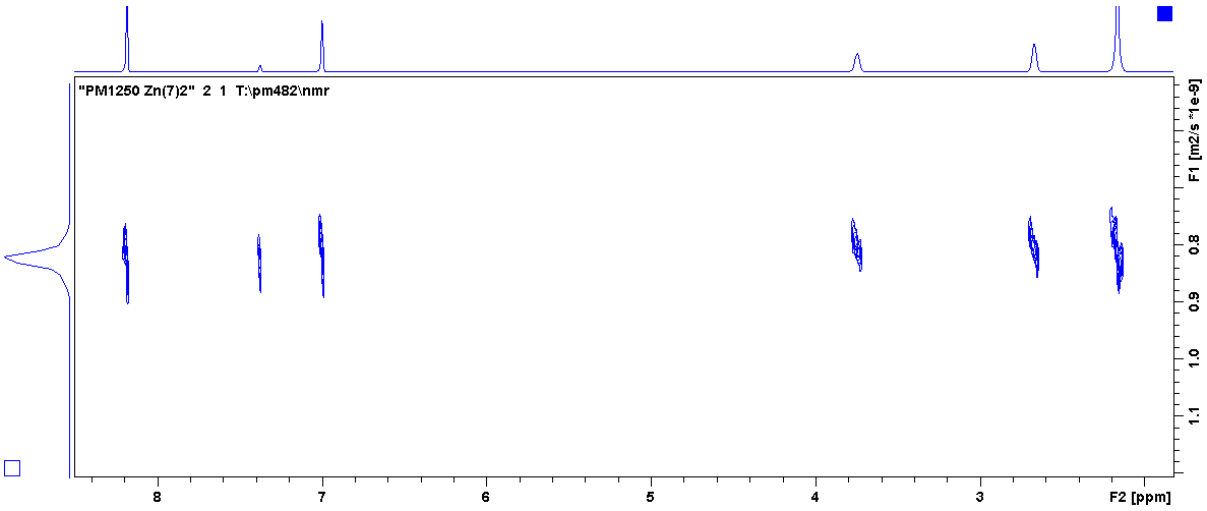

Figure SI36: Zn(**7**)$_2$ DOSY NMR spectra ($CDCl_3$, 500 MHz, D = 8.16×10^{-10} m^2s^{-1}).

Mg(II) complexes

Synthesis of imino monophenolate magnesium complexes, Mg(1-3,5-7)$_2$: Mg(n-Bu)$_2$ (1M, 1 ml, 1 mmol) was added to a solution of ligand (2 mmol) in toluene (10 ml). After complete addition, the solution was stirred for 1 hour before solvent removal. The desired complex was purified *via* washing or recrystallisation from hexane.

Mg(1)$_2$: Recrystallised from hexane. Isolated as pale yellow crystals (0.45 g, 0.75 mmol, 75%). ^{1}H NMR (C_6D_6, 400 MHz) δ = 7.95 (s, 1H; ArCHN), 7.57 (d, *J* = 2.5 Hz, 1H; ArH), 7.05 (d, *J* = 2.5 Hz, 1H; ArH), 3.27 (m, 1H; CH_2), 2.90 (m, 1H; CH_2), 2.57 (m, 1H; CH_2), 2.05 (m, 1H; CH_2), 1.72 (d, *J* = 6.3 Hz, 3H; CH_3), 1.59 (s, 9H; $C(CH_3)_3$), 1.42 (s, 9H; $C(CH_3)_3$), 0.91 (m, 1H; NH). ^{13}C{^{1}H} NMR (C_6D_6, 100 MHz) δ = 169.78 (Ar), 169.76 (ArCHN), 141.1, 132.4,129.3, 120.1 (Ar), 57.8, 51.8 (CH_2), 36.2 (CH_3), 36.1, 34.3 ($C(CH_3)_3$), 32.4, 30.5 ($C(CH_3)_3$).

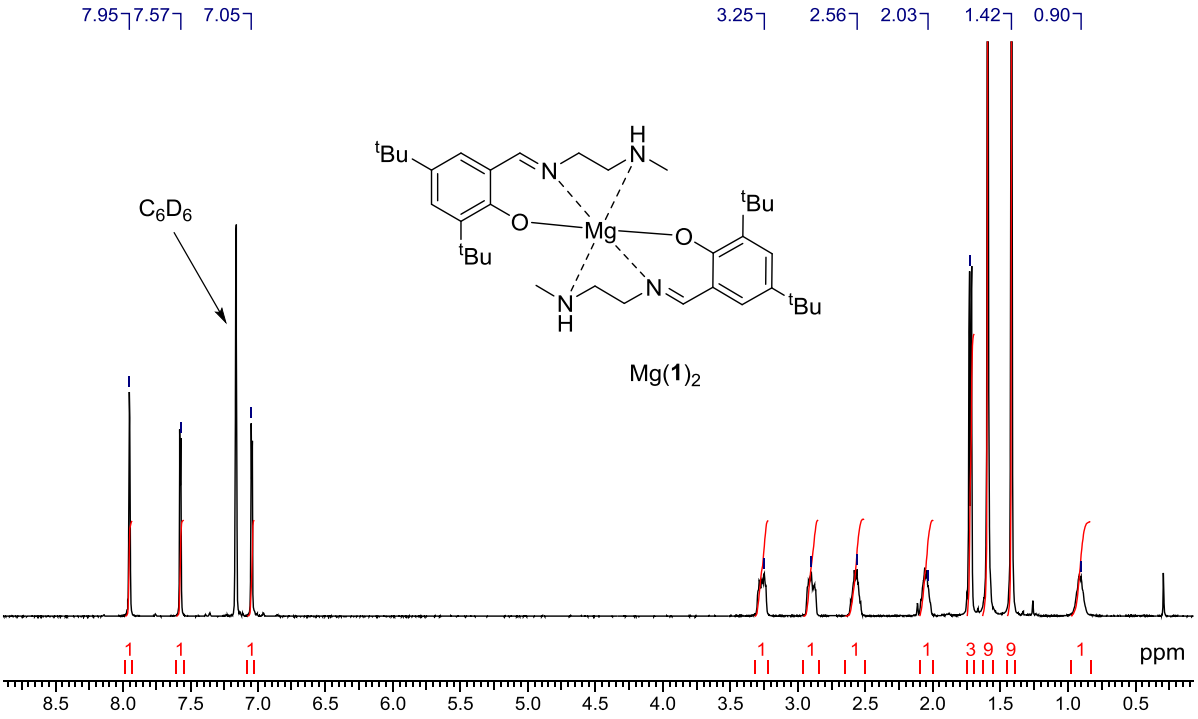

Figure SI37: ^{1}H NMR spectra (400 MHz, C_6D_6) of Mg(**1**)$_2$.

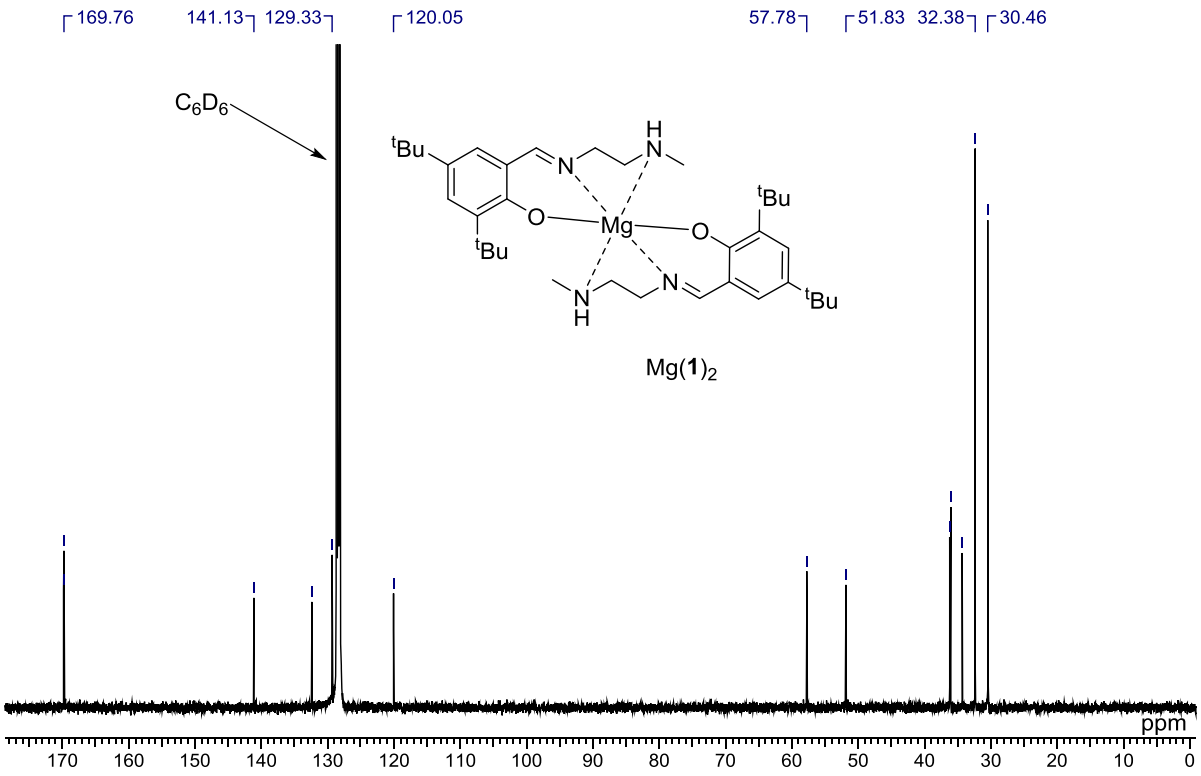

Figure SI38: $^{13}C\{^{1}H\}$ NMR spectra (100 MHz, C_6D_6) of Zn(**1**)$_2$.

Mg(2)$_2$: Recrystallised from hexane. Isolated as pale yellow crystals (0.33 g, 0.87 mmol, 87%). ^{1}H NMR ($CDCl_3$, 400 MHz) δ = 8.19 (s, 1H; ArCHN), 7.14 (t, *J* = 8.4 Hz, 1H; ArH), 7.06 (d, *J* = 7.7 Hz, 1H; ArH), 6.70 (d, *J* = 8.5 Hz, 1H; ArH), 6.40 (t, *J* = 7.4 Hz, 1H; ArH), 3.91 (m, 1H; CH_2), 3.45 (m, 1H; CH_2), 3.06 (m, 1H; CH_2), 2.60 (m, 1H; CH_2), 2.22 (d, *J* = 6.4 Hz, 3H; CH_3), 1.70 (m, 1H; NH). $^{13}C\{^{1}H\}$ NMR ($CDCl_3$, 100 MHz) δ = 170.7 (Ar), 168.5 (ArCHN), 134.7, 133.3,123.2, 120.8, 111.6 (Ar), 57.1, 51.4 (CH_2), 36.3 (CH_3).

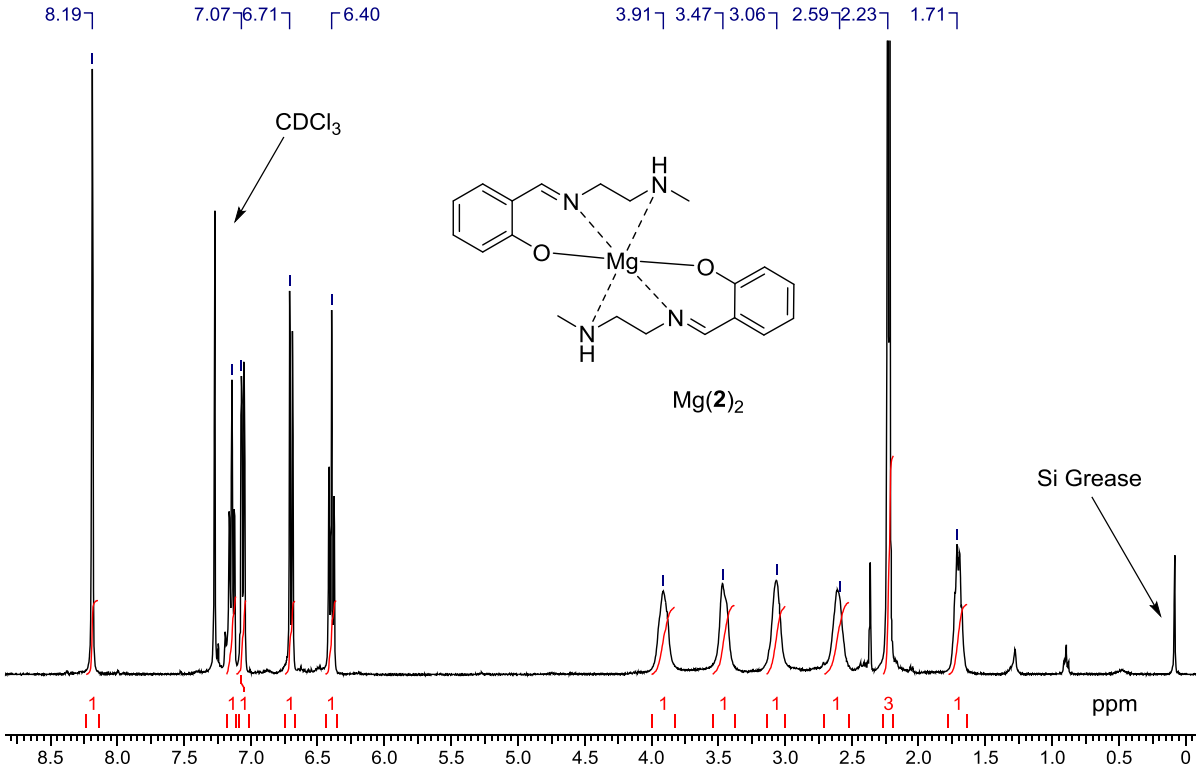

Figure SI39: ^{1}H NMR spectra (400 MHz, $CDCl_3$) of Mg(**2**)$_2$.

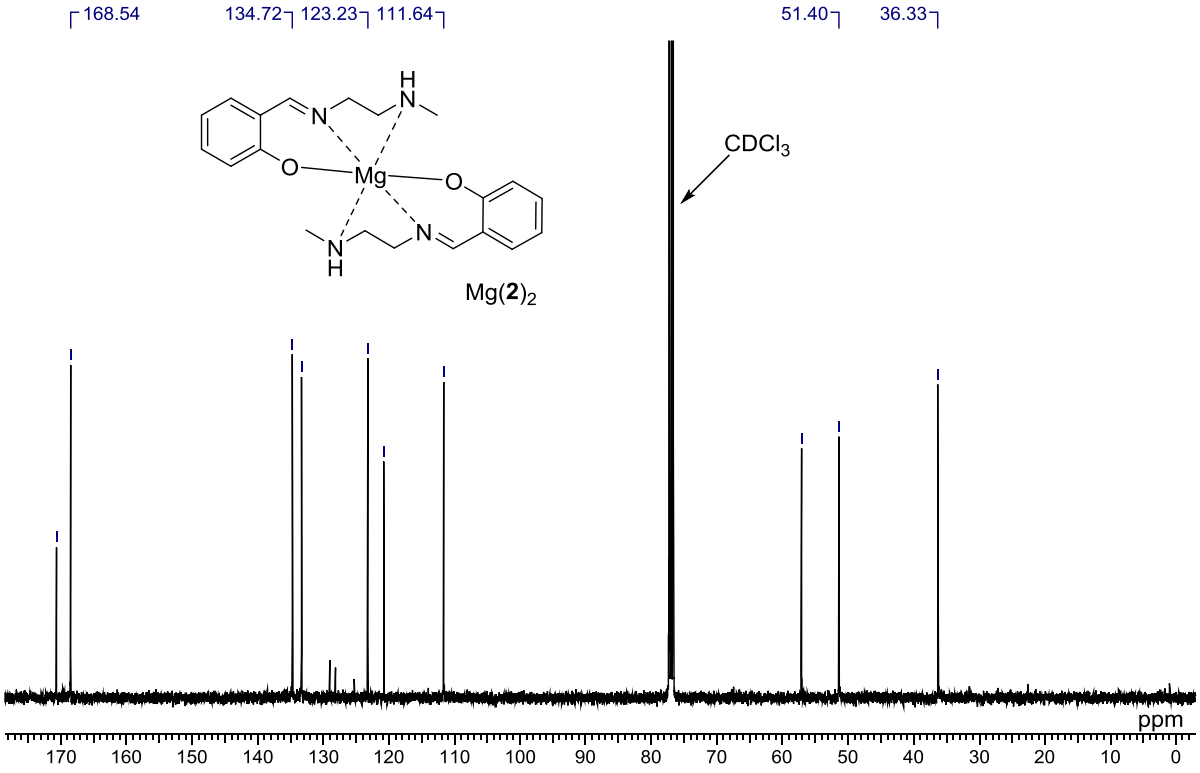

Figure SI40: ^{13}C{^{1}H} NMR spectra (100 MHz, $CDCl_3$) of Mg(**2**)$_2$.

Mg(3)$_2$: Precipitated from toluene. Isolated as pale yellow powder (0.38 g, 0.74 mmol, 74%). ^{1}H NMR ($CDCl_3$, 400 MHz) δ = 8.15 (s, 1H; ArCHN), 7.29 (t, *J* = 2.8 Hz, 1H; ArH), 6.98 (t, *J* = 2.8 Hz, 1H; ArH), 3.91 (m, 1H; CH_2), 4.03 (br s, 1H; CH_2), 3.52 (br s, 1H; CH_2), 3.20 (br s, 1H; CH_2), 2.66 (br s, 1H; CH_2), 2.24 (d, *J* = 6.4 Hz, 3H; CH_3), 1.71 (m, 1H; NH). ^{13}C{^{1}H} NMR ($CDCl_3$, 100 MHz) δ = 166.6 (ArCHN), 163.5 (ArCHN), 132.3, 131.7,127.2, 121.2, 114.6 (Ar), 57.3, 51.4 (CH_2), 36.1 (CH_3).

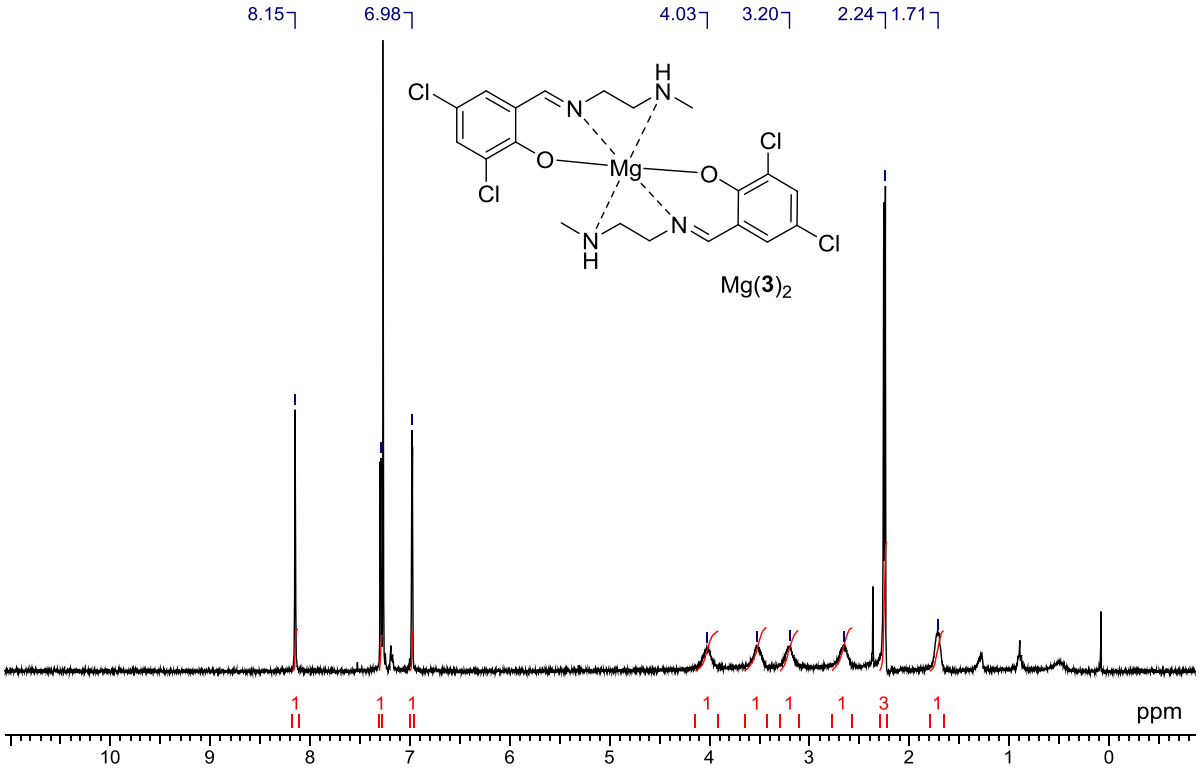

Figure SI41: ^{1}H NMR spectra (400 MHz, $CDCl_3$) of Mg(**3**)$_2$.

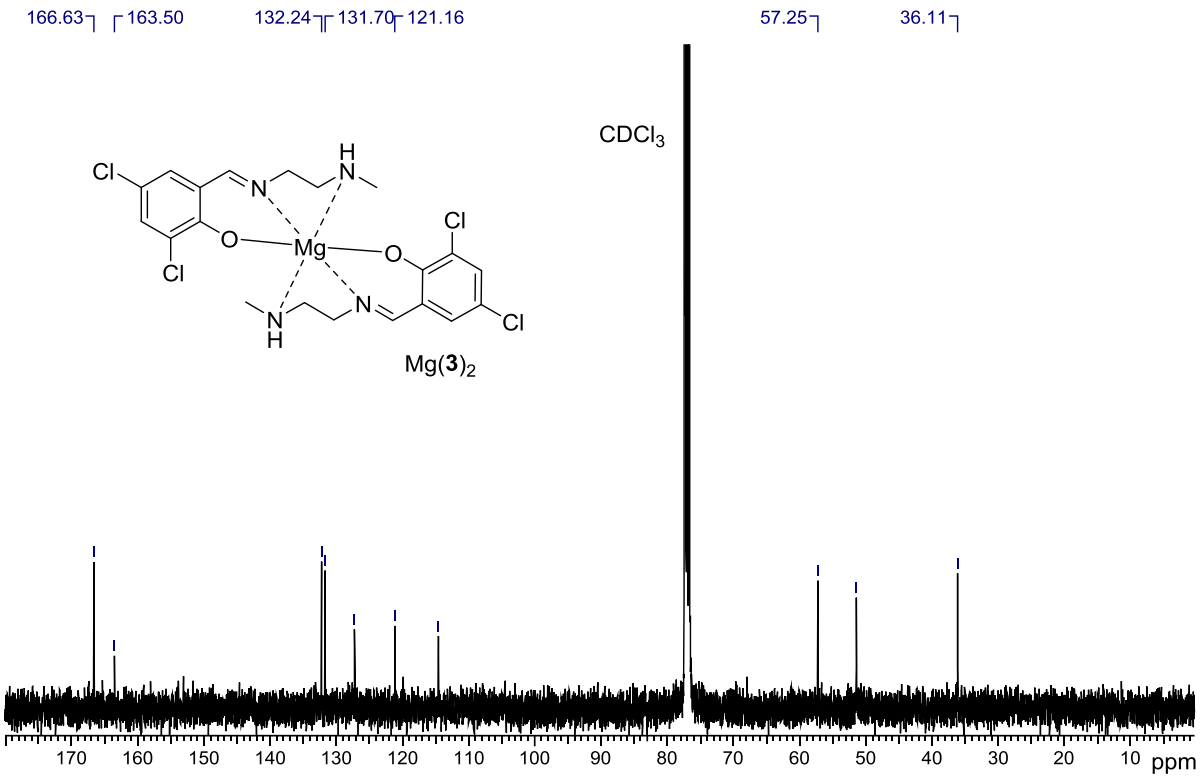

Figure SI42: $^{13}C\{^{1}H\}$ NMR spectra (100 MHz, $CDCl_3$) of Mg(**3**)$_2$.

Mg(5)$_2$: Recrystallised from toluene. Isolated as yellow crystals (0.14 g, 0.22 mmol, 22%). ^{1}H NMR ($CDCl_3$, 400 MHz) δ = 8.19 (s, 1H; ArCHN), 7.28 (s, 1H; ArH), 6.88 (s, 1H; ArH), 3.71 (m, 1H; CH_2), 3.47 (m, 1H; CH_2), 2.68 (m, 1H; CH_2), 2.34 (m, 1H; CH_2), 2.19 (s, 6H; 2 × CH_3), 1.28 (s, 18H; 2 × $C(CH_3)_3$).$^{13}C\{^{1}H\}$ NMR ($CDCl_3$, 100 MHz) δ = 171.3 (ArCHN), 168.4, 140.6, 132.6, 128.4, 128.3, 119.2 (Ar), 60.0, 56.2 (CH_2), 46.2 (CH_3), 35.2, 33.7 ($C(CH_3)_3$), 31.5, 29.5 ($C(CH_3)_3$).

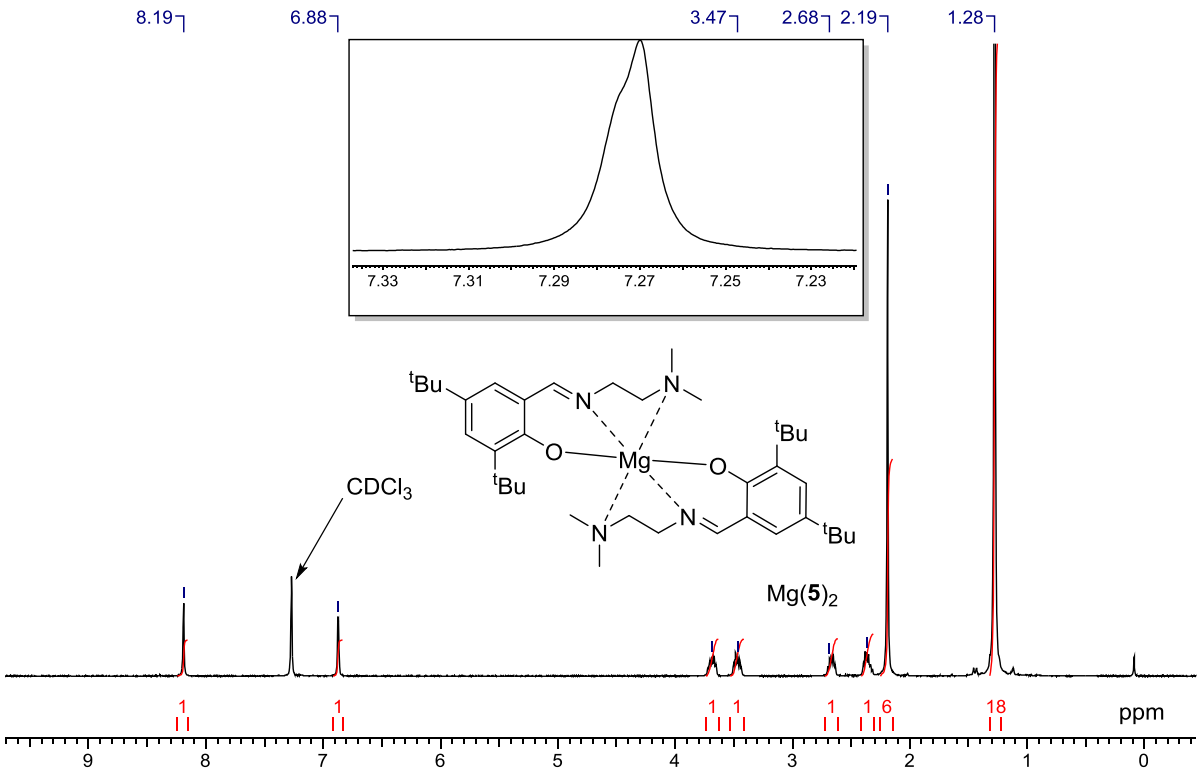

Figure SI43: ^{1}H NMR spectra (400 MHz, $CDCl_3$) of Mg(**5**)$_2$.

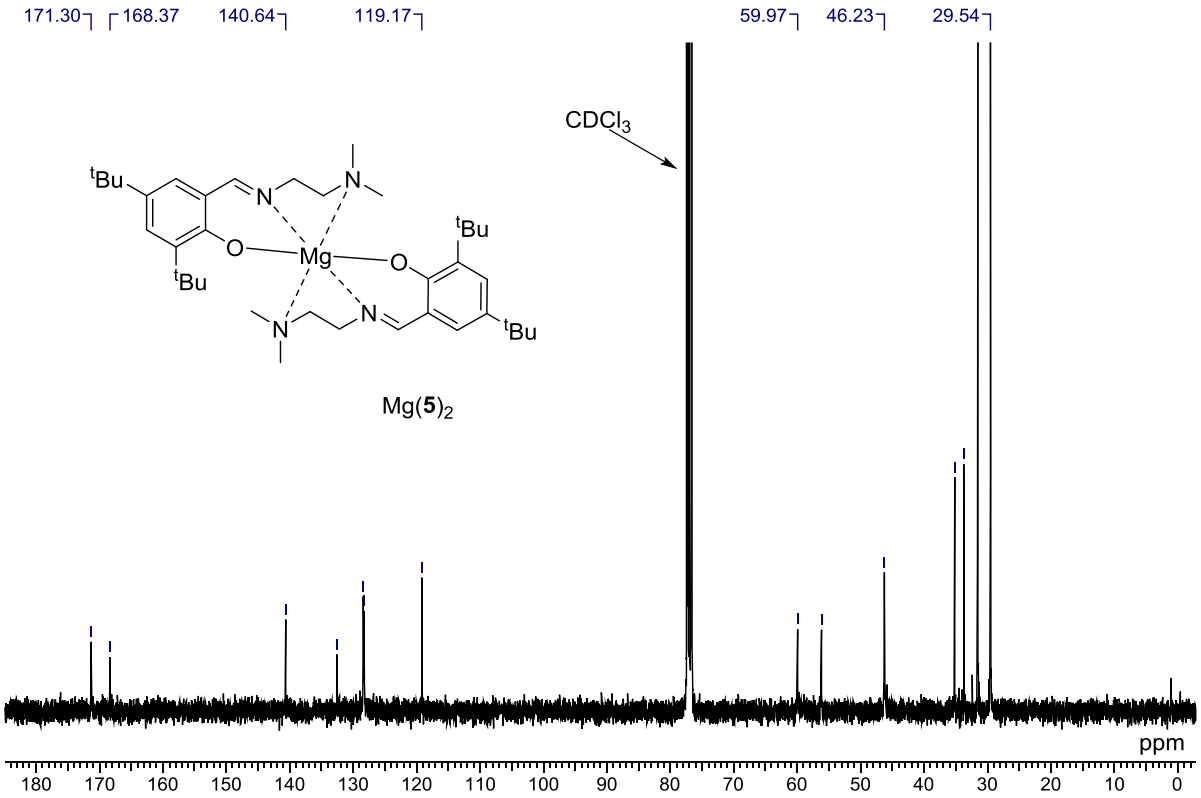

Figure SI44: ^{13}C{^{1}H} NMR spectra (100 MHz, $CDCl_3$) of Mg(**5**)$_2$.

Mg(6)$_2$: Washed with hexane. Isolated as pale yellow crystals (0.13 g, 0.32 mmol, 32%). ^{1}H NMR ($CDCl_3$, 400 MHz) δ = 8.09 (s, 1H; ArCHN), 7.13 (m, 1H; ArH), 6.99 (d, *J* = 7.2 Hz, 1H; ArH), 6.74 (br s, 1H; ArH), 6.39 (br t, *J* = 6.9 Hz, 1H; ArH), 3.54 (br s, 2H; CH_2), 2.38 (br s, 2H; CH_2), 2.03 (s, 6H; 2 × CH_3). ^{13}C{^{1}H} NMR ($CDCl_3$, 100 MHz) δ = 168.4 (ArCHN), 163.2, 132.3, 131.8, 126.9, 121.0, 114.4 (Ar), 59.2, 55.0 (CH_2), 46.8 (CH_3).

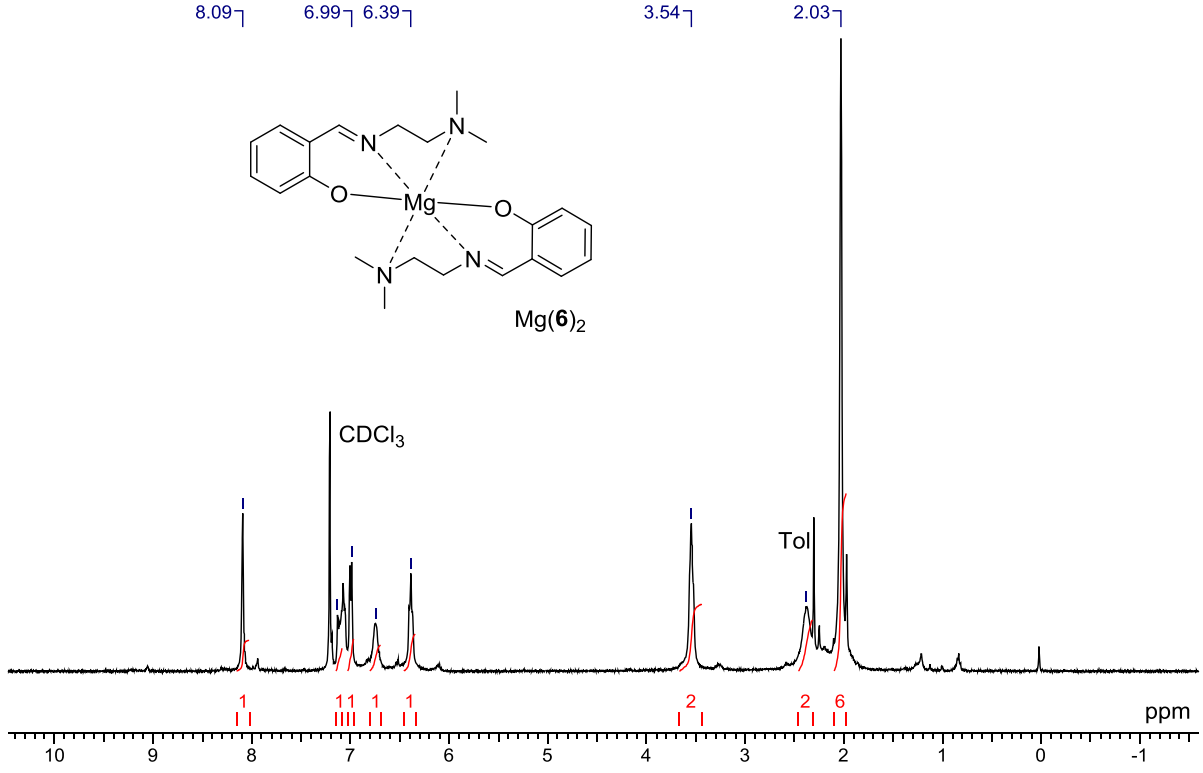

Figure SI45: ^{1}H NMR spectra (400 MHz, $CDCl_3$) of Mg(**6**)$_2$.

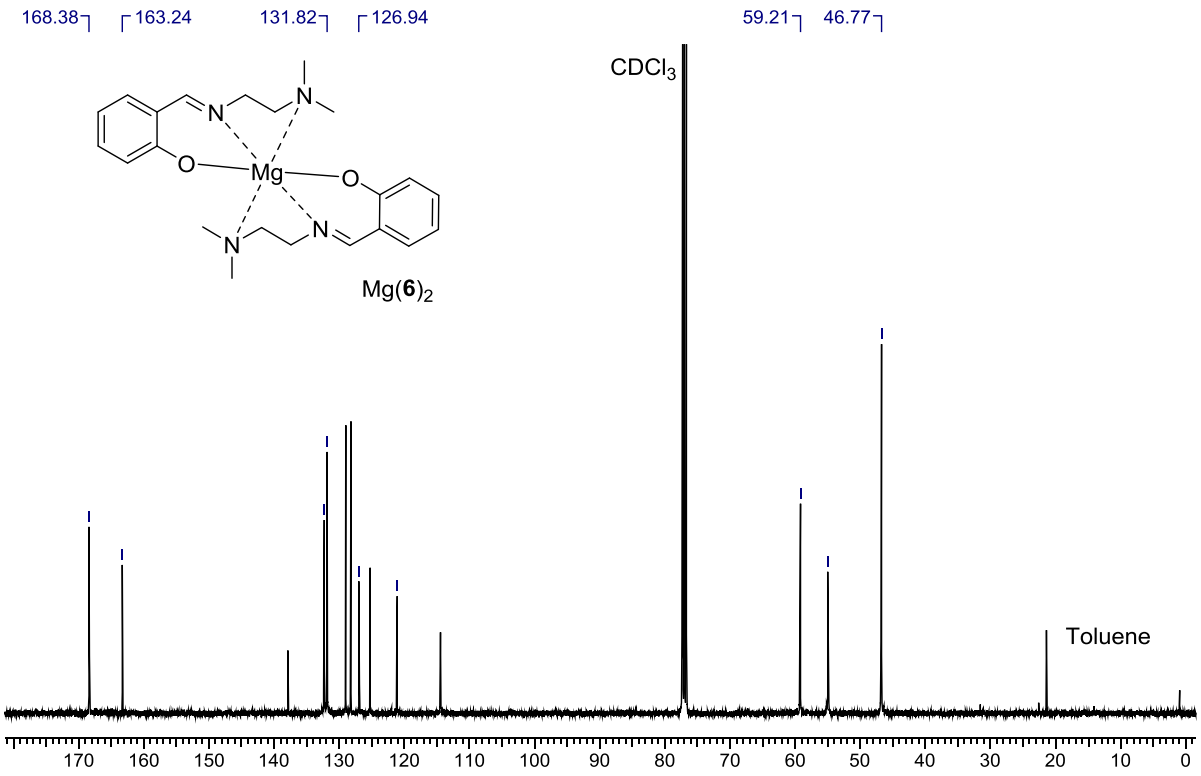

Figure SI46: $^{13}C\{^{1}H\}$ NMR spectra (100 MHz, $CDCl_3$) of Mg(**6**)$_2$.

Mg(7)$_2$: Recrystallised from a mixture of hexane/CH_2Cl_2.Isolated as pale yellow crystals (0.29 g, 0.53 mmol, 53%).

^{1}H NMR ($CDCl_3$, 400 MHz) δ = 8.16 (s, 1H; ArCHN), 7.21 (m, 1H; ArH), 6.95 (s, 1H; ArH), 3.68 (br s, 2H; CH_2), 2.82 (br s, 2H; CH_2), 2.16 (s, 6H; 2 × CH_3). $^{13}C\{^{1}H\}$ NMR ($CDCl_3$, 100 MHz) δ = 170.4 (ArCHN), 134.7, 133.5, 129.0, 128.2, 123.2, 121.1 (Ar), 59.8, 56.0 (CH_2), 46.2 (CH_3).

Elemental analysis ($C_{22}H_{26}MgN_4O_2$) Calcd in %: C, 48.52; H, 4.81; N, 10.29. Found: C, 50.81; H, 5.33; N, 9.42 (Toluene present in crystal structure).

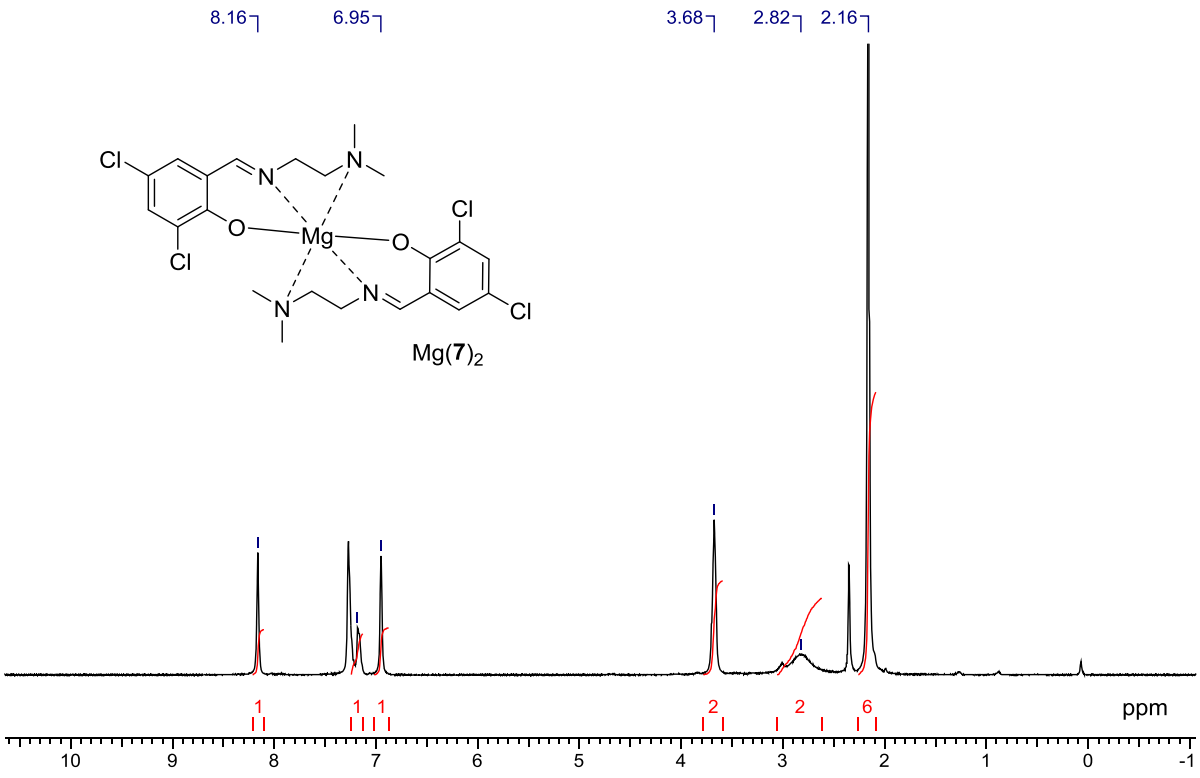

Figure SI47: ^{1}H NMR spectra (400 MHz, $CDCl_3$) of Mg(**7**)$_2$.

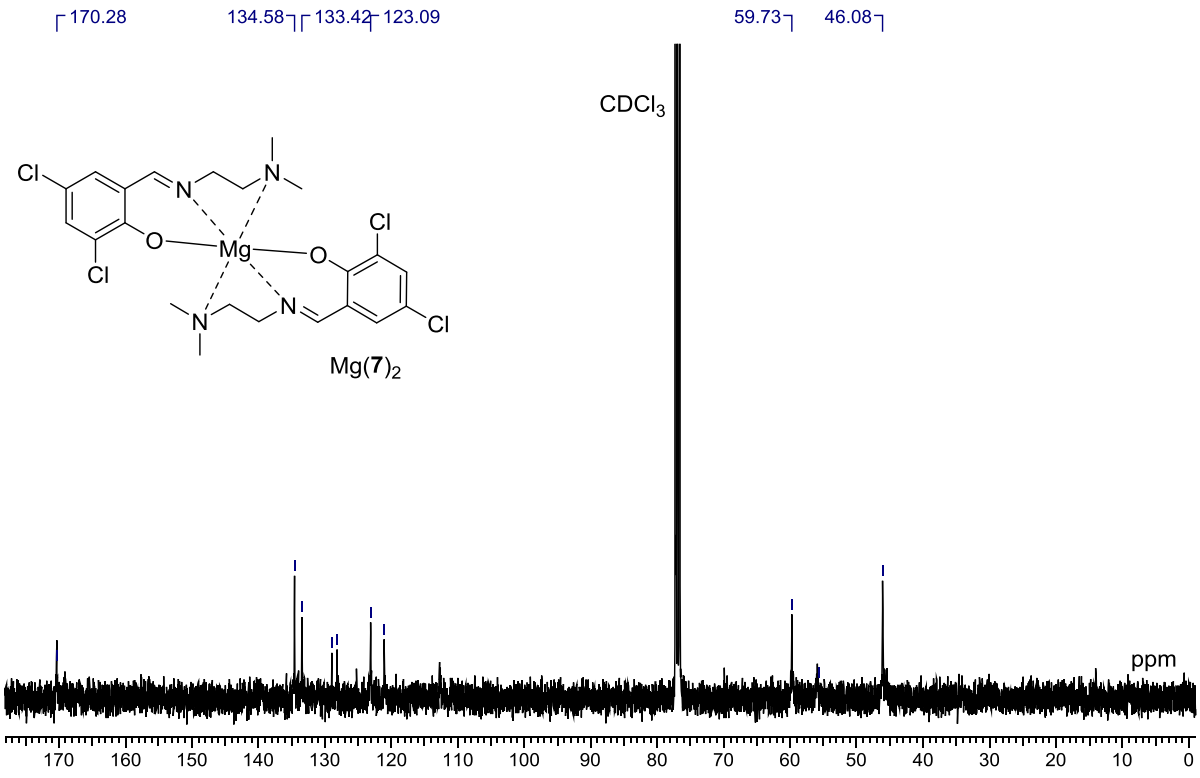

Figure SI48: $^{13}C\{^{1}H\}$ NMR spectra (100 MHz, $CDCl_3$) of Mg(**7**)$_2$.

Polymer characterisation

Mechanistic studies

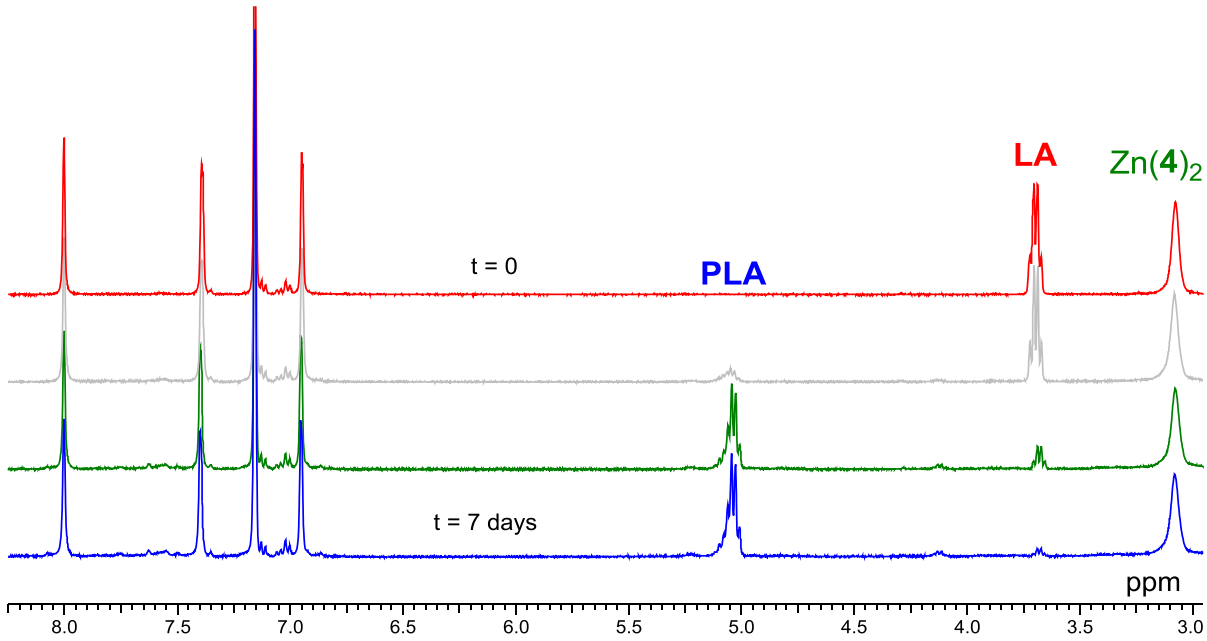

Figure SI49: ^{1}H NMR (400 MHz, C_6D_6) of Zn(**4**)$_2$ + *L*-LA. Polymer is formed after several days with no change in Zn(**4**)$_2$ resonances.

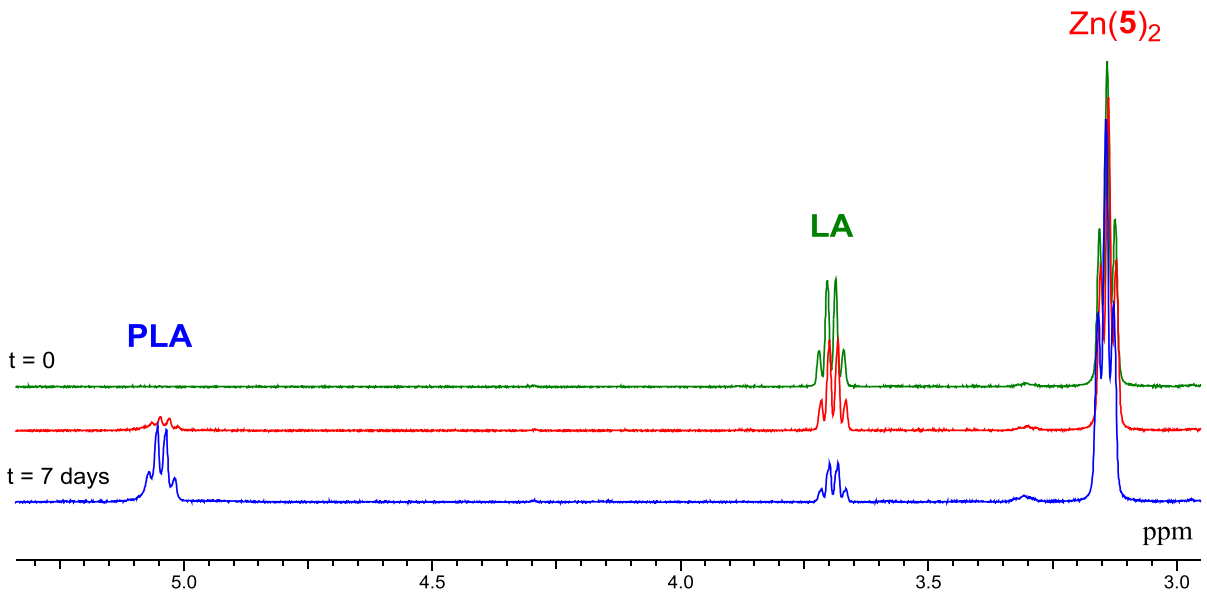

Figure SI50: ^{1}H NMR (400 MHz, C_6D_6) of Zn(**5**)$_2$ + *L*-LA. Polymer is formed after several days with no change in Zn(**5**)$_2$ resonances.

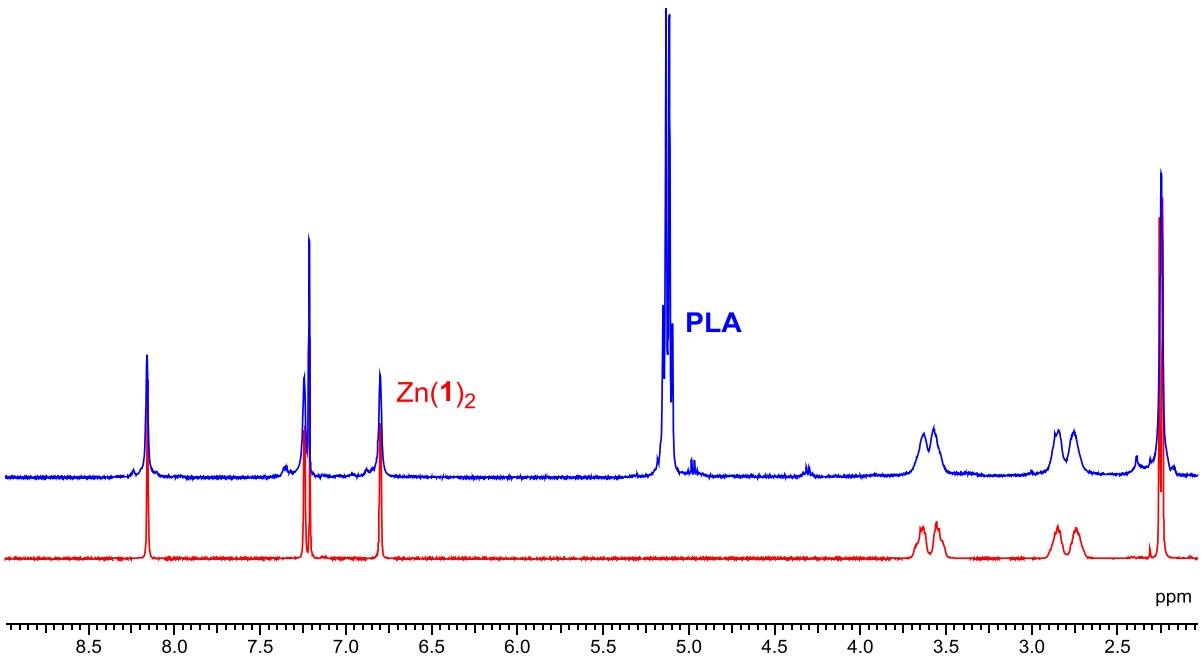

Figure SI51: ^{1}H NMR (400 MHz, $CDCl_3$) of 1. Red spectrum: Zn(**1**)$_2$; 2. Blue spectrum: Zn(**1**)$_2$+ *L*-LA after 1 minute (180°C, 1:5).

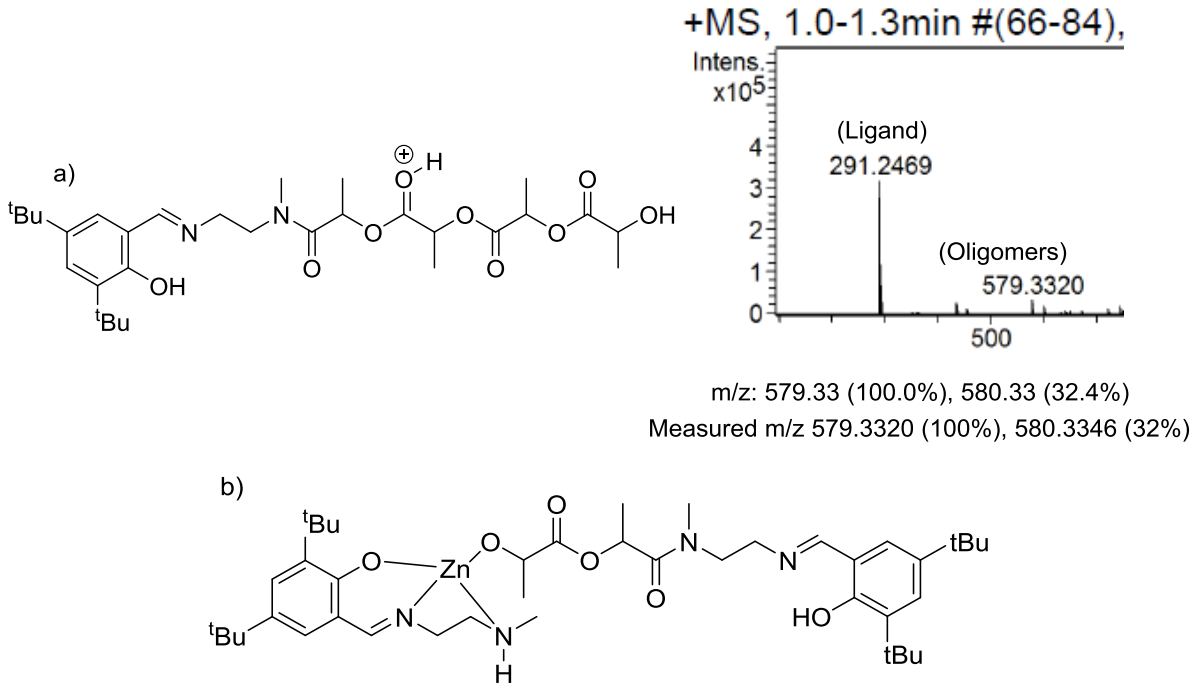

Figure SI52: a) Observed ESI-MS peaks and assignment from solvent free polymerisation {180°C, [Zn(1)$_2$:[*L*-LA] 1:5} .b) Possible propagation species Zn(**1**){Lactyl}. No BnOH added to the polymerisation.

IR-Kinetic data

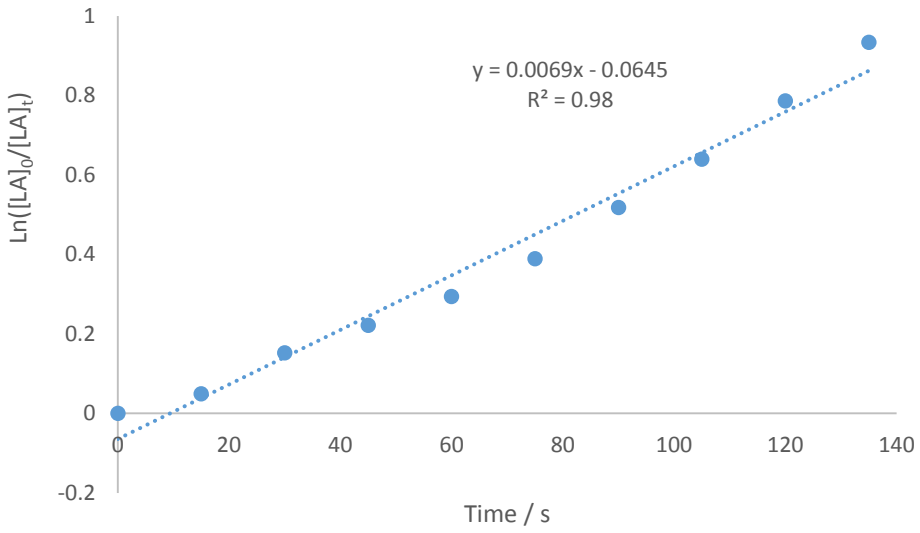

Figure SI53: Semi-logarithmic first order plot with respect to lactide consumption for Zn(**1**)$_2$ (180°C, 10000:1:100) (Table 5, entry 1).

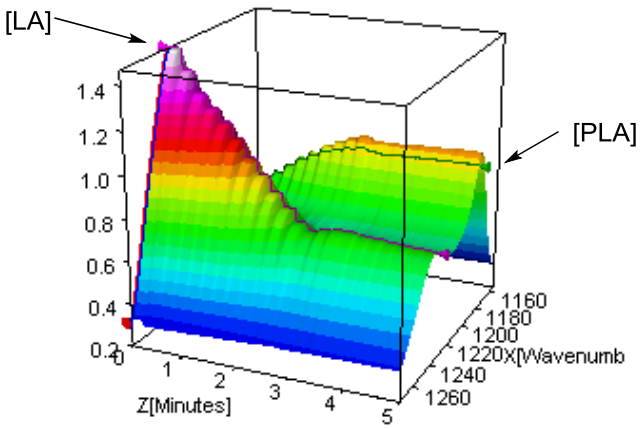

Figure SI54: Change in intensity of IR spectrum due to LA ROP for Zn(**1**)$_2$ (Table 5, entry 1).

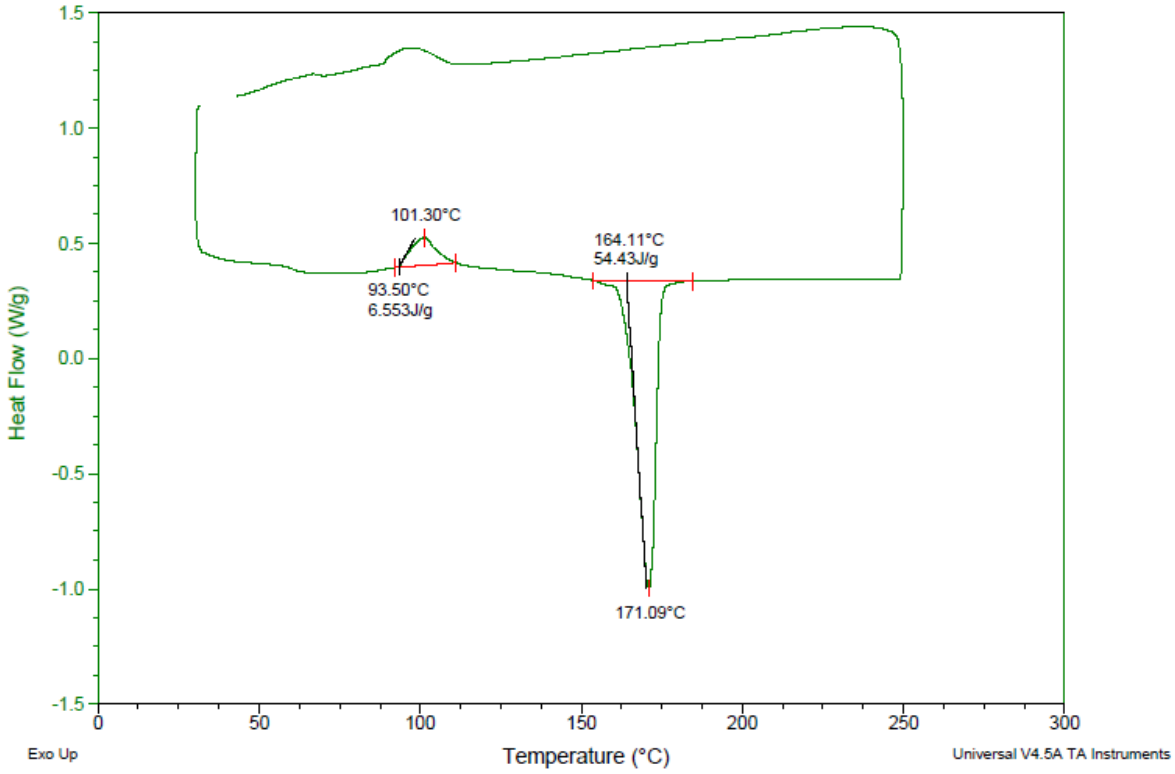

Figure SI55: DSC trace of PLLA produced by Zn(**1**)$_2$ (180°C, 10000:1:100) (Table 5, entry 1).

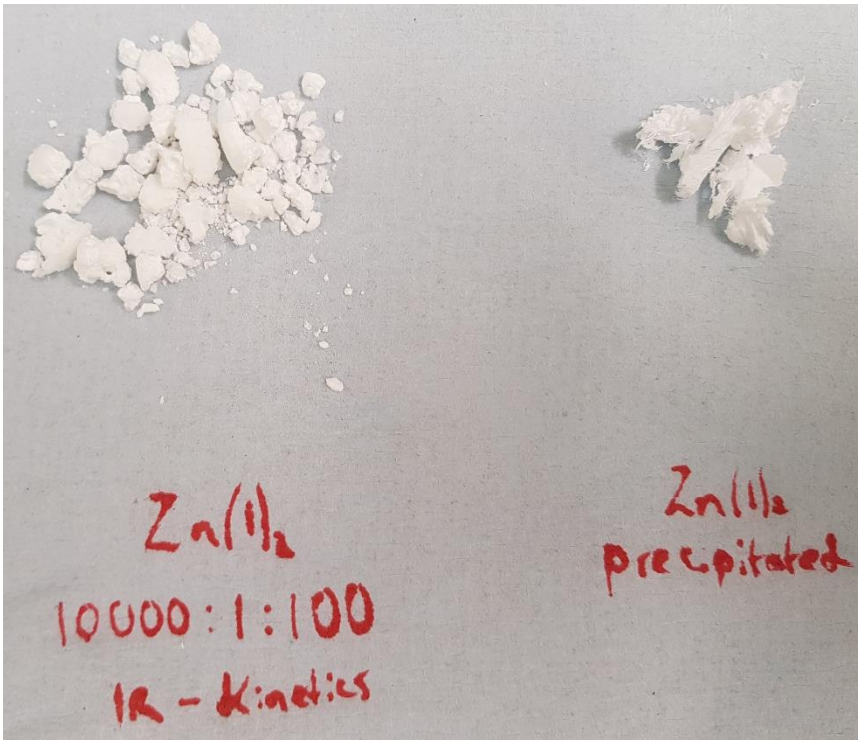

Figure SI56: PLLA produced by Zn(**1**)$_2$ (180°C, 10000:1:100) (Table 5, entry 1).

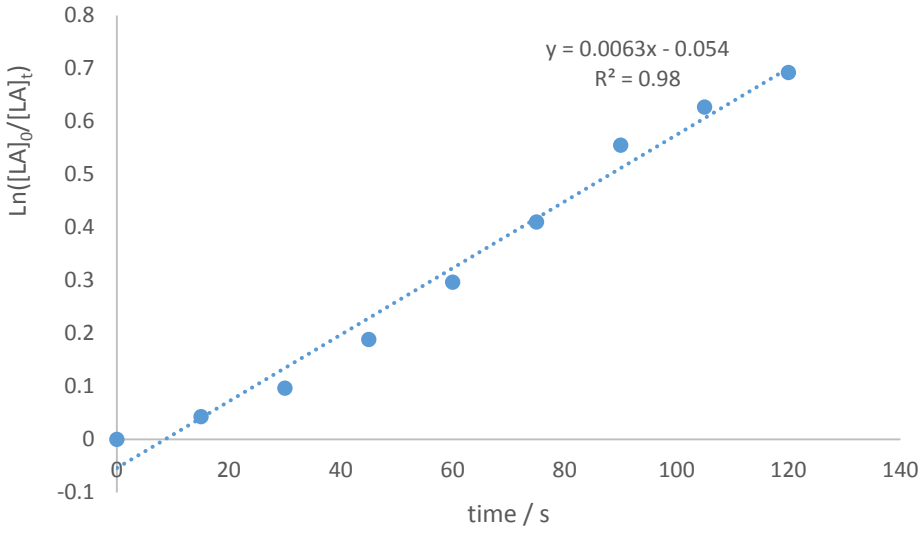

Figure SI57: Semi-logarithmic first order plot with respect to lactide consumption for Zn(**4**)$_2$ (180°C, 10000:1:100) (Table 5, entry 2).

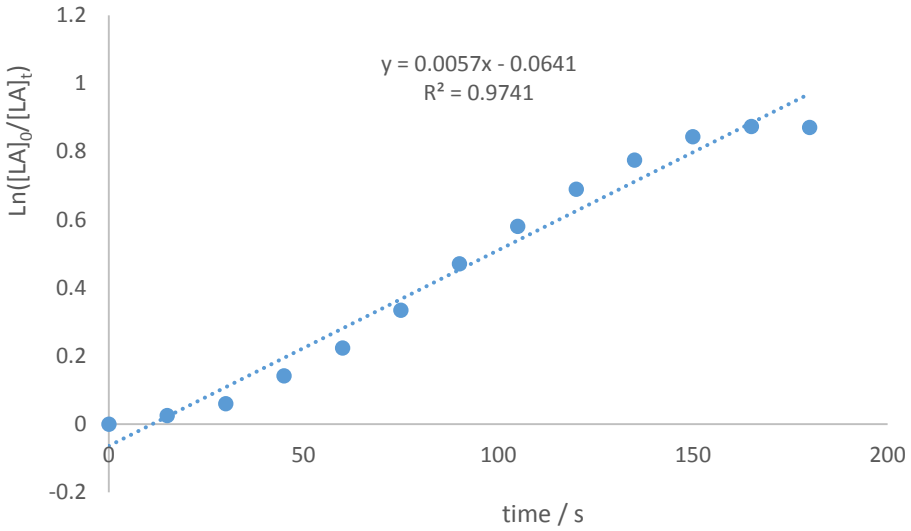

Figure SI58: Semi-logarithmic first order plot with respect to lactide consumption for Zn(**5**)$_2$ (180°C, 10000:1:100) (Table 5, entry 3).

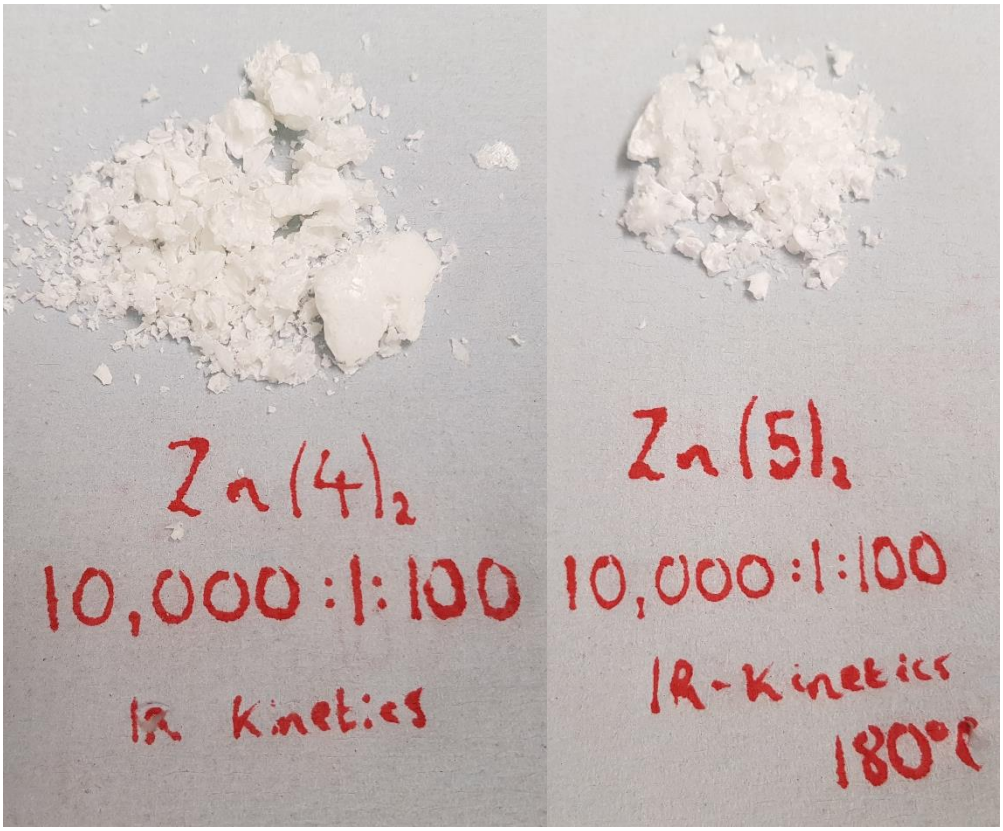

Figure SI59: PLLA produced by Zn(**4**)$_2$ (left) and Zn(**5**)$_2$ (right) (180°C, 10000:1:100) (Table 5, entries 2 and 3).

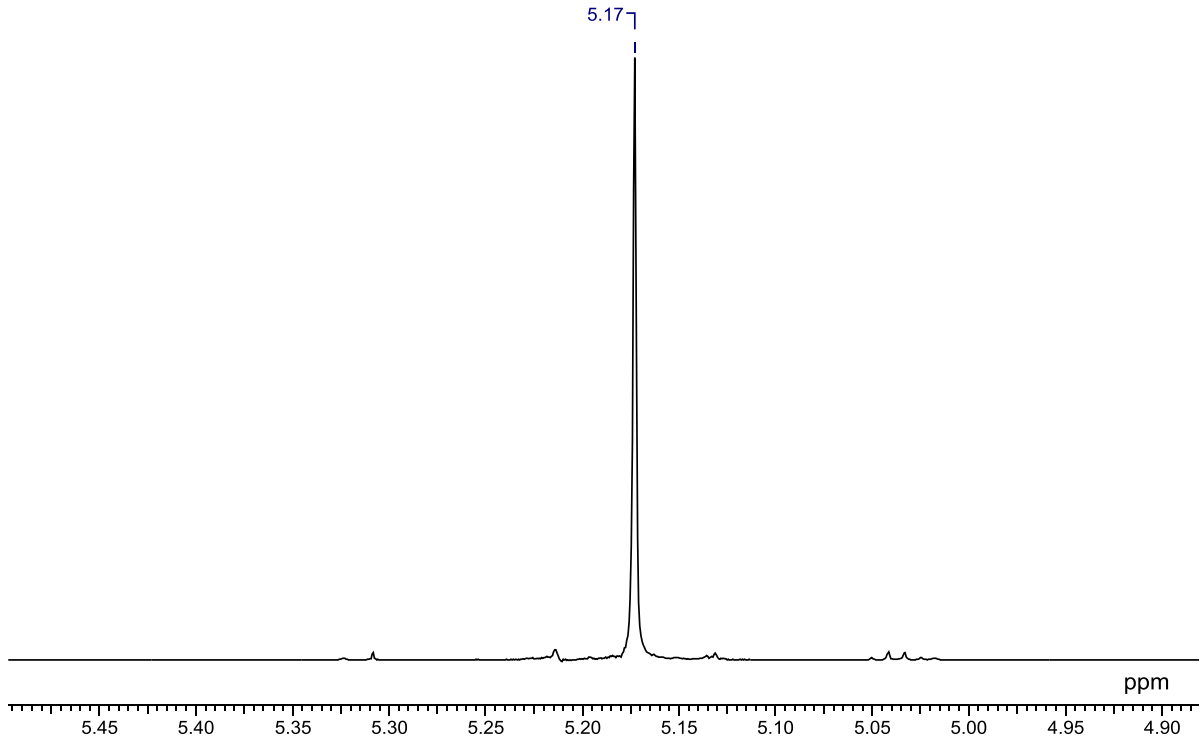

Figure SI60: ^{1}H{^{1}H} NMR spectra of PLLA produced by Zn(**1**)$_2$ (180°C, 10000:1:100) (Table 5, entry 1).

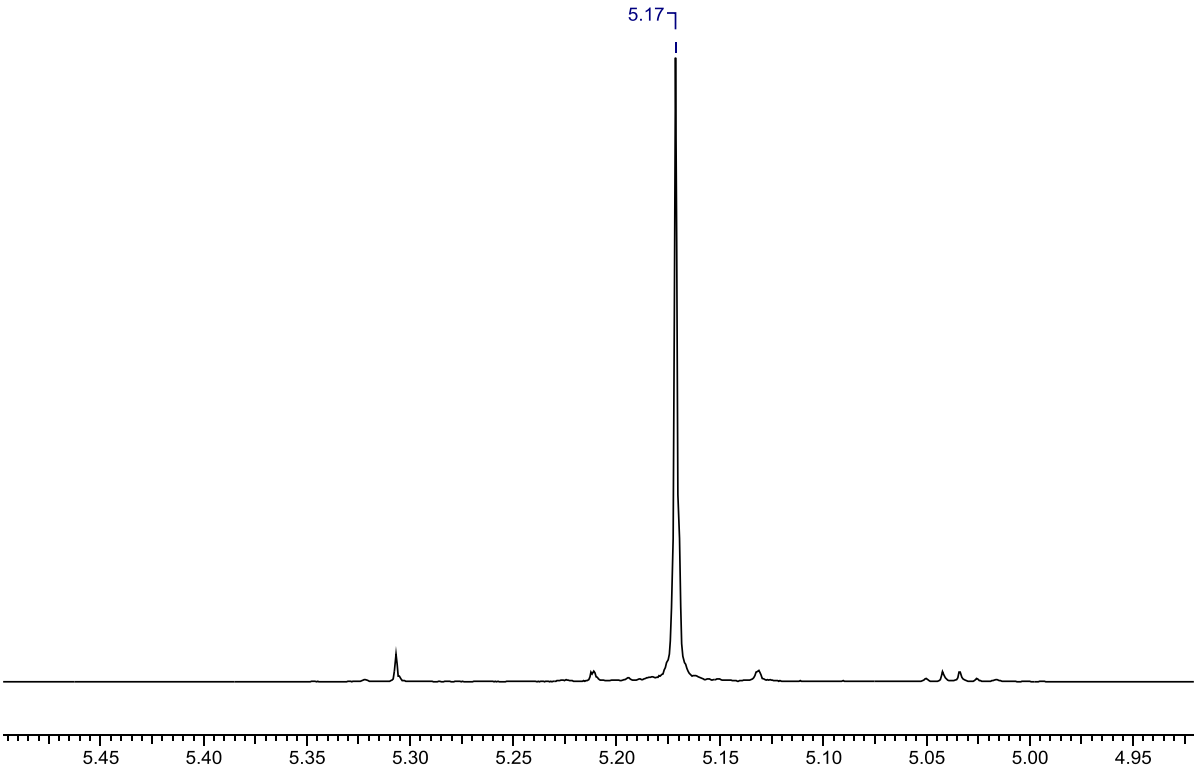

Figure SI61: $^{1}H\{^{1}H\}$ NMR spectra of PLLA produced by Zn(**4**)$_2$ (180°C, 10000:1:100) (Table 5, entry 2).

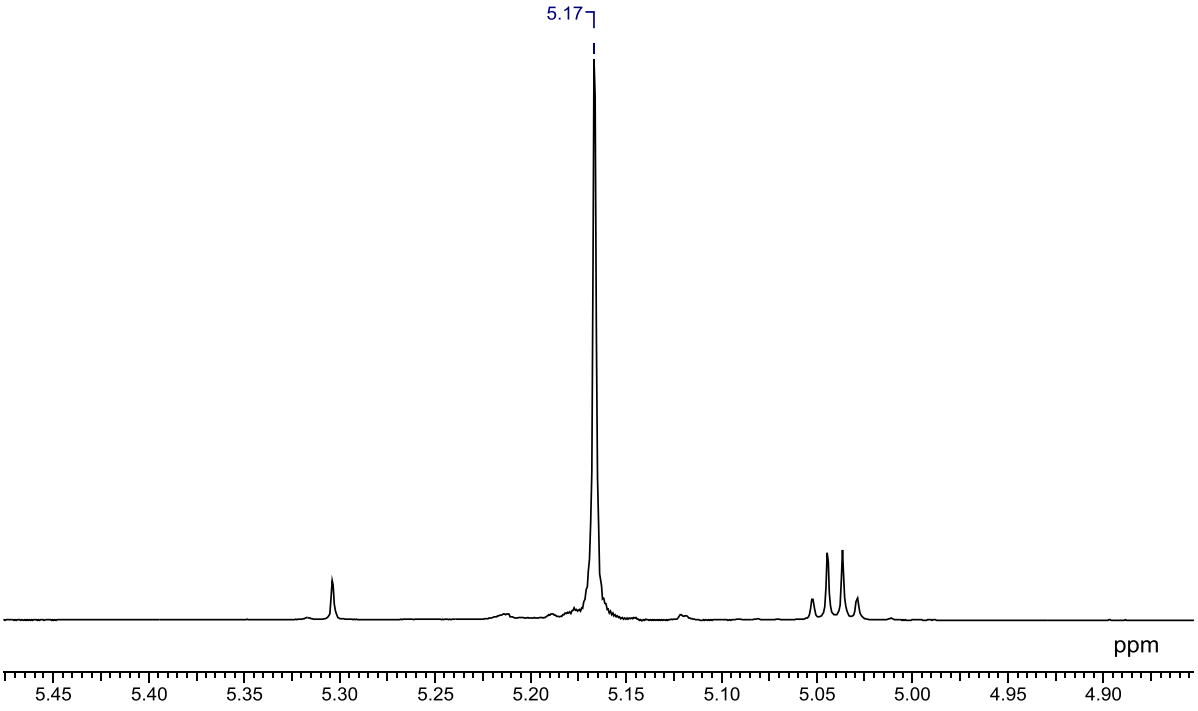

Figure SI62: $^{1}H\{^{1}H\}$ NMR spectra of PLA produced by Zn(**5**)$_2$ (180°C, 10000:1:100)(Table 5, entry 3).

Stereocomplexation data

Table SI1. Stereocomplexation for polymerisation of *L/D*-lactide at 180°C with Zn(II) complexes.

Init.	[LA]:[I]:[BnOH][a]	Time / min	Conv %[a]	$M_{n/theo}$[b]	M_n[c]	Đ[c]	T_m / °C[d]
Zn(1)$_2$	(3000):1:10	5	95	42000	33400	1.62	190

Conditions: ([*L*-LA]+[*D*-LA]):[I]:[BnOH] = (3000):1:10, solvent free (180°C) [a] Determined *via* ^{1}H NMR spectroscopy. [b] Theoretical molecular weight based on conversion and co-initiator added $\{(M_{r,LA} \times 3 \times \%_{conv}) + M_{n,BnOH}\}$. [c] Molecular weight via GPC analysis (in THF). A correction factor of 0.58 has been applied. [d] Determined by DSC.

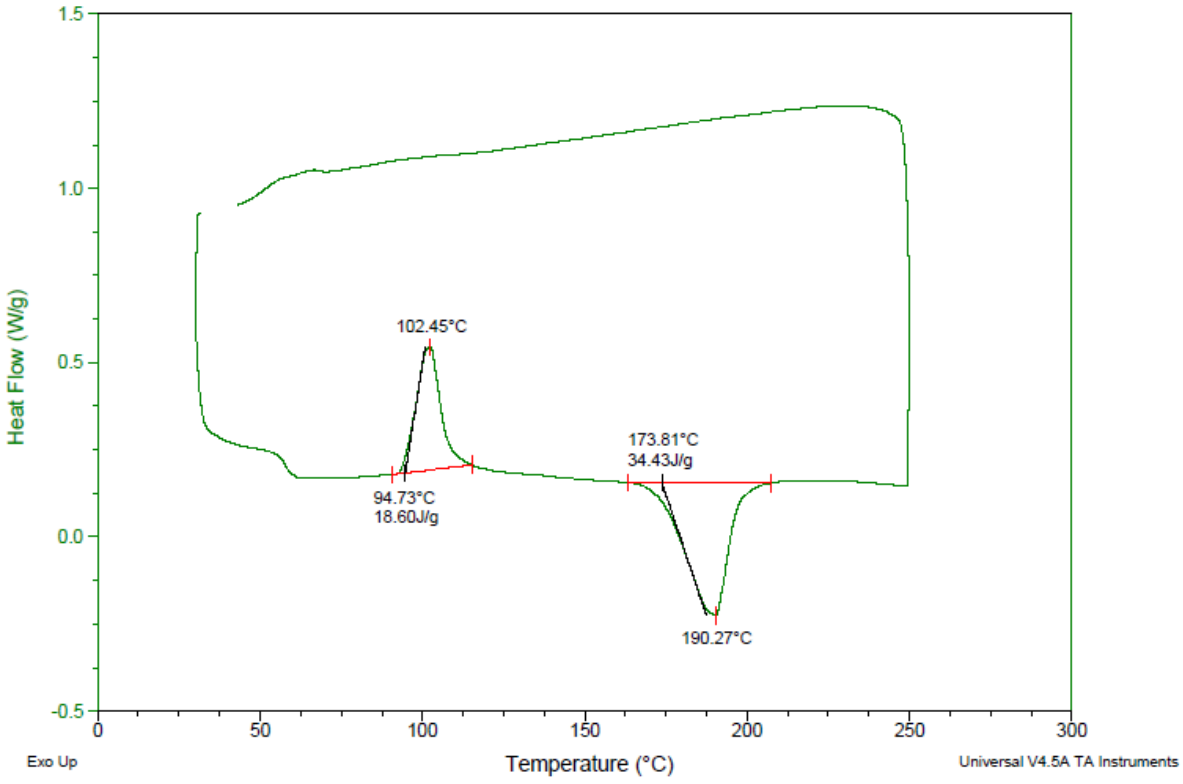

Figure SI63: DSC trace of stereocomplex produced by Zn(**1**)$_2$ (Table SI1).

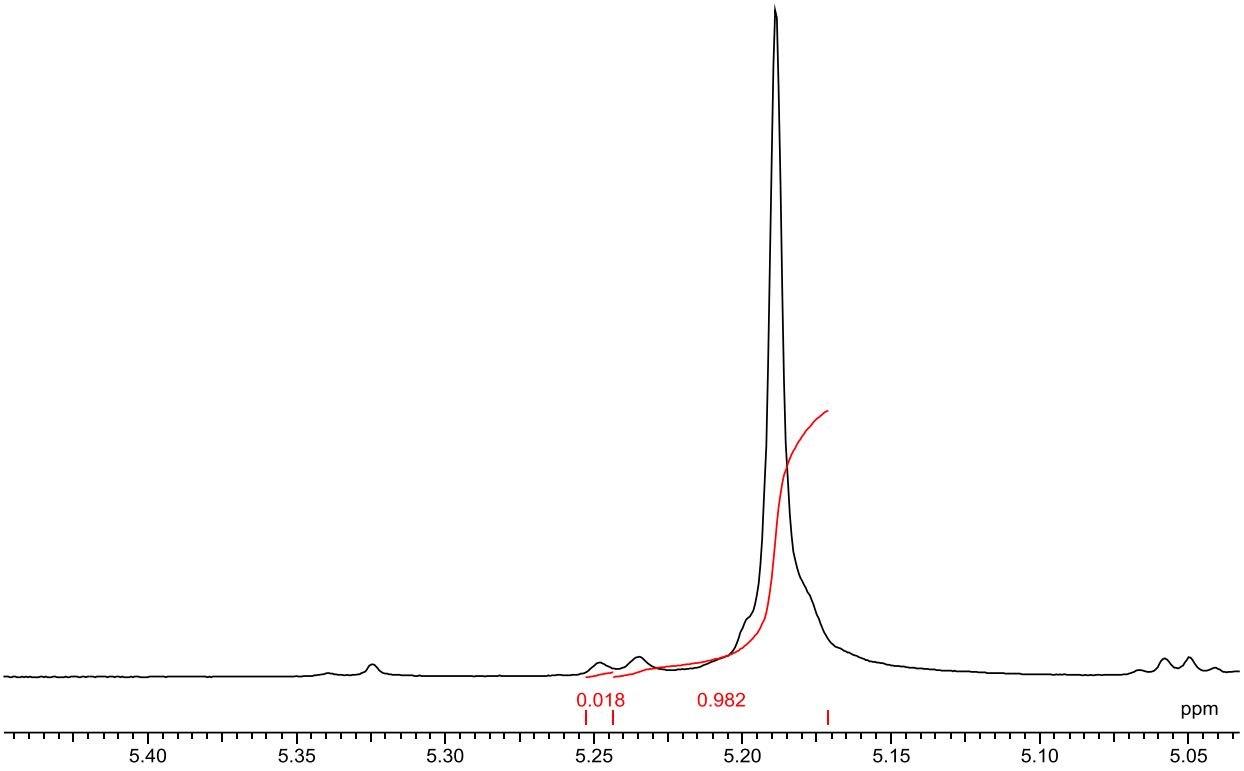

Figure SI64: $^{1}H\{^{1}H\}$ NMR spectra of stereocomplexed PLA produced by Zn(**1**)$_2$ (180°C, 3000:1:10) (Table SI1).

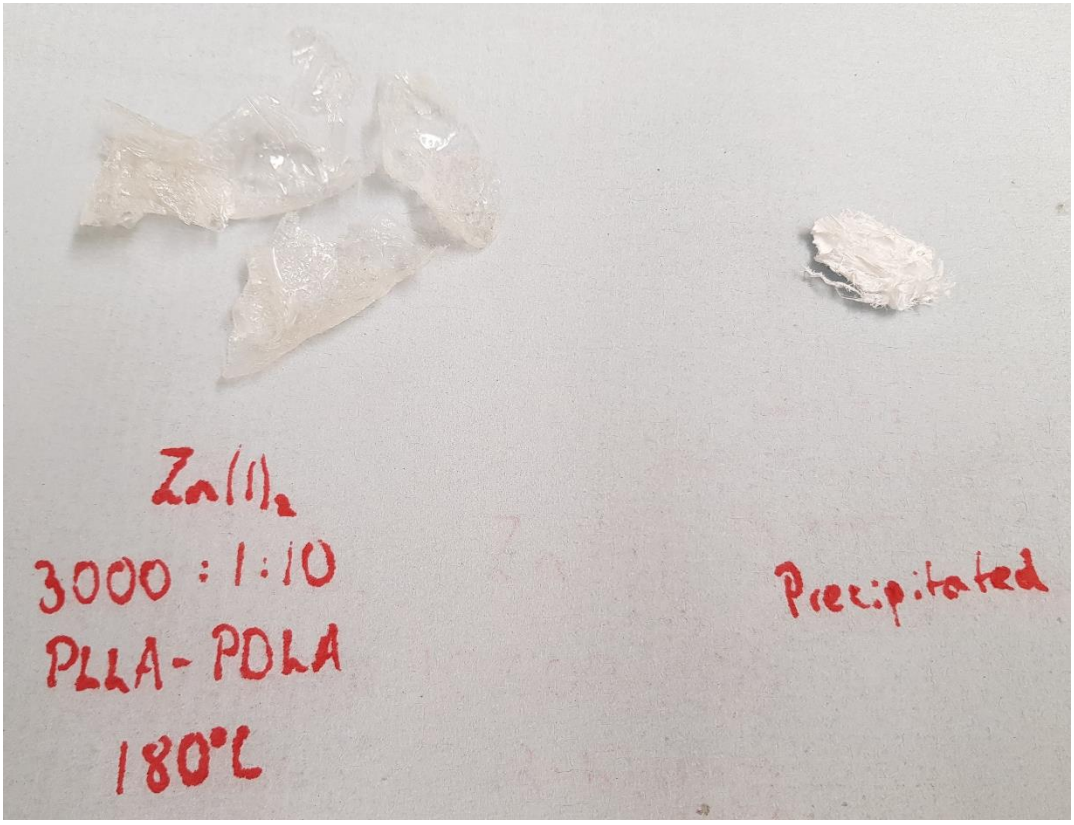

Figure SI65: PLLA-PDLA produced by Zn(**1**)$_2$ (180°C, 3000:1:10) (Table SI1, entry 1).

Select homonuclear decoupled data

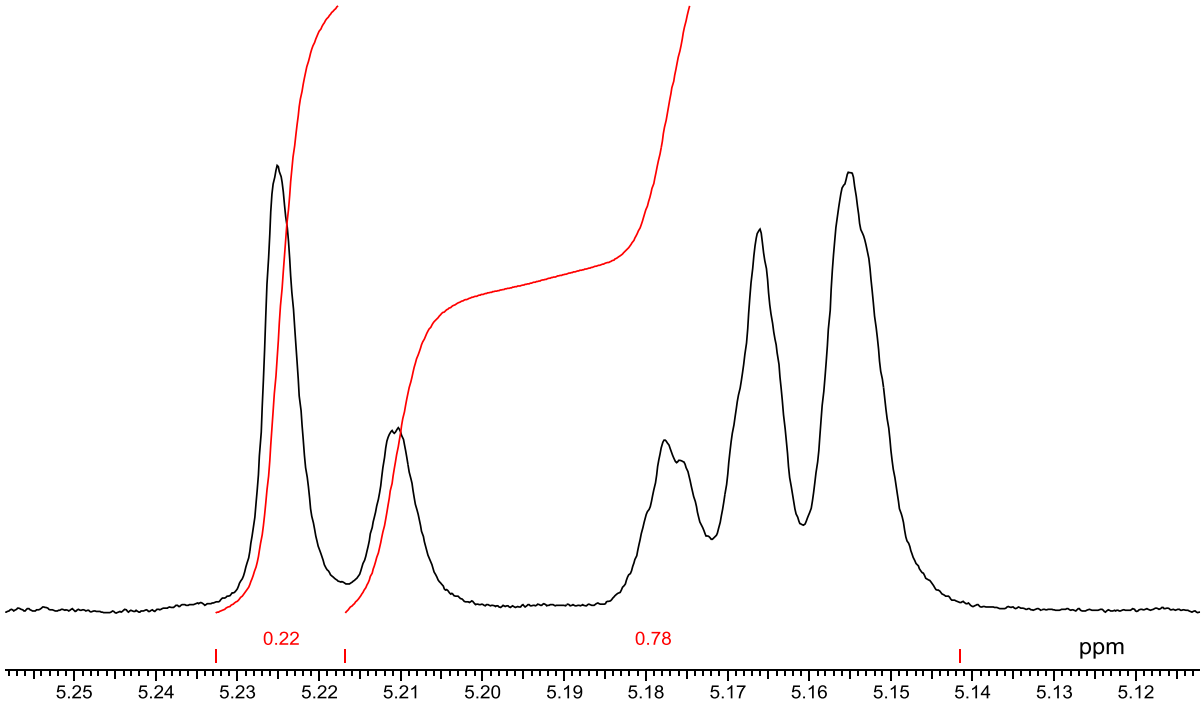

Figure SI66: $^{1}H\{^{1}H\}$ NMR spectra of PLA produced by Zn(**5**)$_2$ (130°C, *rac*-LA 300:1:1) (Table 1, entry 6).

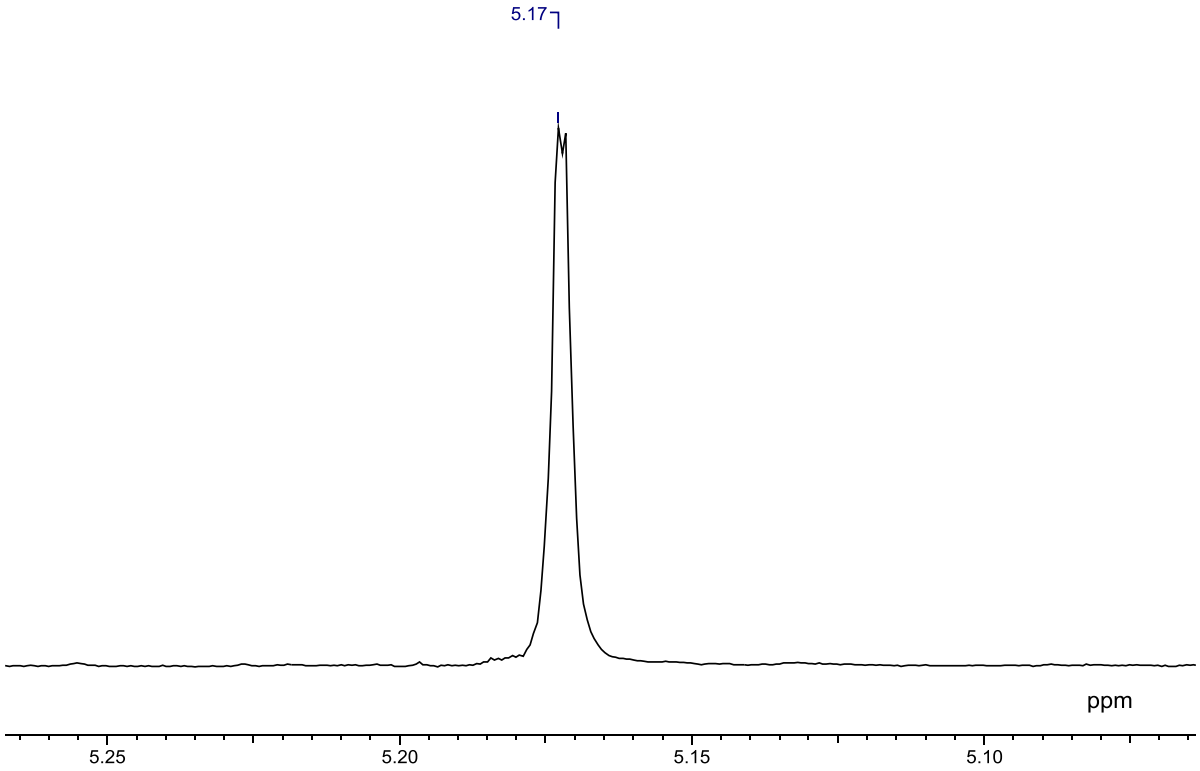

Figure SI67: $^{1}H\{^{1}H\}$ NMR spectra of PLLA produced by Zn(**1**)$_2$ (180°C, 10000:1) (Table 4, entry 4).

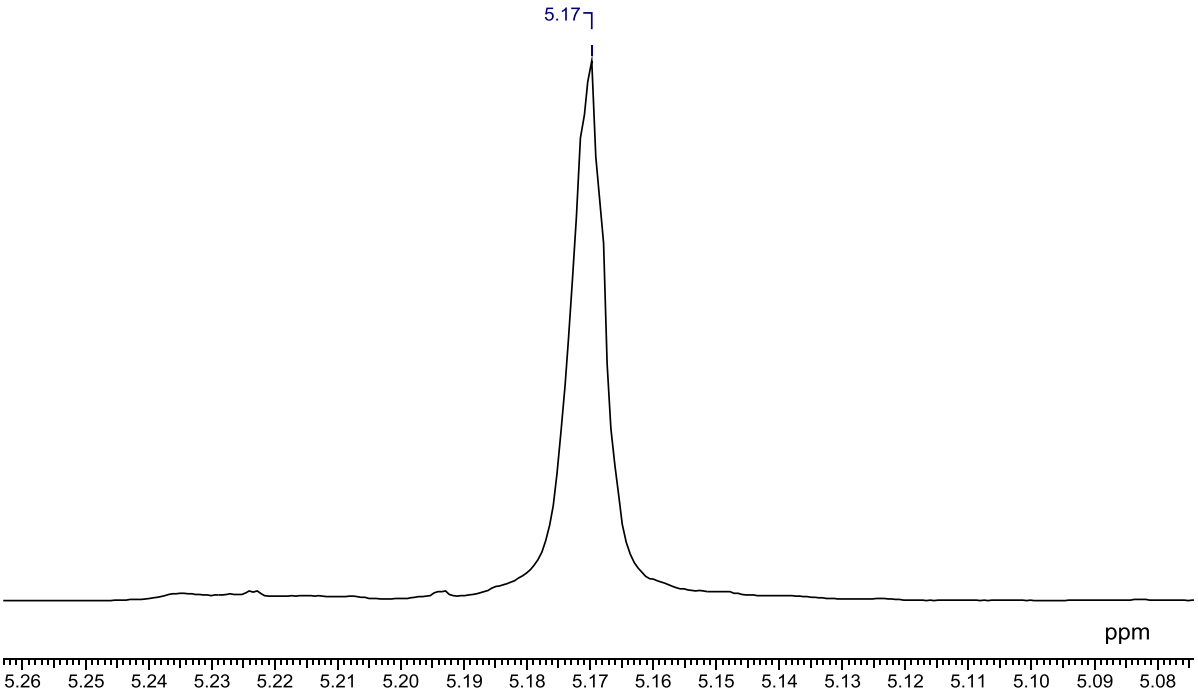

Figure SI68: $^{1}H\{^{1}H\}$ NMR spectra of PLLA produced by Zn(**7**)$_2$ (180°C, 10000:1:100) (Table 4, entry 10).

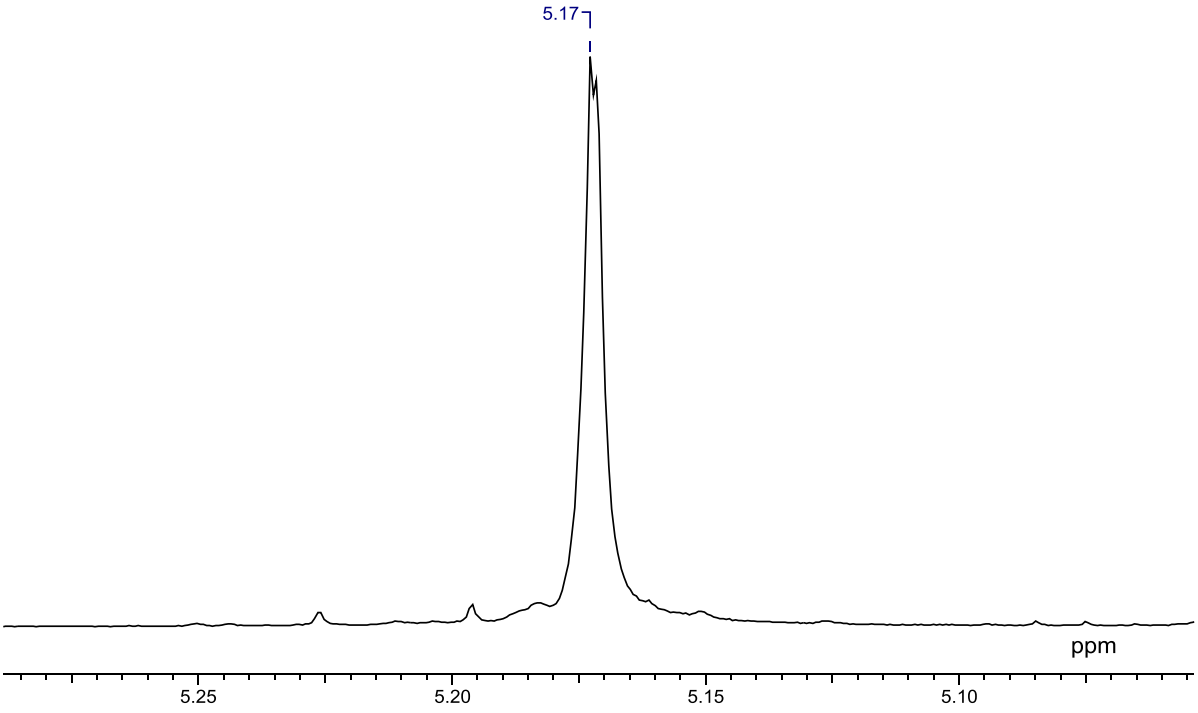

Figure SI69: $^{1}H\{^{1}H\}$ NMR spectra of PLLA produced by Mg(**1**)$_2$ (180°C, 10000:1:100) (Table 4, entry 12).

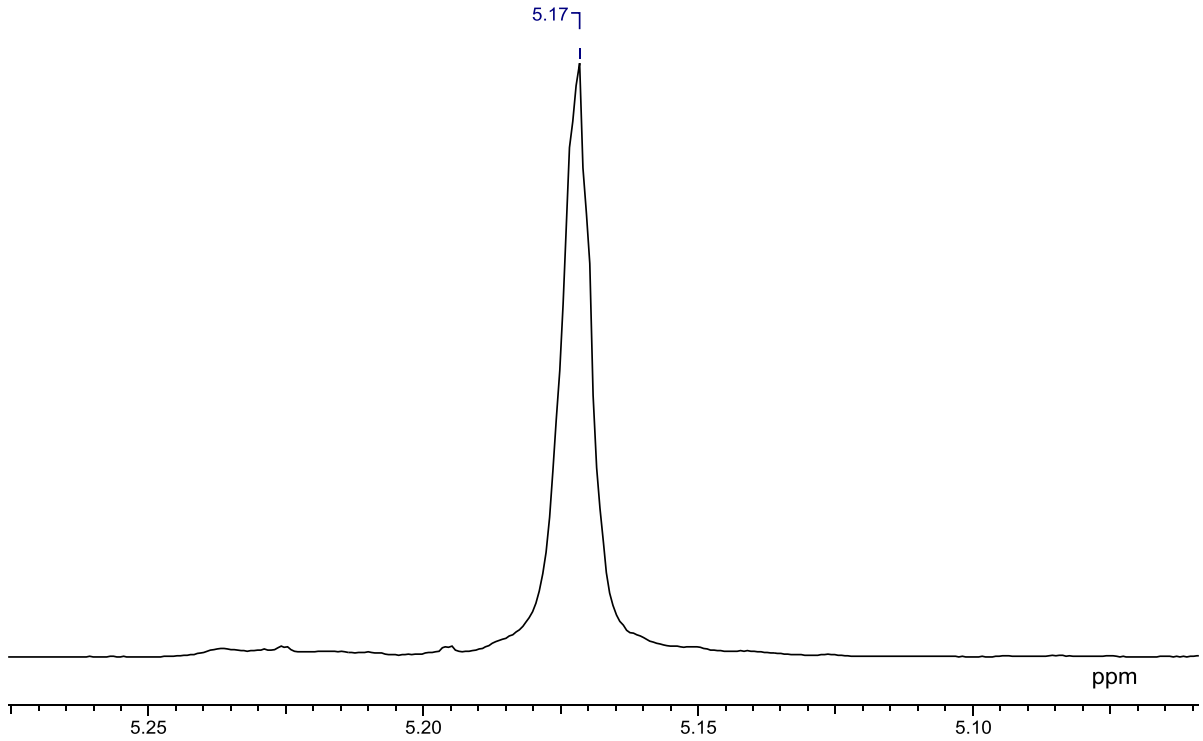

Figure SI70: $^{1}H\{^{1}H\}$ NMR spectra of PLLA produced by Mg(**5**)$_2$ (180°C, 10000:1:100) (Table 4, entry 13).

MALDI-ToF spectra

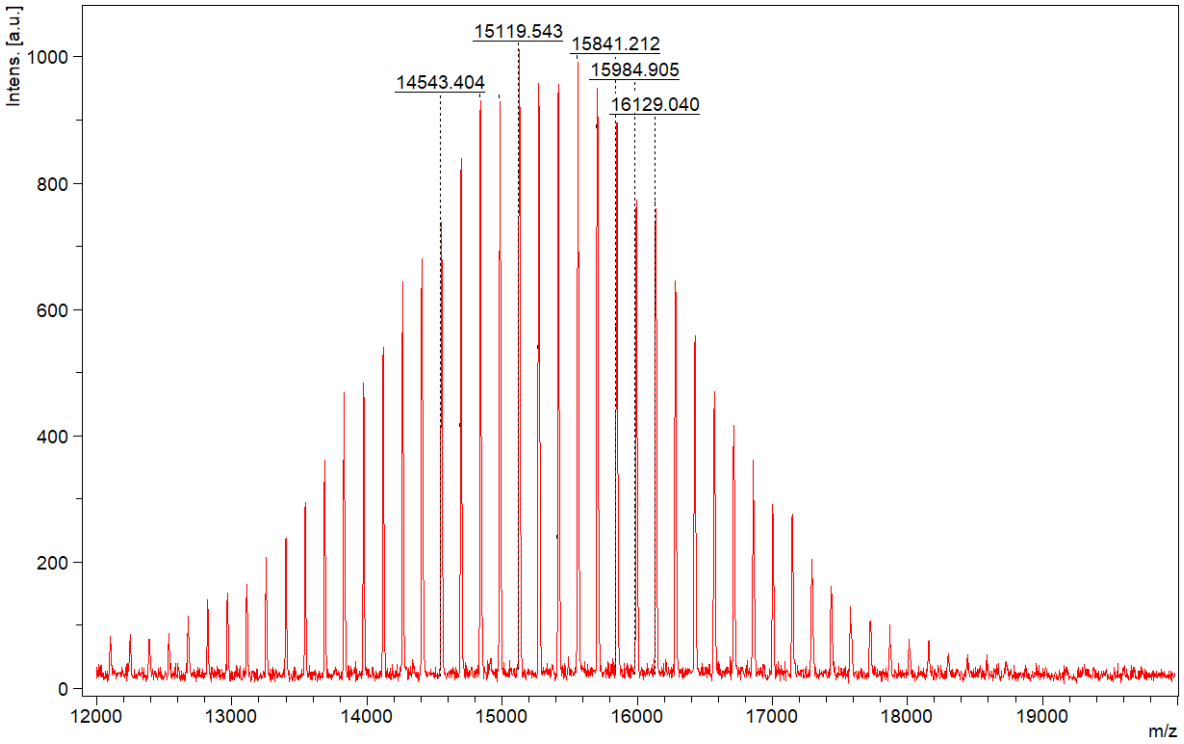

Figure SI71: MALDI-ToF spectra of PLA produced by Zn(**6**)$_2$ (130°C, 300:1:1)(Table 1, entry 7).

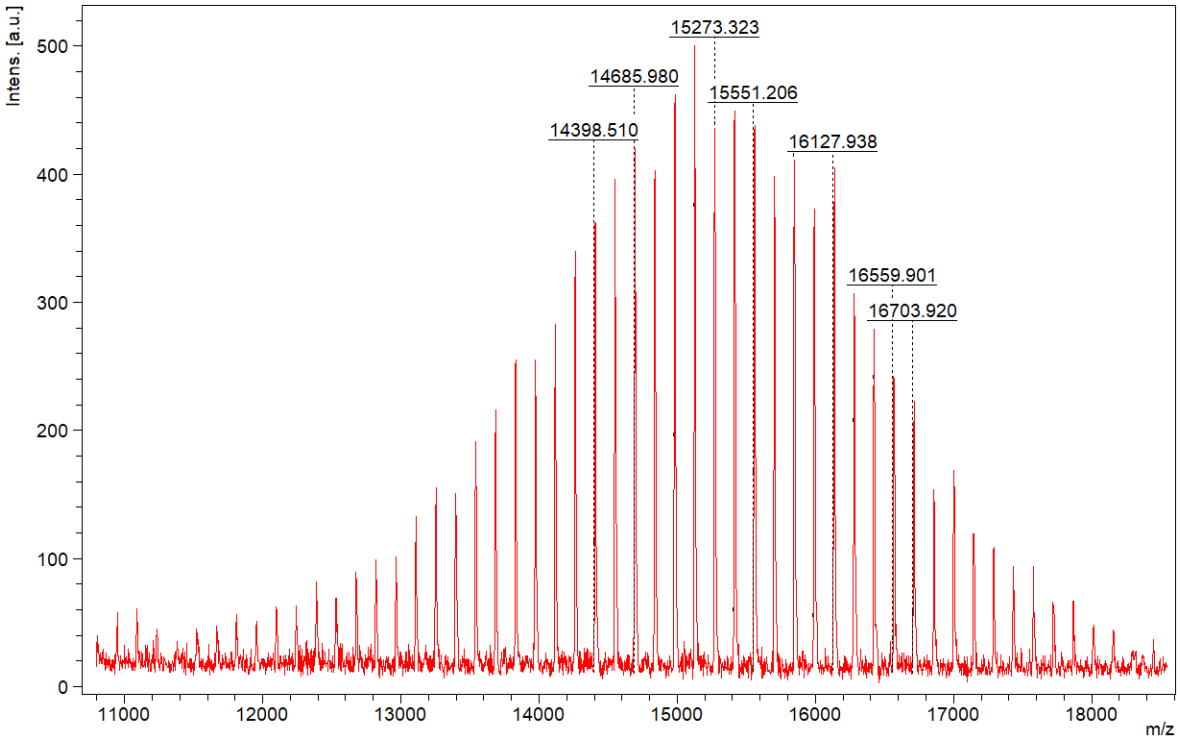

Figure SI72: MALDI-ToF spectra of PLA produced by Zn(**7**)$_2$ (130°C, 300:1:1) (Table 1, entry 8).

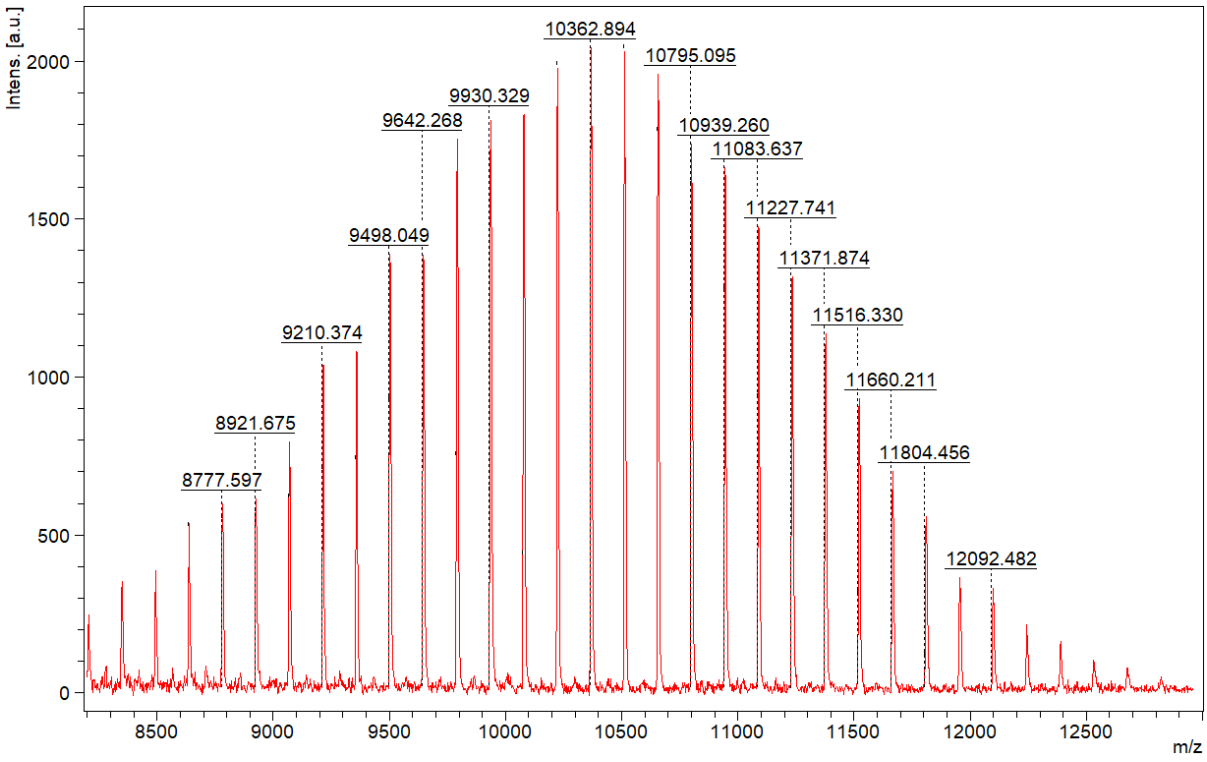

Figure SI73: MALDI-ToF spectra of PLA produced by Zn(**1**)$_2$ (130°C, 10000:1:100)(Table 3, entry 1).

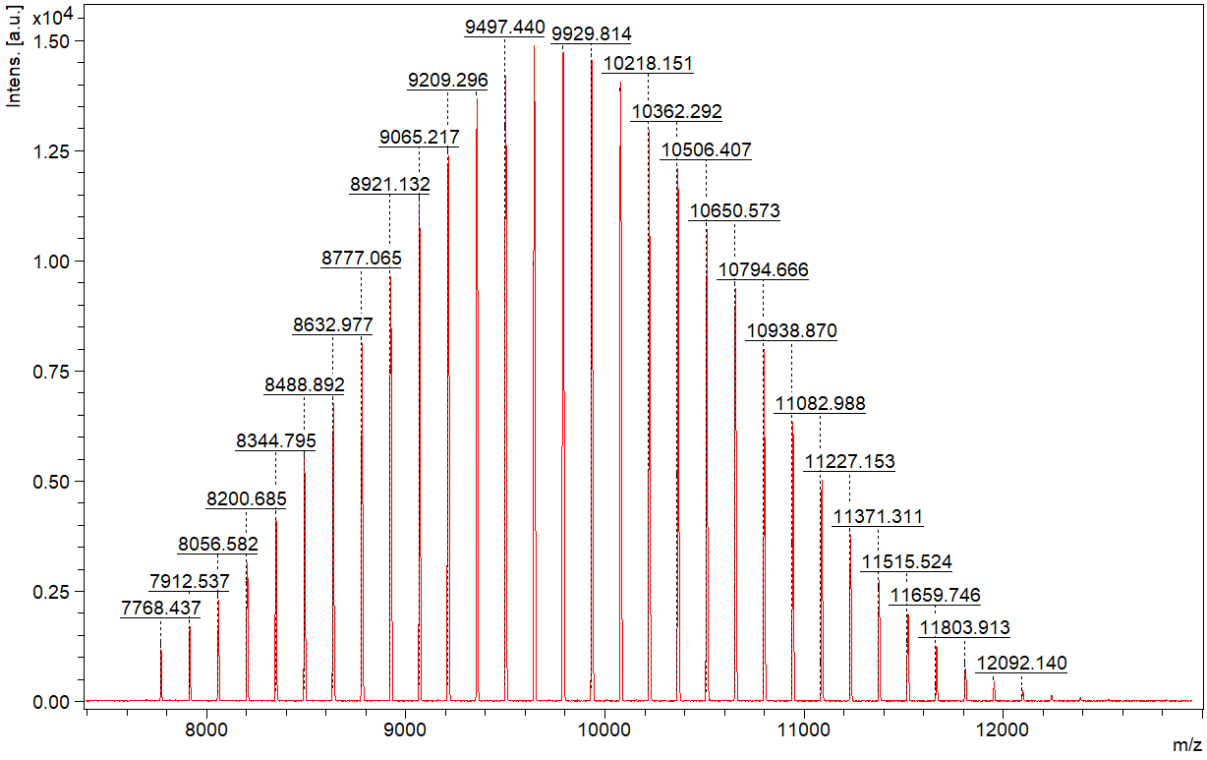

Figure SI74: MALDI-ToF spectra of PLA produced by Zn(**4**)$_2$ (130°C, 10000:1:100) (Table 3, entry 2).

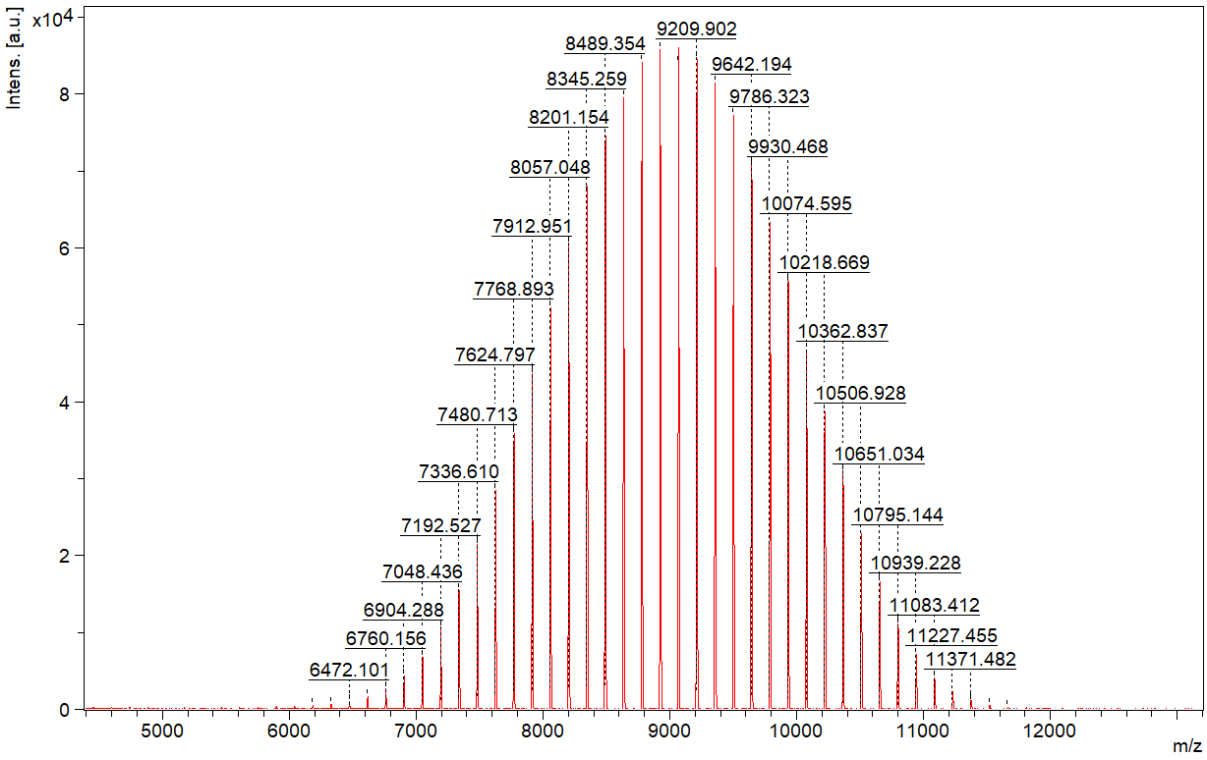

Figure SI75: MALDI-ToF spectra of PLA produced by Zn(**5**)$_2$ (130°C, 10000:1:100) (Table 3, entry 3).

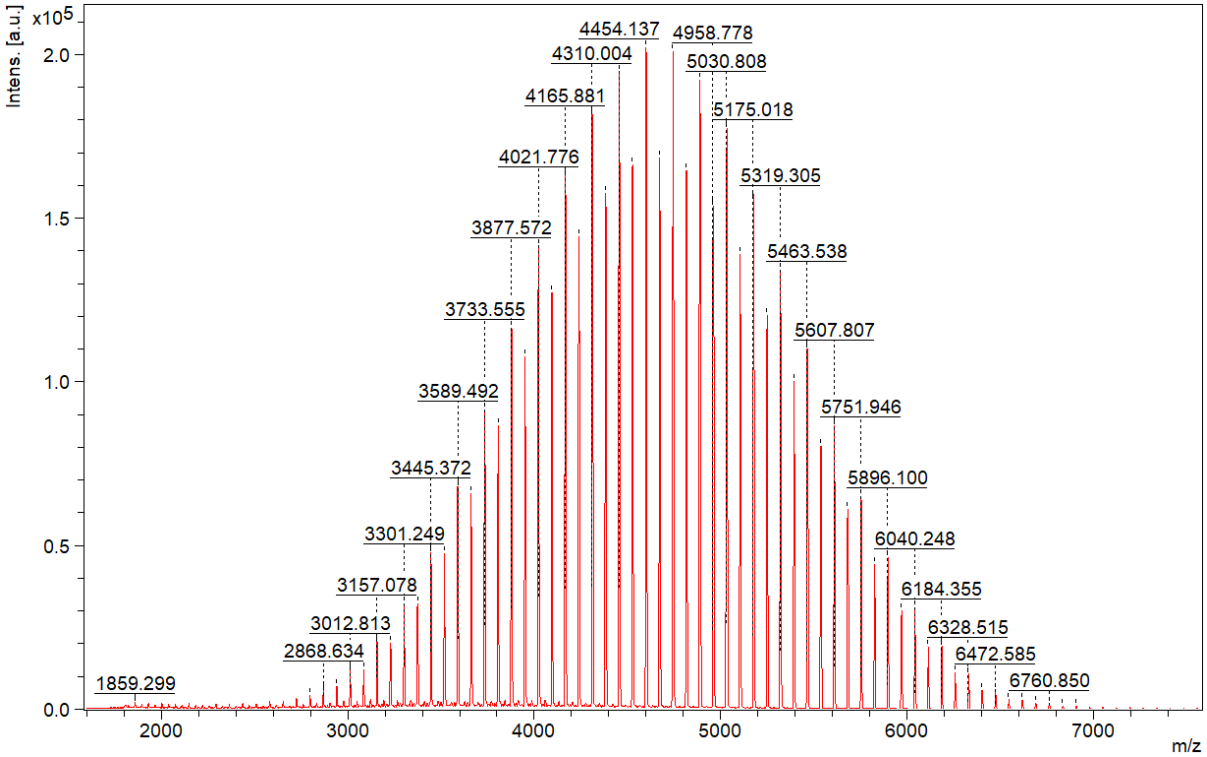

Figure SI76: MALDI-ToF spectra of PLA produced by Mg(**1**)$_2$ (130°C, 10000:1:100) (Table 3, entry 4).

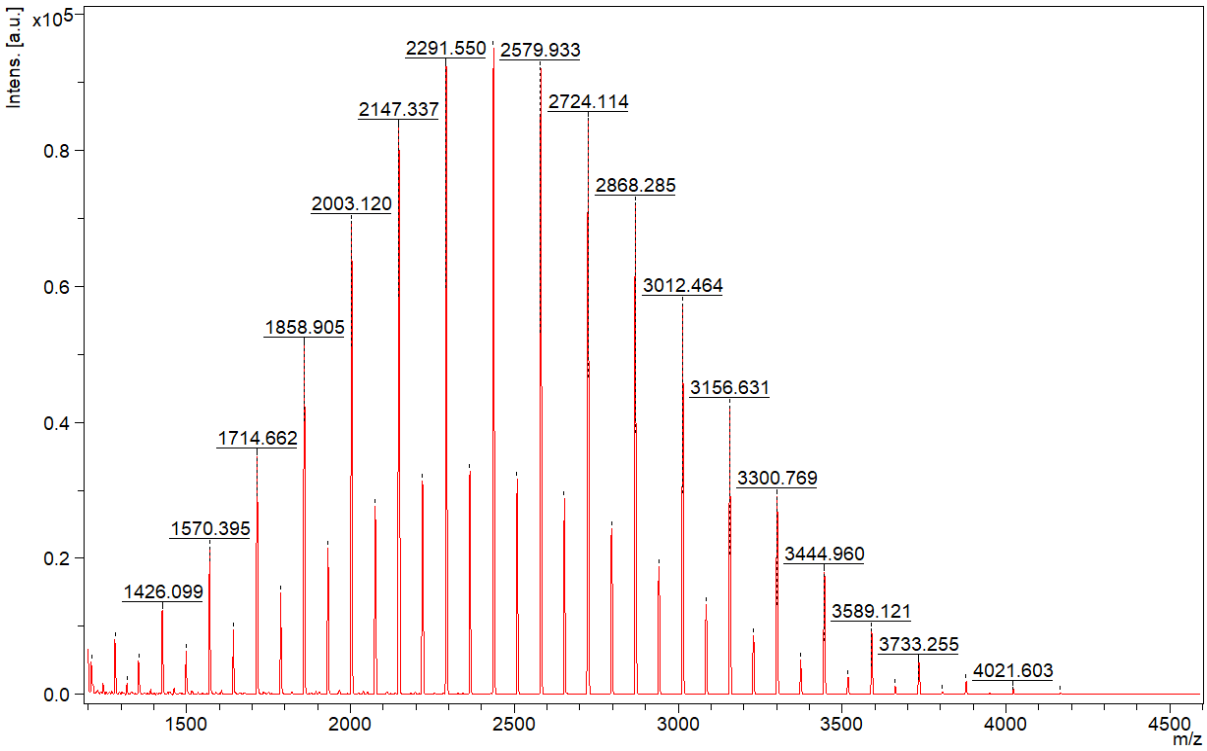

Figure SI77: MALDI-ToF spectra of PLA produced by Mg(**5**)$_2$ (130°C, 10000:1:100) (Table 3, entry 5).

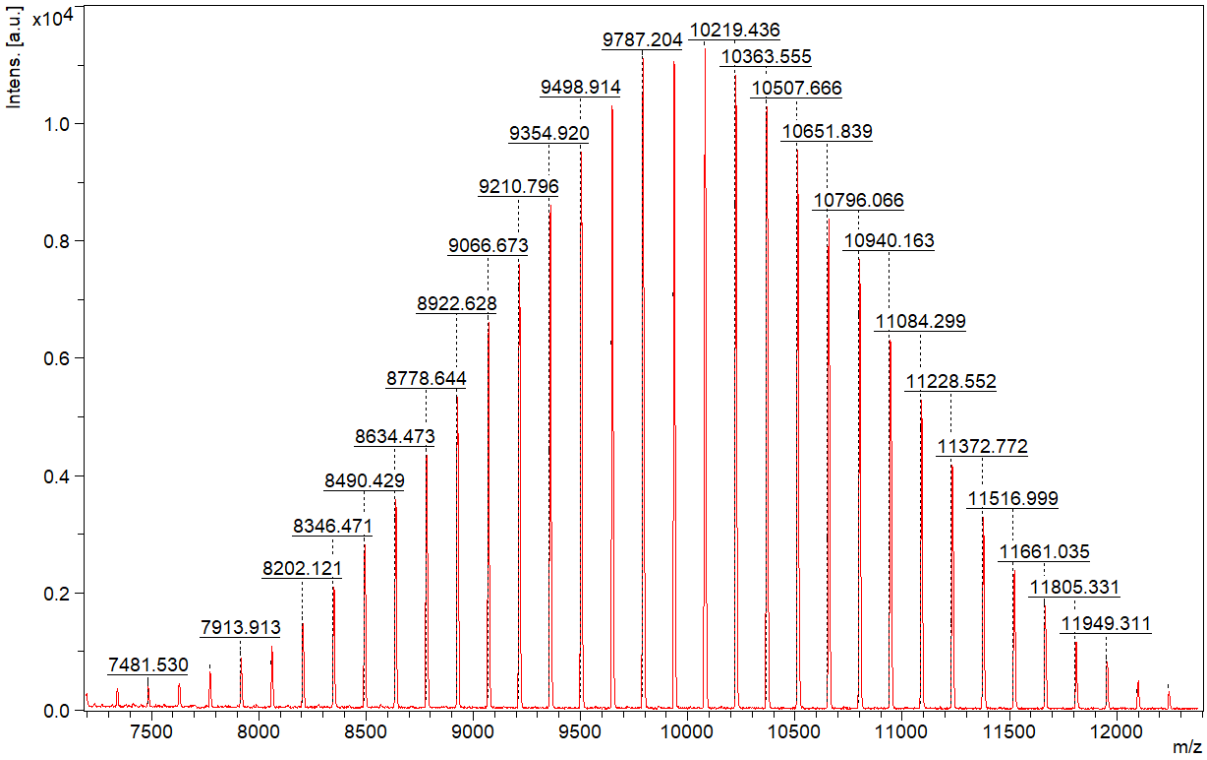

Figure SI78: MALDI-ToF spectra of PLA produced by Zn(**5**)$_2$ (180°C, 10000:1:100) (Table 4, entry 8).

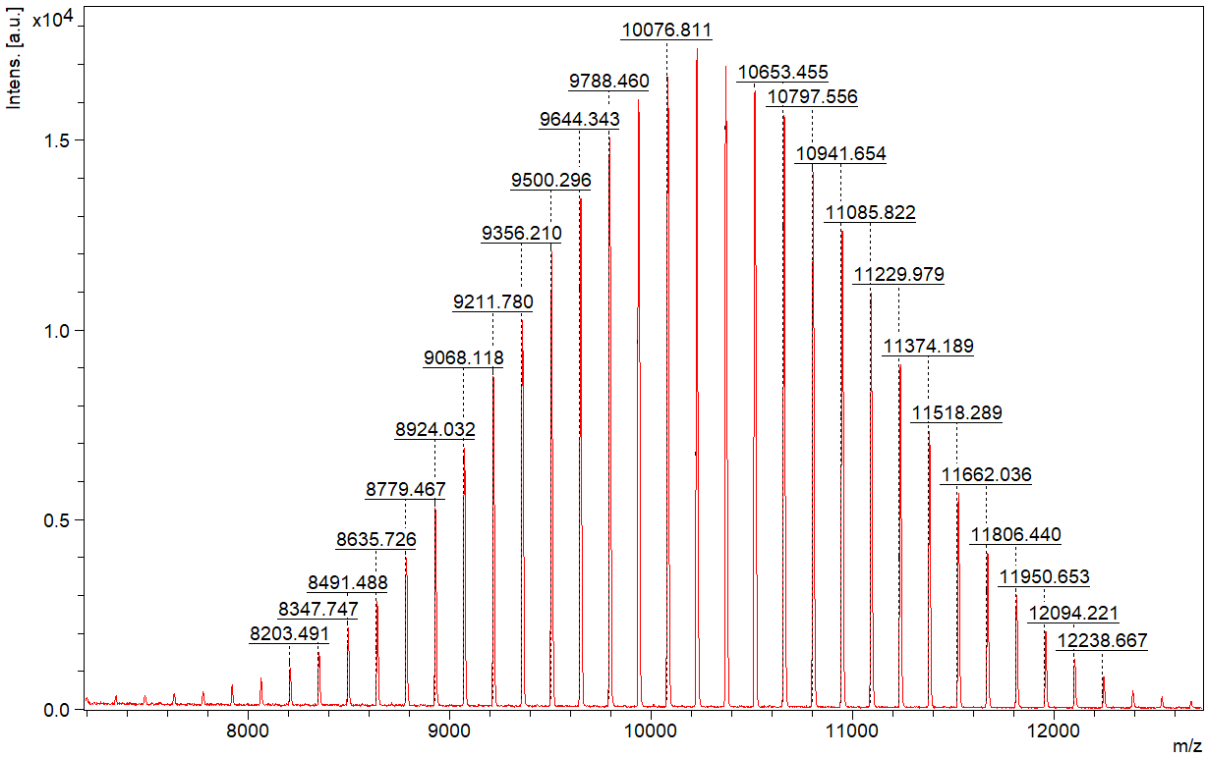

Figure SI79: MALDI-ToF spectra of PLA produced by Zn(**7**)$_2$ (180°C, 10000:1:100) (Table 4, entry 10).

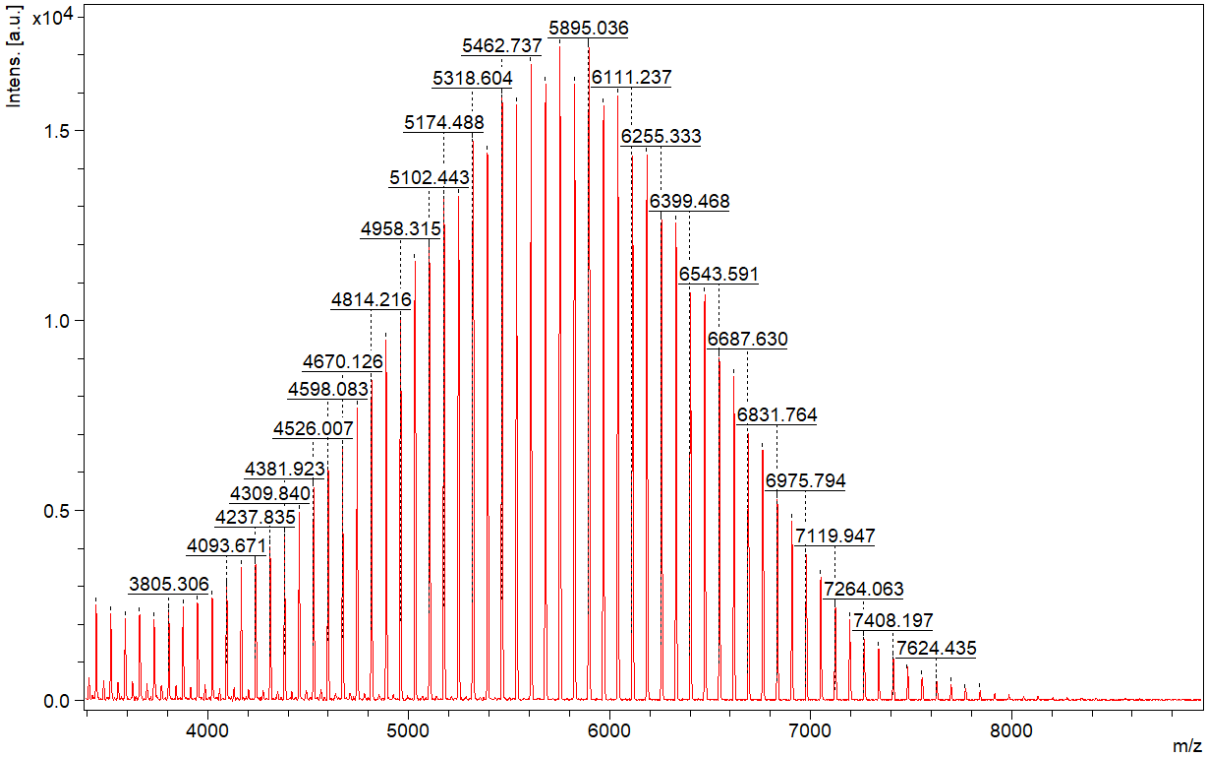

Figure SI80: MALDI-ToF spectra of PLA produced by Mg(**1**)$_2$ (180°C, 10000:1:100) (Table 4, entry 12).

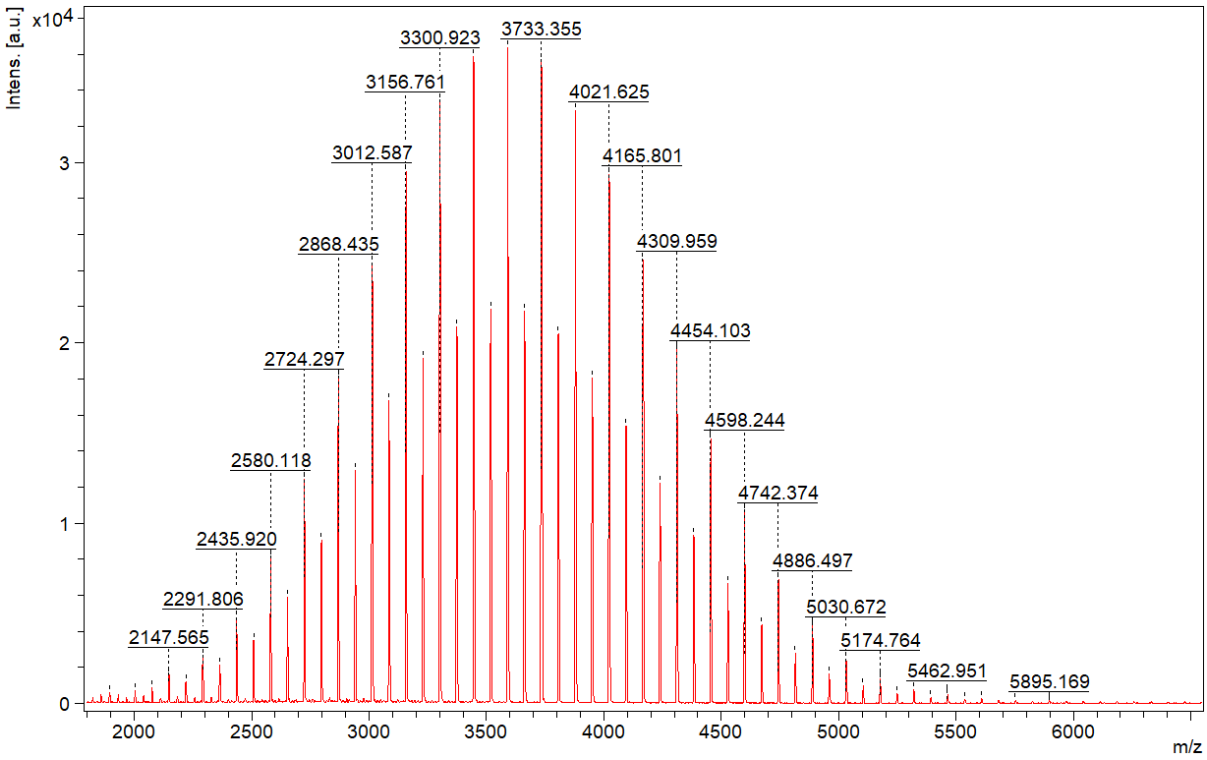

Figure SI81: MALDI-ToF spectra of PLA produced by Mg(**5**)$_2$ (180°C, 10000:1:100) (Table 4, entry 13).

Select GPC spectra

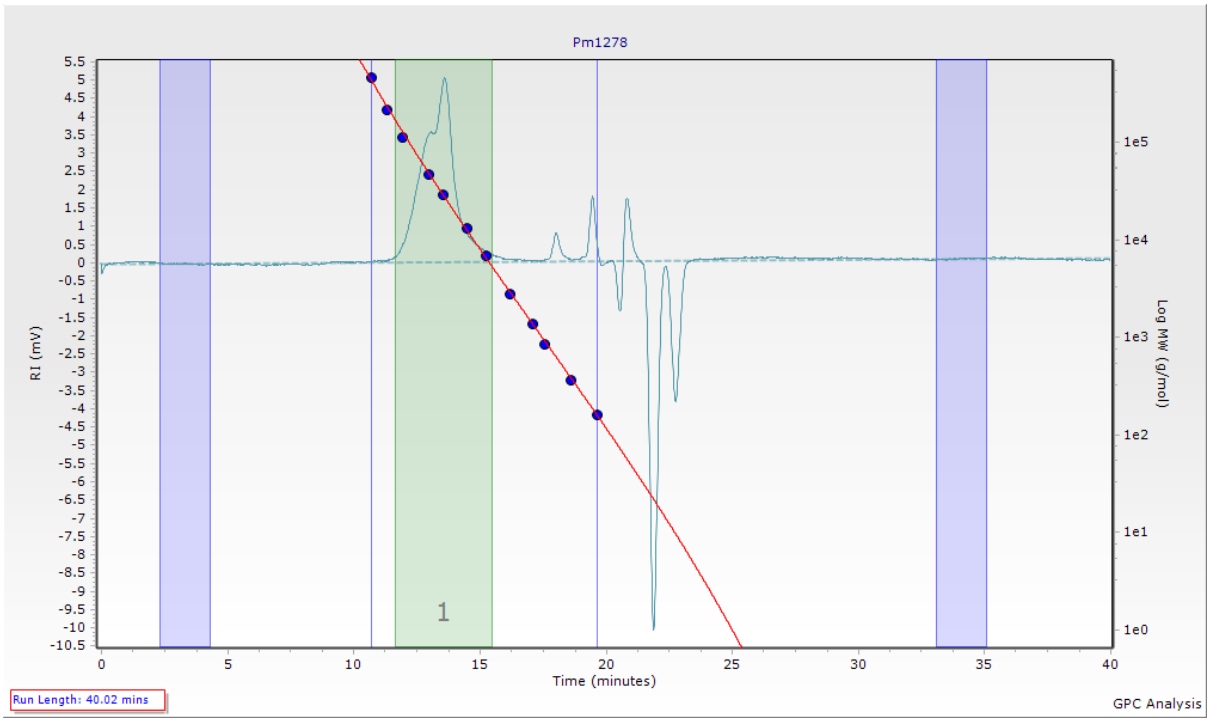

Figure SI82: GPC spectra of PLA produced by Zn(**1**)$_2$ (180°C, 10000:1:100) (Table 4, entry 1).

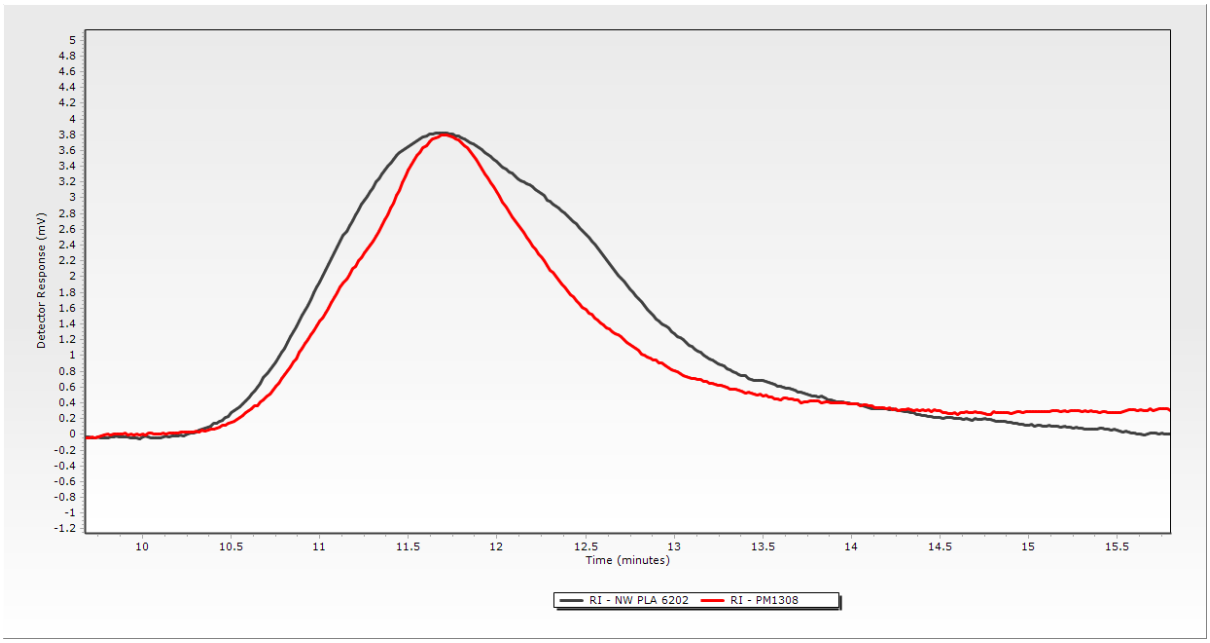

Figure SI83: GPC spectra comparing PLA produced by Zn(**1**)$_2$ (red) and commercial PLA (black) (NatureWorks, 6202D) (180°C, 10000:1:15) (Table 4, entry 3).

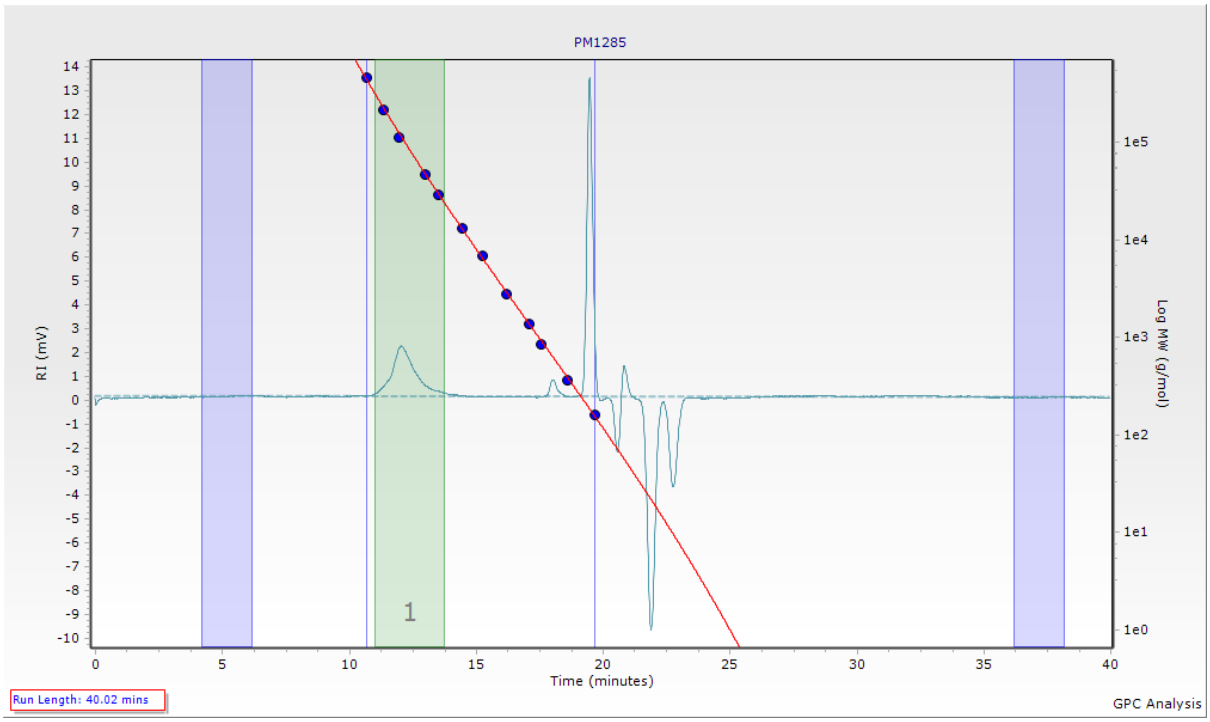

Figure SI84: GPC spectra of PLA produced by Zn(**1**)$_2$ (180°C, 10000:1) (Table 4, entry 3).

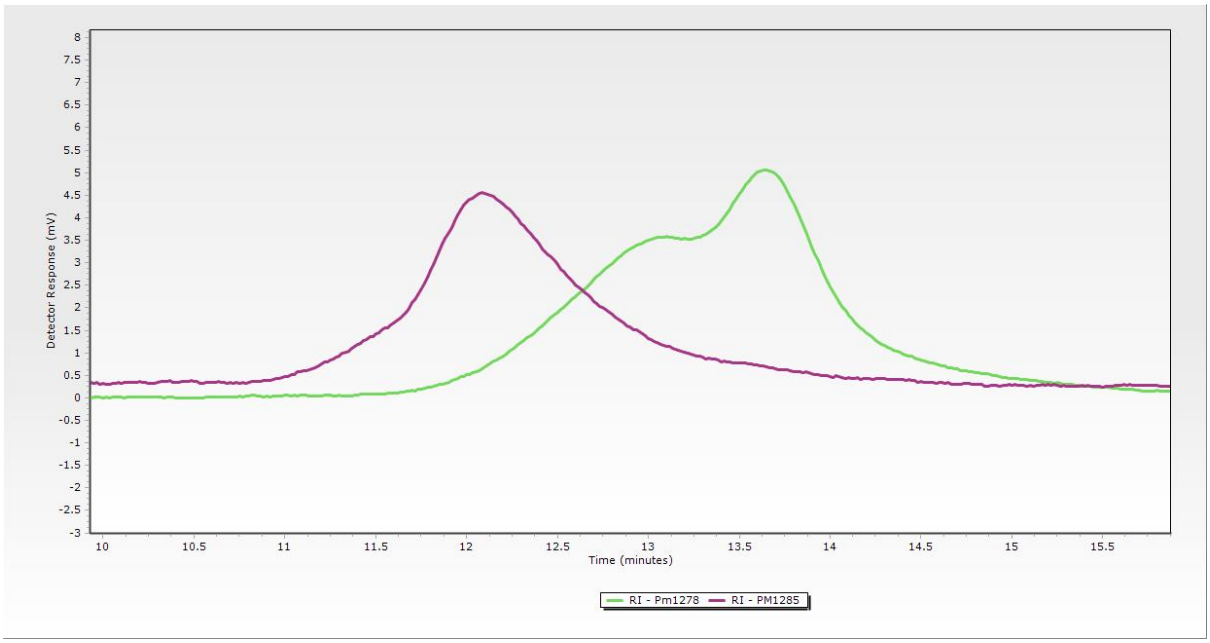

Figure SI85: GPC spectra comparing PLA produced by Zn(**1**)$_2$ with (green) and (magenta) without co-initiator (180°C, 10000:1:{100}) (Table 4, entry 1 vs. 4).

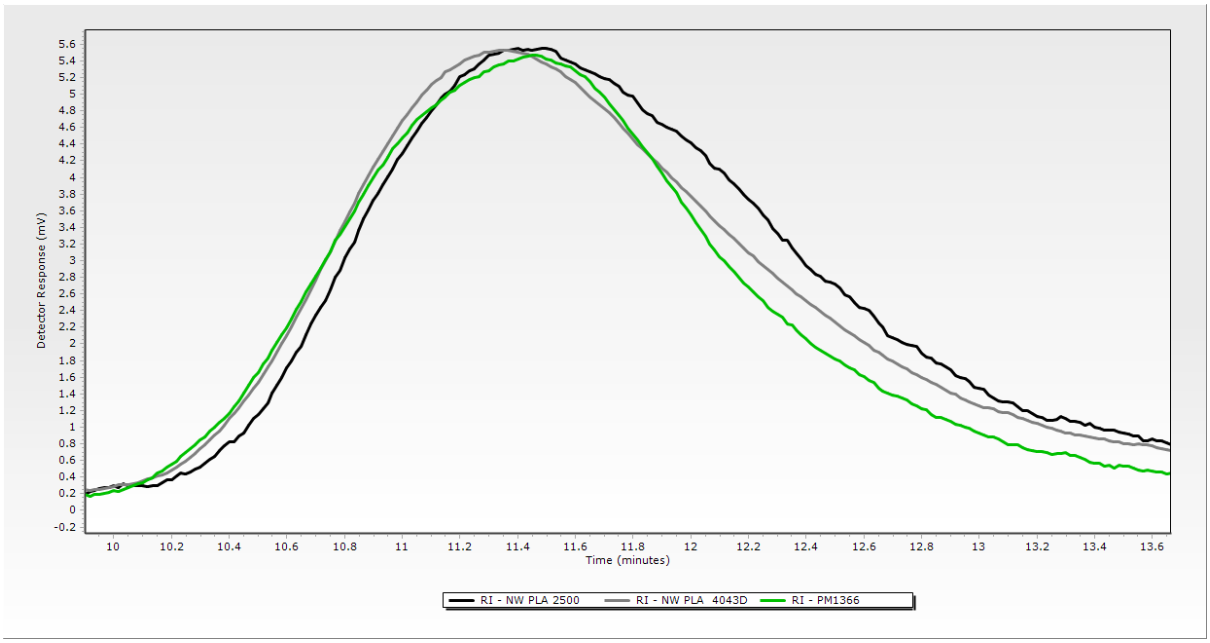

Figure SI86: GPC spectra comparing PLA produced by Zn(**1**)$_2$ (green) and commercial PLA (black/gray) (NatureWorks, 4043D/2500HP) (180°C, 10000:1) (Table 4, entry 5).

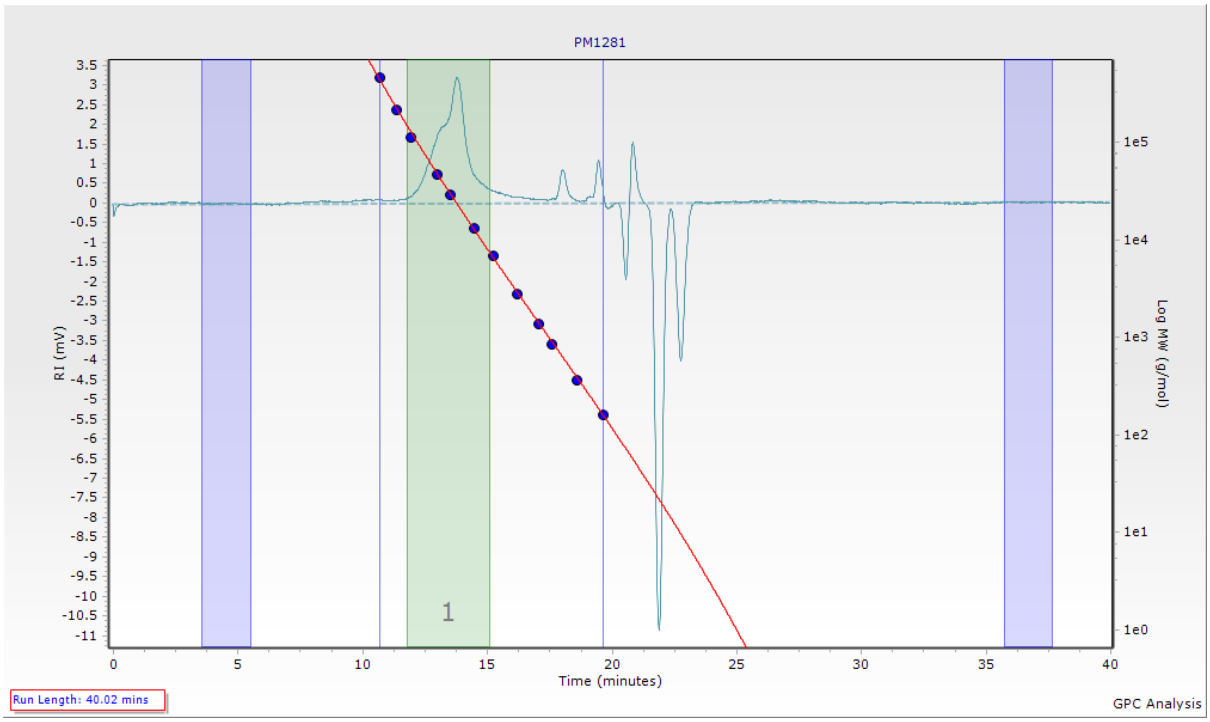

Figure SI87: GPC spectra of PLA produced by Zn(**4**)$_2$ (180°C, 10000:1:100) (Table 4, entry 6).

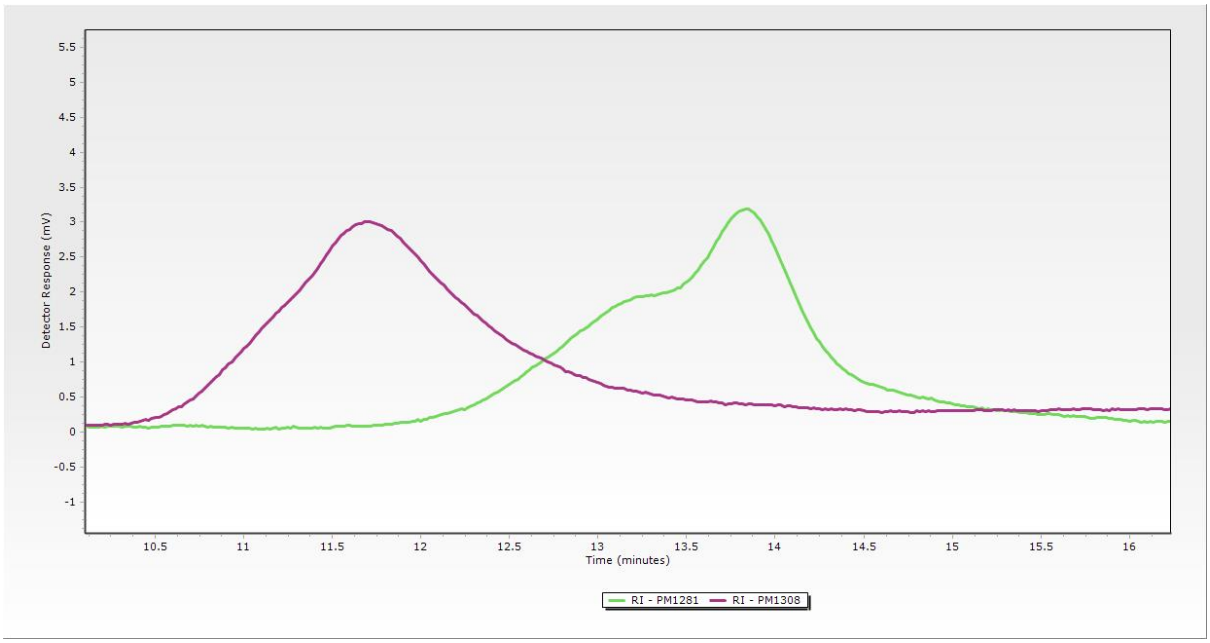

Figure SI88: GPC spectra comparing PLA produced by Zn(**4**)$_2$ (green) with and without (magenta) co-initiator (180°C, 10000:1:{100}) (Table 4, entry 6 vs. 7).

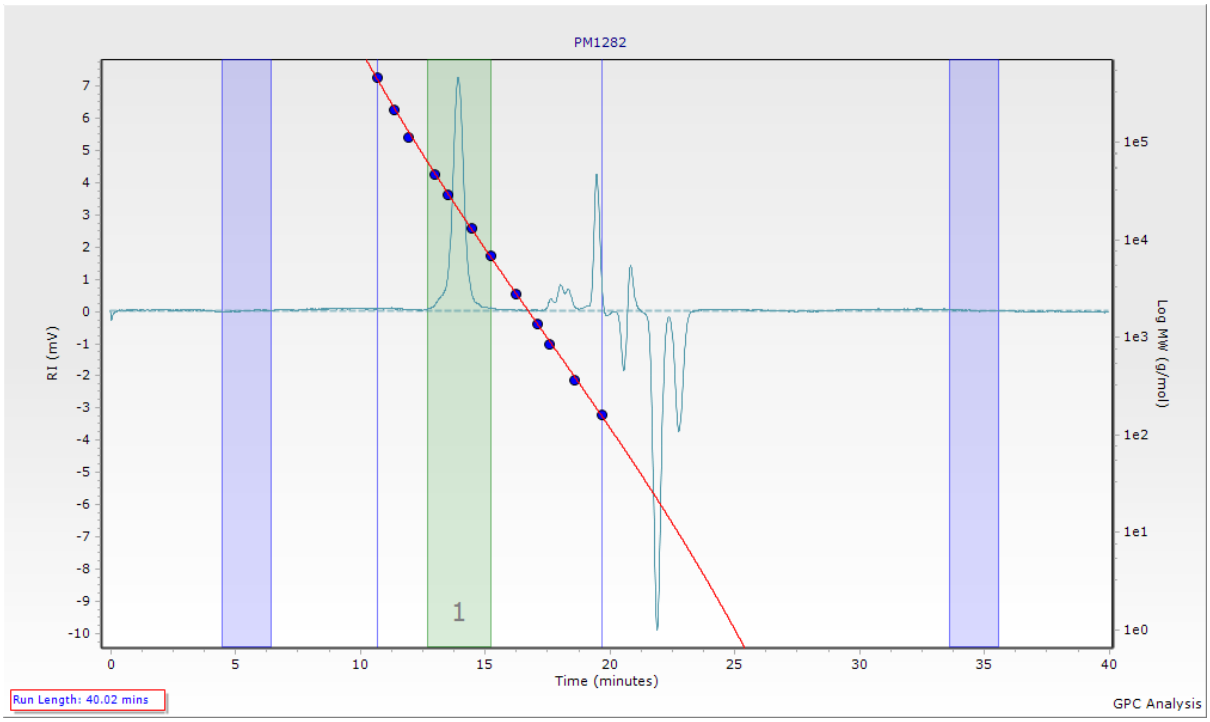

Figure SI89: GPC spectra of PLA produced by Zn(**5**)$_2$ (180°C, 10000:1:100) (Table 4, entry 8).

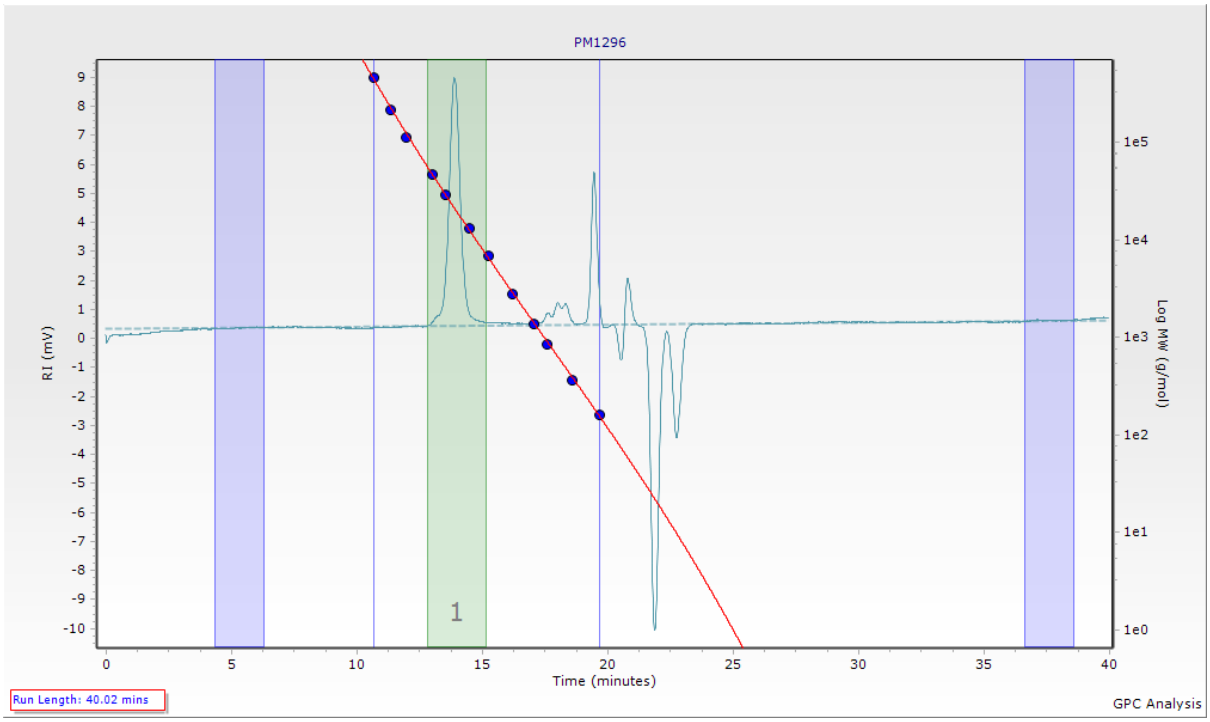

Figure SI90: GPC spectra of PLA produced by Zn(**7**)$_2$ (180°C, 10000:1:100) (Table 4, entry 10).

Crystallographic data

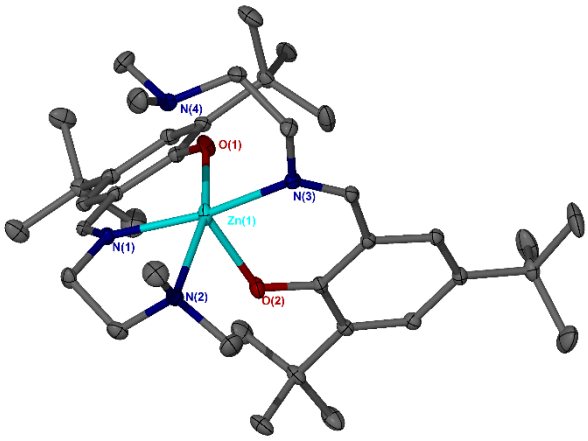

Figure SI91: Solid-state structure of Zn(**5**)$_2$. Ellipsoids shown at 30 % probability level and all hydrogens have been omitted for clarity.

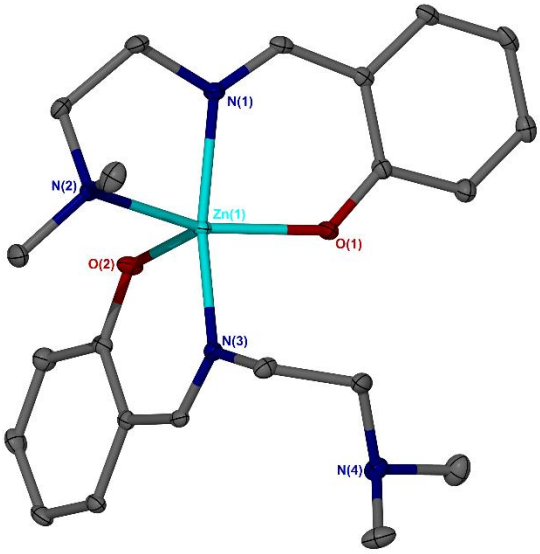

Figure SI92: Solid-state structure of Zn(**6**)$_2$. Ellipsoids shown at 30 % probability level and all hydrogens have been omitted for clarity.

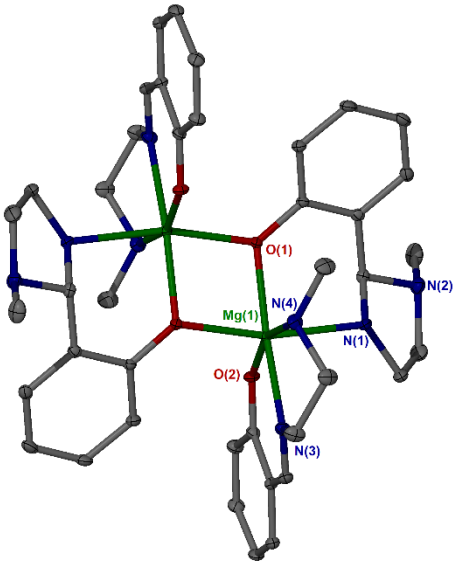

Figure SI93: Solid-state structure of Mg(**2***)(**2**). Ellipsoids shown at 30 % probability level and all hydrogens have been omitted for clarity.

Table SI2 X-ray crystallographic parameters

Compound reference	Zn(**1**)$_2$	Zn(**2**)$_2$	Zn(**3**)$_2$	Zn(**4**)$_4$	Zn(**5**)$_2$	Zn(**6**)$_2$	Mg(**1**)$_2$	Mg(**2**)(**2***)	Mg(**3**)$_2$	Mg(**5**)$_2$
Chemical formula	$C_{36}H_{58}N_4O_2Zn$	$C_{47}H_{60}N_8O_4Zn_2$	$C_{47}H_{52}Cl_8N_8O_4Zn_2$	$C_{54}H_{84}N_4O_2Zn$	$C_{38}H_{62}N_4O_2Zn$	$C_{22}H_{30}N_4O_2Zn$	$C_{36}H_{58}MgN_4O_2$	$C_{40}H_{52}Mg_2N_8O_4$	$C_{51}H_{60}Cl_8Mg_2N_8O_4$	$C_{38}H_{62}MgN_4O_2$
Formula Mass	644.23	931.77	1207.30	886.62	672.28	447.87	603.17	757.51	1181.29	631.22
Crystal system	Monoclinic	Monoclinic	Triclinic	Monoclinic	Monoclinic	Tetragonal	Monoclinic	Monoclinic	Monoclinic	Monoclinic
a/Å	17.3189(3)	12.0930(10)	11.3788(3)	13.4614(7)	17.0865(3)	24.06310(10)	19.8993(3)	9.4092(5)	39.731(4)	17.1130(2)
b/Å	12.4391(3)	14.8544(12)	11.6856(2)	11.9750(7)	15.0333(2)	24.06310(10)	14.4435(2)	13.8925(12)	11.9213(9)	15.0517(2)
c/Å	17.5819(3)	13.2064(15)	21.1747(5)	31.0390(13)	30.0246(4)	7.46520(10)	25.6572(4)	14.8093(10)	23.8229(19)	29.9562(4)
α/°	90	90	105.712(2)	90	90	90	90	90	90	90
β/°	104.339(2)	105.887(11)	94.301(2)	90.965(4)	91.1930(10)	90	92.1430(10)	95.647(5)	99.266(8)	90.8720(10)
γ/°	90	90	104.647(2)	90	90	90	90	90	90	90
Unit cell volume/Å^3	3669.70(13)	2281.7(4)	2590.97(11)	5002.8(4)	7710.6(2)	4322.60(7)	7369.12(19)	1926.4(2)	11136.4(16)	7715.22(17)
Temperature/K	150(2)	150(2)	150(2)	150(2)	150(2)	150(2)	150(2)	150(2)	150(2)	150(2)
Space group	$P2_1/n$	$P2_1$	$P\bar{1}$	$P2_1/n$	$I2/a$	$P\bar{4}\,2_1c$	$P2_1/c$	$P2_1/n$	$C2/c$	$I2/a$
No. of formula units per unit cell, *Z*	4	2	2	4	8	8	8	2	8	8
Radiation type	CuKα	MoKα	CuKα	MoKα	CuKα	CuKα	CuKα	CuKα	MoKα	CuKα
Absorption coefficient, μ/mm^{-1}	1.184	1.103	5.354	0.534	1.146	1.774	0.671	0.981	0.479	0.660
No. of reflections measured	82933	33276	20075	68799	30120	29566	32351	11021	38040	28402
No. of independent reflections	7370	9784	10229	9486	7675	4104	13991	3401	10155	7598
R_{int}	0.0439	0.0649	0.0233	0.0733	0.0317	0.0335	0.0363	0.0466	0.1014	0.0253
Final R_1 values ($I > 2\sigma(I)$)	0.0349	0.0538	0.0360	0.0501	0.0335	0.0210	0.0572	0.0394	0.0610	0.0505
Final $wR(F^2)$ values ($I > 2\sigma(I)$)	0.0896	0.0725	0.0876	0.1137	0.0893	0.0547	0.1450	0.0932	0.0854	0.1415
Final R_1 values (all data)	0.0384	0.0824	0.0399	0.0822	0.0377	0.0215	0.0773	0.0564	0.1590	0.0557
Final $wR(F^2)$ values (all data)	0.0922	0.0800	0.0901	0.1271	0.0924	0.0551	0.1585	0.1003	0.1139	0.1444

References

1. A. S. Altieri, D. P. Hinton and R. A. Byrd, *J. Am. Chem. Soc.*, 1995, **117**, 7566.
2. R. Evans, Z. Deng, A. K. Rogerson, A. S. McLachlan, J. J. Richards, M. Nilsson and G. A. Morris, *Angew. Chem. Int. Ed.*, 2013, **52**, 3199.
3. J. Baran, A. Duda, A. Kowalski, R. Szymanski and S. Penczek, *Macromol. Rapid Commun.*, 1997, **18**, 325.
4. M. Sun, T. Xu, W. Gao, Y. Liu, Q. Wu, Y. Mu and L. Ye, *Dalton Trans.*, 2011, **40**, 10184.